A NUMERICAL STUDY OF WASTE HEAT RECOVERY POTENTIAL OF THE EXHAUST GASES FROM A POWER GENERATION DIESEL ENGINE

A Thesis Submitted to the Graduate School of Engineering and Science of İzmir Institute of Technology In Partial Fulfillment of Requirements for the Degree of

MASTER OF SCIENCE

In Energy Engineering

By
Buket BOZ

January 2017
İZMİR

We approve the thesis of **Buket BOZ**

Examining Committee members:

_____

Assistant Professor Alvaro DIEZ

Mechanical Engineering, İzmir Institute of Technology

_____

Assistant Professor Turhan ÇOBAN

Mechanical Engineering, Ege University

_____

Assistant Professor Ünver ÖZKOL

Mechanical Engineering, İzmir Institute of Technology

27 January 2017

_____

Assistant Professor Alvaro DIEZ

Supervisor, İzmir Institute of Technology

_____

Assistant Professor Onursal ÖNEN

Co-supervisor, İzmir Institute of Technology

_____

Professor Gülden GÖKÇEN AKKURT

Head of the Department of Energy Engineering

_____

Professor Aysun SOFUOĞLU

Dean of the Graduate School of Engineering and Sciences

ACKNOWLEDGMENTS

I would like to express my deepest appreciation to my supervisor, Assistant Professor Alvaro Diez and my co-advisor Assistant Professor Onursal Önen for their guidance and support through the study.

Specifically, I would like to sincerely thank to my supervisor Assistant Professor Alvaro Diez. I truly consider myself lucky to have him as my supervisor. Without his great patient, guidance and attention, the thesis would not have been as productive it is. His approach to the problems and the way that he teaches will keep enlighten me for my future works.

I am thankful to my exam committee, Assistant Professor Turhan Çoban and Assistant Professor Ünver Özkol for their valuable comments to refine my study.

I am also grateful to my lecture professors during my Master Degree. I also want to thank my friends who supported and cheered me during my hard times while I was writing the thesis.

Lastly, I am profoundly thankful to my great family for their unconditional love and patient, and their support through my education.

ABSTRACT

A NUMERICAL STUDY OF WASTE HEAT RECOVERY POTENTIAL OF THE EXHAUST GASES FROM A POWER GENERATION DIESEL ENGINE

Recently, producing and using energy in an efficient way is one of the challenges through the world. Additionally, the severe environmental issues regarding global warming and ozone depletion have risen. Having taken into consideration two aspects, waste heat recovery systems can be an effective solution to solve some of these problems. This study presents the waste heat recovery potential applied to stationary internal combustion engines. Through the work, three different diesel engines' exhaust gases are applied as the heat sources. Three Organic Rankine Cycle (ORC) configurations are designed, a Simple Organic Rankine Cycle and Regenerative Organic Rankine cycle which are thermally powered by exhaust gases and Pre-heating and Regenerative Organic Rankine Cycle with the usage of exhaust gas and the engine cooling water as the heat sources. In order to assess the differences between the chemical classes regarding the ozone depletion and global warming potential, eight candidate working fluids are chosen. A selecting procedure is created to obtain the most appropriate working fluid for the suitable cycle configuration.

The first law of thermodynamic analysis is conducted with the variations of the working fluids, heat sources and the cycle designs in order to accomplish the greatest thermal efficiency with the most suitable working fluid and the configuration. It was found that it is possible to achieve a high thermal efficiency outcome using zero ozone depletion and global warming potential fluids under the Regenerative Organic Rankine configuration.

ÖZET

ELEKTRİK ÜRETEN DİZEL MOTORLARININ EGZOZ GAZLARINDAN ATIK ISI GERİ KAZANIM POTANSİYELİNİN SAYISAL YÖNTEMLERLE İNCELENMESİ

Son zamanlarda, enerjiyi verimli bir şekilde üretmek ve kullanmak dünya çapındaki sorunlardan biridir. Buna ek olarak, küresel ısınma ve ozon tabakası incelmesi çevresel sorunlar olarak ciddi bir oranda artmaktadır. Bütün bu iki görüşler dikkate alındığında, atık ısı geri kazanım sistemleri etkili bir çözüm olabilir.

Bu çalışma, Organik Rankine Çevrimi ile sabit İçten Yanmalı Motorlarda atık ısı geri kazanımı potansiyelini sunmaktadır. Çalışma sırasında, üç farklı dizel motorun egzoz gazları ısı kaynağı olarak kullanılmıştır. Üç farklı ORÇ kurulumu tasarlanmış, Basit Organik Rankine Çevrimi, termal ısı kaynağı olarak egzoz gazı kullanılmaktadır, Rejeneratif Organik Rankine Çevrimi, termal ısı kaynağı olarak egzoz gazı kullanılmaktadır, Ön Isıtmalı ve Rejeneratif Organik Rankine Çevrimi, termal ısı kaynağı olarak egzoz gazı ve motor soğutma suyu kullanılmaktadır. Ozon tabakası delinmesi ve küresel ısınma potansiyeline ilişkin, kimyasal sınıflar arasındaki farkları değerlendirmek için sekiz aday çalışma sıvısı seçilir. Uygun çevrim yapılanması için en uygun çalışma akışkanını elde etmek için bir seçim prosedürü oluşturulmuştur.

Termodinamiğin birinci kanununa göre, en yüksek ısıl verimi elde etmek için, çalışma akışkanlarının ve çevrimlerin çeşitlerinin analizleri yapılmıştır. Gösterilen sonuçlar doğrultusunda, %18,lik termal verim Rejeneratif Organik Rankine Çevrimi ve R-1233zd(E) çalışma sıvısı ile elde edilmiştir.

TABLE OF CONTENTS

LIST OF TABLES

LIST OF FIGURES

Figure **Page**

LIST OF ABBREVIATIONS/SYMBOLS

℃	Celsius
ALT	Atmospheric Lifetime
ASHRAE	American Society of Heating, Refrigerating and Air Conditioning Engineers
CFC	Chlorofluorocarbon
CO_2	Carbon dioxide
EGR	Exhaust Gas Recirculation
EPA	Environmental Protection Agency
GWP	Global Warming Potential
HCFC	Hydrocholorfluorocarbon
HFC	Hydrofluorocarbon
ICE	Internal Combustion Engine
K	Kelvin
Kg	Kilogram
kJ	Kilo Joule
kPa	Kilo Pascal
kW	Kilo Watt
L	Liter
m	Meter
min	Minutes
Min	Minimum
MWe Mega	Watt Electrical
ODP	Ozone Depletion Potential
ORC	Organic Rankine Cycle
PRORC	Pre-Heating Regenerative Organic Rankine Cycle
RORC	Regenerative Organic Rankine Cycle
s	Second
SORC	Simple Organic Rankine Cycle
WHR	Waste Heat Recovery

NOMENCLATURE

$\dot{Q}_{in}$	Heat transfer rate
$\dot{W}_{net}$	Net work per unit of mass
$\dot{W}_{pump}$	Pump work per unit of mass
$\dot{W}_{turbine}$	Turbine work per unit of mass
$\dot{m}$	Mass flow rate
$\dot{m}_{exh}$	Exhaust mass flow rate
$\dot{m}_{wf}$	Working fluid mass flow rate
ΔT	Temperature difference
ΔT_{pp}	Pinch point temperature difference
$\Delta T_{approach}$	Temperature difference between the fluids in the heat exchanger
C_{pexh}	Exhaust gas specific heat capacity
η_{cycle}	Organic rankine cycle efficiency
η_{pump}	Isentropic pump efficiency
$\eta_{turbine}$	Isentropic turbine efficiency
h	Enthalpy
P	Pressure
s	Entropy
T	Temperature
$T_{exh,\ in}$	Exhaust gas inlet temperature
$T_{exh,\ out}$	Exhaust gas outlet temperature
$T_{w,\ in}$	Water inlet temperature
$T_{w,\ out}$	Water outlet temperature
ξ	Inverse of the slope of the saturated vapour curve

CHAPTER 1

INTRODUCTION

The incremental environmental issues induce scientists to develop more efficient, environmentally friendly and sustainable energy production systems. In the Izmir Institute of Technology, one of the aim of the study is to create a much more sustainable campus in terms of the energy. The idea of the study relies on investigating the possibility of waste heat recovery on the generators to help to increase the sustainability in the campus. Since, the number of the generators in the campus cannot be disregarded, a numerical study of the waste heat recovery on the generators is proposed. In point of fact that the 35% of the energy in an internal combustion is rejected as the residual energy in the exhaust system. The dissipated heat can be recovered and converted into useful energy. Thus, the efficiency of the engine ascends and the emissions are reduced at the same time.

In Chapter 2, an overview of the Waste Heat Recovery (WHR) techniques and applicability for energy systems and diesel engines is introduced. In power generations plants, Waste Heat Recovery systems are employed widely in order to increase the thermal efficiency. Several WHR techniques can be named, Organic Rankine Cycle, Thermoelectric Generators, Mechanical Turbo-Compounding etc. However, the Organic Rankine Cycle seems to be the most attractive approach. Thus, the Organic Rankine Cycle is the main topic of the study. Besides that, a profound analysis of the effective parameters on the ORC is presented. The one of most vital parameter is the working fluid. A selecting procedure has created to obtain the most suitable organic fluid.

Furthermore, the fundamental automobile producers are fascinated by the increment of the efficiency and the reduction of the emissions. Hence, the applications of the Waste Heat Recovery systems are not limited by the stationary employments.

Notwithstanding the improvements on the Waste Heat Recovery systems with the Organic Rankine Cycle, there are still innumerable challenges due to the cycle design and the suitable working fluids.

In Chapter 3, a detailed thermodynamic analysis of the three configurations has been indicated. The three designs are proposed and discussed through an extensive energy analysis of the system to enlighten the benefits of the waste heat recovery.
The characteristics of the candidate working fluids are also introduced particularly. In addition, the diesel generators are demonstrated with regard to the engine features. For each case, the inputs, relevant assumptions and the thermodynamic states are provided and are applied on Matlab and Refprop.

Chapter 4 provides an in-depth discussion of the results. The simulation models of the three ICE-ORC systems will provide an opportunity to choose the proper configuration with the organic fluid for the engine's characteristic with regard to the exhaust temperature easily. The investors and the energy system researchers will distinguish the differences on the combined system. Hence, the selecting the right combination will be less painful in terms of time and costs.

In Chapter 5, the final conclusions and remarks of this work are presented.

CHAPTER 2

LITERATURE SURVEY

The fluctuation of fuel prices and the rise of the importance of the environmental impacts of energy production lead scientists to develop more efficient and environmentally friendly energy generating systems. One of the crucial problems of the world is the global warming, which is caused mostly by the greenhouse gas emissions from mankind activities. As a result, the earth's temperature is above than it should be (Kokic, Crimp, & Howden, 2014). In the last two decades, notwithstanding the adoption by the United Nations of climate change policies to reduce the greenhouse gas emissions (Unfccc, 2009), the energy consumption in the world has risen significantly, which has been estimated approximately 30% (Houghton, Jenkins, & Ephraums, 1990). Hence, within the inefficient processes the energy losses in the form of residual heat increase significantly. Regarding this, the development and promotion of waste heat recovery technologies are vital to confirm a sustainable and low-emission future for industrial processes. In addition, the depletion of the fossil fuel reserves leads the conventional energy sources to be less available. Despite the fact that the demand of energy and the prices have been increasing recently, energy in the form of low-grade is still being wasted throughout the some energy-intensive process industries. Hence, using available energy sources more efficiently could help to reduce the requirement for fuel and consequently the emissions of CO_2.

More specifically, internal combustion engines (ICE) have been an essential power source for automobiles, long-haul trucks and power generation over a century. Moreover, the usage of ICEs can be seen on large scale power plants or industries. As a result of the idea of the increase efficiency and reuse of the low-grade heat, the concept of the waste recovery is proposed. In most of the thermal power plants or industrial processes a large percentage of fuel power cannot be converted into mechanical or electrical power, whilst this power is removed in the form of waste heat. It is an inherent

and abundant residual product of the systems. By converting this by product into the useful power such as electricity, the efficiency of the engine system could be improved. On the other hand, industrial waste heat's temperature which is extracted from the system is too low to convert the heat into useful energy by conventional steam cycles. Despite that, different waste heat recovery (WHR) techniques can be suggested to be implemented even with low temperatures. Organic Rankine Cycle, thermoelectric generators, mechanical turbo-compounding and electrical turbo-compounding, turbocharger and other thermodynamic cycles (the Rankine cycle, Stirling cycle etc.) can be given as examples (Punov et al., 2015), (Hossain & Bari, 2013).

- -Mechanical turbo-compounding: an additional power turbine is implemented in the downstream of the turbocharger and it is mechanically coupled to the engine crank shaft by a gear train in order to rise the engine power output (Hossain & Bari, 2013).
- -Electrical turbo-compounding: a system that converts waste exhaust heat to shaft work using a turbine which is utilised on an electric generator (Algrain & Hopmann, 2003).
- -Thermoelectric generators (TEG): the technology directly converts a portion of the exhaust gas heat to electrical power through thermos-electric systems without the utilization of mechanical components (DT Hountalas, Katsanos, Kouremenos, & Rogdakis, 2007). Due to the high prices of thermoelectric materials, the system is not widely used in practical applications.
- -Organic Rankine Cycle (ORC): It is a thermodynamic cycle which uses a circulating organic fluid pumped around the circuit and heated by waste heat in the evaporator to produce vapour that expands to generate electricity (Qiu & Hayden, 2012). In accordance with (Desideri, Gusev, van den Broek, Lemort, & Quoilin, 2016), the ORCs have been proven to be a mature and viable technology for low quality waste heat recovery applications. Hence, Organic Rankine Cycle (ORC) can be proposed one of the most promising waste heat recovery techniques from low temperatures. ORCs rely on the same principle as conventional steam/water Rankine cycles. ORCs use organic fluids as a working fluid. The main components of the cycle are akin to the Conventional Rankine cycle namely, the turbine, evaporator, generator, condenser and pump.

ORC system for WHR is the most common system in the studies because of its simplicity and applicable characteristic (Sprouse & Depcik, 2013). Furthermore, ORCs can be applied to heavy-duty diesel engines as well as to light duty automobiles (Punov et al., 2015).

2.1. Waste Heat Recovery on Diesel Engines

A simple analysis of heat balance of a diesel engine depicts that the input fuel energy is separated into three main parts: energy that converts to useful work, energy that loses through the exhaust gas and energy that dissipates to the coolant. The efficiency of the engines can be estimated around 35% (Hossain & Bari, 2013). Hence, a considerable amount of the input energy is rejected to the ambient environment. Not only the improvement of the engine efficiency but also the environmental pollution problems, are fundamental reasons to use of waste heat recovery systems.

The Rankine cycle can be defined as a steam generator employed to produce steam using the exhaust heat which is expanded in a turbine to generate extra power. It is a closed-loop system where a working fluid repeatedly circulates through four components. If the working fluid is chosen as an organic fluid instead of water, the cycle system is called Organic Rankine Cycle. Geothermal energy, biomass applications, solar energy and the recovery of waste heat can be given as examples of ORC applications. In engine field, ORC systems are also a proven technology in terms of taking advantage of low/medium temperature heat sources (Bianchi & De Pascale, 2011).

Apart from the ORC, the Kalina cycle is also under examination in term of recovering residual heat from the systems. The Kalina cycle is another thermodynamic cycle used in waste heat recovery applications. The Kalina cycle generates electricity from waste heat using a mixture of two fluids with different boiling points (Shu, Yu, Tian, Wei, & Liang, 2014). Due to the fact that the mixture evaporates gradually over a range temperatures, more heat can be extracted from the heat sources in contrast to some pure working fluids (Matsuda, 2014). In comparison between the ORC and the Kalina cycles, the ORC has higher thermal efficiency, smaller systems volume and weight. However, the Kalina cycle has a better thermodynamic performance (Tian, Shu, Wei, Liang, & Liu, 2012). Even though there is a small gain in the performance, the Kalina cycle requires a complicated plant scheme, large surface heat exchangers and particular high resistant and

no corrosion materials (Zhang, He, & Zhang, 2012). In (Bombarda, Invernizzi, & Pietra, 2010), they show that the Kalina cycle can be adapted in geothermal power plants but the need for high pressure resistant and no-corrosion materials should be taken into consideration. Moreover, in (Law, Harvey, & Reay, 2013) study, the efficiency of the Kalina cycle was found 3% higher in comparison to the ORC. However, the application of the Kalina cycle is not still the best choice with regard to the complexity and the high costs. Especially, the high prices of the no-corrosion materials increase the capital outlay of the project. According to (Hossain & Bari, 2013), the mechanical turbo-compounding and Rankine cycle are the most promising candidate techniques regarding waste heat recovery and break specific fuel consumption in diesel engines. However, the increase in the back pressure and pumping losses on the application of the turbo-compounding cause serious problems. Therefore, it is not widely used in comparison to the Rankine cycle**.** (Weerasinghe, Stobart, & Hounsham, 2010)'s study is based on the numerical comparison between mechanical turbo-compounding systems and the Rankine cycle. The results indicate that 7.8% power is recovered by using the Rankine cycle system, whereas only 4.1% power was recovered by using mechanical turbo-compounding system. The ORCs' advantages outweigh the disadvantages with regard to the engine pumping losses, the system has not crucial impact on it (DT Hountalas et al., 2007). In accordance with the many studies, the Rankine cycle is the most applicable method for WHR systems in terms of the high efficiency. In (Daccord et al., 2013) study, the cycle efficiencies obtained for an organic Rankine cycle and water based Rankine cycle were 6.7% and 10.3% respectively.

The ORC system has been investigated in different aspects such as, working fluid selection, performance analysis and system designs. The key point of the ORC system is the selection the working fluid. Researches mainly considered in diverse screening and assessment criteria for organic fluids (Z. Wang, Zhou, Guo, & Wang, 2012).

The ORC technology has been widely used to recover residual heat in a plenty of industrial fields. The one of main ideas of applying ORCs in industries is to increase the overall efficiency of the plants. In order to reach the possible highest cycle efficiency, different cycle configurations are researched in the studies. For instance, in (Vaja & Gambarotta, 2010) study, three different cycle set-ups were considered. The first setup was the simple ORC thermally powered by engine exhaust gases, the second one was the pre-heating ORC thermally powered by engine exhaust gases and engine refrigerant

water. Meanwhile, the different organic fluids were also tried on the study. The last configuration was regenerated ORC thermally powered by engine exhaust gases. The highest efficiency was obtained from the regenerated and preheated phases. The maximum efficiency was slightly close to 12.5%. Moreover, in (Dolz, Novella, García, & Sánchez, 2012), two different cycle configurations were applied which were single and binary cycles respectively. The results were depicted in terms of power increment. The binary cycle and single cycles' power increases were 19% 10% respectively. In addition, the working fluids R245fa and water were used. As a result of using two different working fluids, the organic fluid was found much more suitable in comparison to water regarding the engine's different operating conditions. Furthermore, in (Peris, Navarro-Esbrí, & Molés, 2013) study, six different ORC configurations with ten non-flammable working fluids were simulated in terms of efficiency, safety, costs and environment. The key point of the study was to compare the efficiencies of different cycle designs with unique working fluids. The first bottoming ORC configuration was the Basic ORC. The second one was obtained as Regenerative ORC. The following design was Double Regenerative ORC. The fourth, fifth and the last configurations were named, Reheat Regenerative ORC, Ejector ORC and Transcritical Regenerative ORC respectively. In consequence of this study, the single Regenerative ORC with R236fa as the working fluid and the Reheat Regenerative ORC were acquired as the suitable configurations among the rest of them. The net efficiency was calculated 6.55%, the ICE efficiency rose up to 4.6%. In the work of (Uusitalo, Honkatukia, Turunen-Saaresti, & Larjola, 2014) the ORC process was investigated in terms of different working fluids which were toluene, n-pentane, R245fa and cyclohexane. With regard to the large scale turbocharged engine's different exhausts gas temperatures for ORC application, toluene and cyclohexane gave the highest power outputs in contrast to the other two selected working fluids. As the case of this work, a large-scale gas-fired engine was chosen. The maximum power increase of 11.4% was obtained from the exhaust gas. The increment from the charge air heat was only 2.4%. Hence, the greatest heat recovery potential was related to exhaust gases.

WHR is not only applied to stationary generators or power plants. Among the other technologies, the RC promises high potential and is already well established in many industrial applications such as gas and steam, solar, geothermal and biomass power plants (Bredel, Nickl, & Bartosch, 2011; Horst, Tegethoff, Eilts, & Koehler, 2014). The application of WHR by means of ORC to vehicles is also a burning issue regarding

reductions in fuel consumption and decrease of CO_2 emissions. Notwithstanding the implementations of advanced engine technologies such as direct fuel injection, turbo-charging or variable valve actuation, the peak efficiency of a modern internal combustion engines used in passenger cars does not exceed 43% (Pischinger, Klell, & Sams, 2009). Thus, the remaining energy from the fuel is emitted into the ambient in the form of exhaust and coolant waste heat. Furthermore, the increase of restrictions on environmental regulations plays a crucial role on finding alternative ways to reduce emissions whilst, the efficiency of the vehicles rises. Various WHR techniques are applied to the on-road vehicles. For instance, turbo-compounding is currently used in heavy duty trucks. In the work of (Dimitrios Hountalas & Mavropoulos, 2010) with the application of mechanical turbo-compounding, the brake specific fuel consumption decrease was obtained 1% to 5%. Besides that, (Weerasinghe et al., 2010) stated the increment of the power output of the engine was 4.1%. Despite the improvements, the back pressure which affects the gas exchange processes of the engine, particularly at lower loads appears as a problem. In order to avoid the back pressure issue, thermoelectric generators are suggested as an alternative WHR technique. Even though, back pressure is not a problem on TEG applications, the efficiency rate in the conversion of residual heat to electrical power is slightly lower in contrast to other WHR techniques (Punov et al., 2015). A number of studies have indicated that the RC is the most promising application on the vehicle applications by means of heat recovery (Teng, 2010b)-(Domingues, Santos, & Costa, 2013). The RC can be used in heavy duty diesel engines as well as in automobile applications (Glavatskaya, Olivier, Podevin, & Shonda, 2011). However, the most comprehensive studies are performed on heavy-duty Diesel engines for truck applications (Horst et al., 2014). Nevertheless, in contrast to the success of stationary WHR applications, challenges remain for vehicle operations. The cost and complexity of WHR systems are generally considered to be prohibitive to develop WHR systems for small vehicles (Teng, Klaver, Park, Hunter, & van der Velde, 2011). In the work of (Punov et al., 2015) a tractor engine was studied in terms of WHR with the RC and the ORC. The peak efficiency of the cycle was obtained with the water as the working the fluid which was 15.8% whilst, ethanol as the working fluid, the ORC performed less. The calculated power output was 6.05 kW (14.2%). In this study, using organic materials as the working fluids de-escalated the efficiency of the RC.

The existent implementation of the ORC cannot be limited to on-road vehicle applications. In the different part of the world, the ORC has been installed in order to recover heat from low operating temperature from various sources, solar energy, geothermal heat, biomass etc. (Tchanche, Lambrinos, Frangoudakis, & Papadakis, 2011).

In order to obtain a high efficiency cycle, the type of the heat source is also crucial point to be considered. In (Auld, Berson, & Hogg, 2013), the ORC model was applied with three different heat sources which are named as, internal combustion engine, hot brines and industrial plant. While the ORC application is specifically applied on internal combustion diesel engines, there are also more than one possible heat sources. For instance, the heat which comes from jacket water, EGR or through the exhaust can be used as a heat source for the ORC. In accordance with previous studies, the heat rejected to the ambient through the EGR and exhaust on ICEs was used as the primary heat source for WHR. The application of high temperature heat sources to the Organic Rankine Cycle systems increases the cycle efficiency (Dolz et al., 2012). In this study, several heat sources were investigated which are the exhaust gas heat energy, the EGR cooler, the intercooler where the low pressure compressor outlet air is cooled, the aftercooler where the high pressure compressor outlet air is cooled and engine block cooling water.

2.1.1. Organic Rankine Cycle

ORC systems on waste heat recovery process are suitable for producing electricity from relatively low-temperature waste sources (Uusitalo et al., 2014). The one of most crucial point on the design of ORCs is the selection of the working fluid. In the previous studies numerous organic materials were investigated in order to increase the overall efficiency (Punov et al., 2015; Vaja & Gambarotta, 2010). Thus, the efficiency of the system highly depends on the working fluid. As a consequence, numerous screening criteria of working fluids can be suggested such as, the shape of the temperature-entropy diagram, safety and environmental properties (Kuo, Hsu, Chang, & Wang, 2011). However, the most widely used criteria is the slope criteria of the saturation vapour curve in the temperature-entropy diagram (He et al., 2012). If the slope is vertical, the fluid is an isentropic fluid. If the slope of the T-S diagram is positive, the fluid is named as dry fluid. The ultimate option is the negative slope of the T-S diagram which represent the wet fluid (Peris et al., 2013). Generally, the wet fluids are considered as inappropriate for

ORC applications due to the mechanical problem of the condensation during the expansion which might damage the turbines' blades (Hung, 2001).

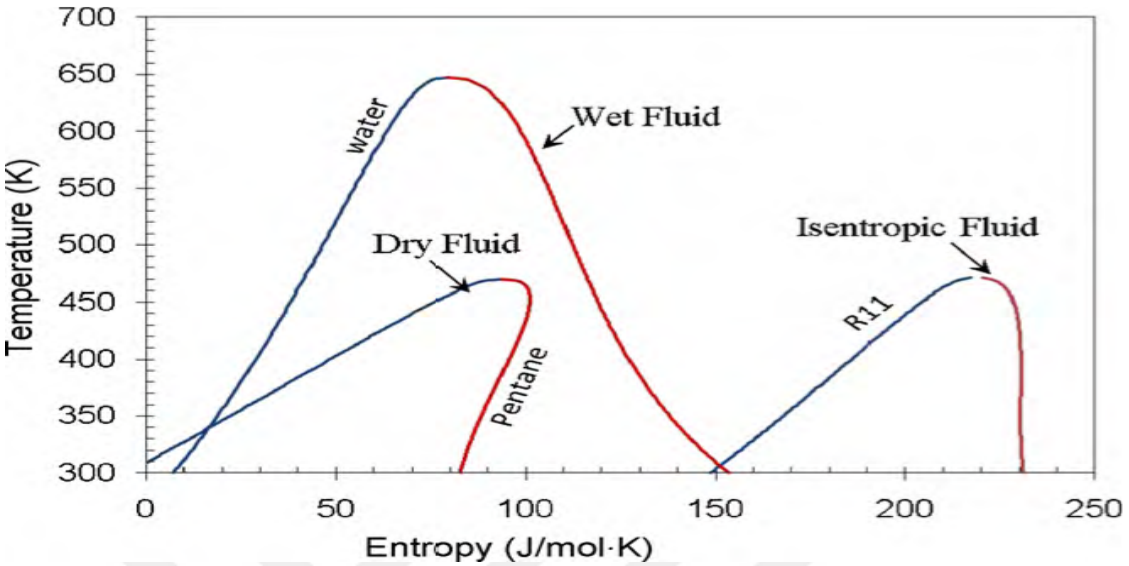

Figure 2. 1. The three different working fluids; wet, dry, isentropic
(Source: Chen, Goswami, & Stefanakos, 2010)

ds/dT> 0 Dry fluid; ds/dT=0 Isentropic fluid; ds/dT<0 Wet fluid (Amicabile, Lee, & Kum, 2015)

In (Amicabile et al., 2015), the working fluid screening criteria were divided into three sections, thermodynamic criteria which contained molecular weight and critical point, environmental criteria, Ozone Depletion Potential (ODP), Global Warming Potential (GWP) and Global Safety criteria which were health, fire and specific hazards. In order to obtain the influence of molecular complexity, the ORC working fluids were evaluated in three categories; dry, isentropic and wet respectively. The working fluid selection part has been one of the burning topics with regard to the ORCs. However, no universal optimum working fluid has been obtained since, the choice is highly relied on the target application. In addition, the working fluid should not affect the ozone layer, null ozone depletion potential (ODP), the global warming potential should be taken into account during the selection of the working fluid (P. UNION, 2006).

2.1.2. Working Fluid on ORC Applications

The enhancement of an ORC depends on various criteria regarding the cycle configuration, choosing the right working fluid etc. The working selection must be taken into consideration in term of the shape of slope, environmental impacts such as GWP (Global Warming Potential and ODP (Ozone Depletion Potential). The most widespread organic fluids in ORC applications are R134a, which is generally used in geothermal power plants and low-temperature heat utilization, and R245fa, whose main application is waste heat recovery of low to medium temperature heat (Eyerer, Wieland, Vandersickel, & Spliethoff, 2016; Quoilin, Van Den Broek, Declaye, Dewallef, & Lemort, 2013). Currently, dominating working fluids for ORCs have a significant drawback with regard to GWP (P. UNION, 2006). In terms of chemical classes of the compounds, R245fa is an example for HFCs (hydrofluorocarbons) which have no effect on the ozone layer but extremely high GWP values. In accordance with the Kyoto Protocol, they have been considered as one of six main greenhouse gases (Unfccc, 2009). As a consequence of this problems, HFOs (hydrofluoroolefins) have been proposed as the last generation organic fluids in order to reduce the environmental drawbacks of the current organic fluids (W. Liu, Meinel, Wieland, & Spliethoff, 2014). In the previous studies of (Shu, Li, et al., 2014; Siddiqi & Atakan, 2012), alkanes are suggested suitable working fluids for medium and high temperature WHR applications.

The selection and the properties of the working fluids are going to be expanded on the latter sections.

2.2. The Working Fluids

The most vital design parameters in ORC applications can be stated as, the evaporator and the condenser's pressure and the temperature. At the same time, the working fluid plays a crucial role in terms of system's operating conditions, critical pressure and temperature. Since, the type of the working fluid has a great effect on the system's performance, environmental and safety impact (Chen et al., 2010).

The fundamental difference between the Organic Rankine cycle and the conventional Clausius-Rankine cycle is the organic fluid which operates the system. The reasons why

the ORC is chosen in waste heat recovery applications were stated in the previous chapters. Even though water has numerous advantages such as, abundant, easily reachable, high thermal and chemical stability, low cost and no side reaction with environment, it is not applicable for low and high temperature waste heat recovery application due its high critical pressure and inappropriate saturation curve (Jumel, Feidt, & Kheiri).

The selection is an elaborate task with regard to the different specification of the organic fluids. In order to eliminate the working fluids, a procedure is prepared.

A procedure for the screening the organic fluids is proposed with the following steps:

- Literature survey on existing and under operation working fluid for the ORC applications
- The primary selection relies on the convenience with the working temperature range (The critical temperature and the pressure of the candidate working fluid)
- The shape of the saturation curve of the organic fluid (Wet, dry, isentropic)
- The second one focuses on the environmental and safety issues (Kyoto Protocol, Montreal Protocol etc.). The attention is on the ODP and GWP values.
- Comparison of thermodynamic properties

Throughout this thesis, the working fluids are going to be obtained regarding this procedure in order to find the most suitable organic fluid for waste heat recovery applications.

2.2.1. Thermodynamic Properties

Each of the organic fluids has different features in terms of thermodynamics and chemical classes. In order to distinguish the proper fluid for waste heat recovery with the ORC application, the properties should be identified. In general, as mentioned before, the organic working fluids are categorized in three different groups regarding the slope of the saturation curves on T-s diagrams respectively, wet, dry and isentropic fluids. The slope of the T-s diagram is positive, the organic fluid considers as dry whereas, the slope is negative, the working fluid is wet. If the slope is vertical, the fluid represent the isentropic group (Peris et al., 2013). As the dT/ds term goes to the infinity, the class of the fluid is expressed as an inverse function of the saturation slope ($\xi = ds/dT$). If the term is greater than zero, the fluid is counted as dry fluid, whilst the fluid is wet, ξ is below zero

(Amicabile et al., 2015). Additionally, in the work of (B.-T. Liu, Chien, & Wang, 2004) an empirical equation is proposed to estimate the exact value of the ξ and the group of the working fluid. In this work, the reliability of that equation was proofed at the fluid's normal boiling points. The further work of (Chen et al., 2010) depicts the resultant of a large deviation on the equation. Hence, the appropriate way to predict visually whether the fluid is dry, wet or isentropic is to plot the T-s diagram.

After the expansion process, dry fluids stay in one phase which means avoiding the liquid formation. Therefore, this condition can be used to increase the cycle efficiency. Since, at the outlet of the turbine, there is an excessive superheated vapour form of the working fluid which can be recovered by internal heat exchanger as in regenerative organic Rankine cycle. In case of application of wet fluid for this type of waste heat recovery applications, it is highly possible to face two phase region which can cause mechanical damage on the turbine blades. This is the reason why the wet fluids are regarded as inconvenient (Oluleye, Jobson, Smith, & Perry, 2016).

2.2.2. Environmental and Safety Issue

One of the core reasons to investigate the candidate working fluids on ORC applications is to determine the most suitable organic fluid for this kind of operations. While, the screening of the possible working fluids is on the progress, environmental properties of these fluids must be taken into account due the fact of the global warming problem and the increment of the greenhouse gases. EPA (United States Environmental Protection Agency) plays a crucial role defining and controlling the greenhouse gases and the refrigerants, such as R-134a, R245fa etc. Even though, EPA is based in the USA, it is considered as one of the leader organisation through the world in terms of environment (EPA, 2016).

Ozone Depletion Potentials (ODP) supplies a relative measure of the expected effect on ozone per unit mass emission of a gas compared to that expected from the same mass emission of CFC-11 integrated over time (Solomon, Mills, Heidt, Pollock, & Tuck, 1992). In accordance with the Montreal Protocol, the ODP of CFC-11 is defined as 1.0. Beside that the other CFCs and HCFCs' ODP values range between 0.01 and 1.0. However, the chemical class of HFCs have zero ODP due to the fact that, in their chemical compound does not contain any chlorine (Secretariat, 2000).

Global Warming Potential (GWP) is the ratio of the warming caused by a substance to the warming caused by a similar mass of CO_2. Moreover, the GWP ratio of CFC-12 is 8500, while CFC-11 has GWP of 5000. In contrast to ODP ratios of HCFCs and HFCs, the GWP values of these substances are fairly high 93 to 12000 respectively (Secretariat, 2000). Furthermore, ODP and GWP ratios are crucial to identify how hazard the fluid is for the environment (CHANGE, 2007).

Atmospheric Lifetime (ALT) is defined how long it takes for a substance to restore the equilibrium following a sudden increment or decrement of the concentration in the atmosphere of the greenhouse gases. In order to assess the long term impact of a greenhouse, ALT plays a critical role.

Under the Montreal Protocol (M. Protocol, 1987), ozone depleting substances have phased out by the countries. For instance, CFCs had phased out at the end of 1995 in the developed countries, for the developing countries the date was target as 2010. In addition, some of the substances such as R-21, R-22 etc. have been targeted to phase out in 2020s.

From the safety point of view, the possible working fluids are investigated regarding the ASHRAE Standard-34 (Standard, 2001). In accordance with the standard, the refrigerants are divided into six different main classes and two subclasses with regard to the toxicity and flammability.

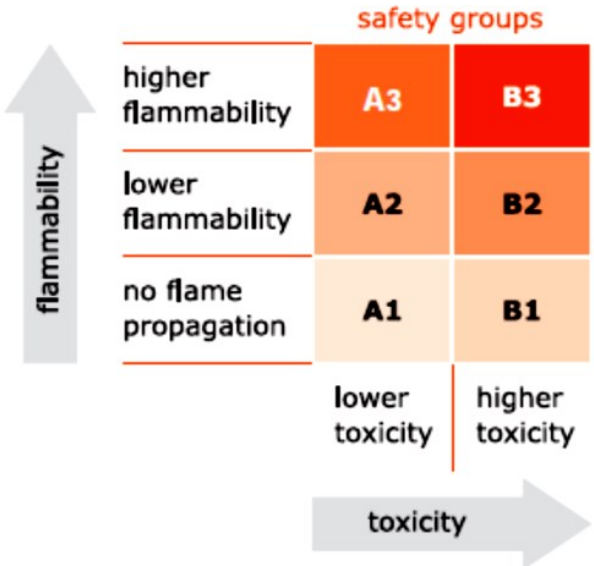

Figure 2. 2. ASHRAE Standard 34-2007 safety classification (Source: Designation, 1993).

2.2.3. The Procedure to Select the Working Fluid

Since the selection of the working fluid on ORC applications is a critical issue, unlimited possible organic fluids have appeared. Within the help of the set procedure, the suitable candidates have been designated.

In accordance with the literature survey, four main chemical classes have become prominent in terms of waste heat recovery with ORCs which are named as, hydrofluorocarbons, hydrofluoroolefins, alkanes and siloxane. (Gao et al., 2012; Hærvig, Sørensen, & Condra, 2016; Jumel et al.; E. Wang et al., 2011).

Refrigerants used for HVAC (heating, ventilation and air conditioning) systems can be categorized in four generations. The first generation of the working fluids' representative is CFCs (chlorofluorocarbons) such R11 and R12. Meanwhile, the second generation refrigerants are HCFCs (hydrochlorofluorocarbons), R22 can be given as an example (Eyerer et al., 2016). The two generations were applied widely on the applications due to their good performances and convenient handling until their side effects of ozone depletion potential was discovered. Under the control of the Montreal Protocol (M. Protocol, 1987), the usage of these substance were prohibited based on the depletion on the ozone layer. By the reason of ODP problem, the third generation of working fluids, HFC (hydrofluorocarbons) are presented and the current state of art working fluids for ORC applications. R245fa and R134a are being used considerably. However, the significant problem of the third generation fluids is their high GWP values (Secretariat, 2000). Hence, HFCs were determined as greenhouse gases under the Kyoto Protocol (K. Protocol, 1997). In most of the developed countries within the help of regulations, the usage is tried to be taken under control. Recently, the phase out of the fluorinated greenhouse gases (F-gases) has been controlled by two legislations in the European Union, The MAC Derivative and the F-Gas Regulation (E. Union, 2006). The profound difference between the two legislations is, F-Gas Regulation targets to eliminate the usage of these gases, whereas MAC Derivative aimed prohibiting the usage of refrigerants with a GWP value is higher than 150 for air condition systems of motor vehicles from 2017 onwards. In order to assess the regulations and prevent the side effects of the third generation working fluids, the fourth generation of refrigerants seem a logical settlement (Eyerer et al., 2016).

One of the most applied refrigerant on waste recovery application with ORC is R-134a the other suitable working fluid is R245fa (Saleh, Koglbauer, Wendland, & Fischer, 2007). On the study of (Bracco, Clemente, Micheli, & Reini, 2013), the net electrical efficiency was obtained as 8% with R-245fa. Even though, the main refrigerants have been applied widely in ORC application both low and high and medium temperatures, a current topic is the replacement of these working fluids with more environmentally friendly organic fluids (Eyerer et al., 2016; Invernizzi, Iora, Preßinger, & Manzolini, 2016). Having regard to this issue, the two suitable HFOs are proposed for the replacement of R-134a, R1234yf and R1234ze(E) (Invernizzi et al., 2016). The application of the working fluids is investigated in different studies. For instance, (Yang & Yeh, 2016) researched the suitability on geothermal applications. Meanwhile, (Yang & Yeh, 2015) published how R1234yf is applicable for waste heat recovery in large diesel engines. For the refrigerant systems, R1234yf has been deliberated as an excellent replacement for HCF-134a (Jarall, 2012).

Furthermore, (Petr & Raabe, 2015) approximated R1234ze(E) the drop-in for R245fa for heat sources which ranged between 100℃ and 250℃. As a consequence, the replacement of R245fa to R1234ze(E) seemed convenient. According to (Luo, Mahmoud, & Cogswell, 2015), a suitable approach was developed to obtain the high performance and low GWP working fluids with respect to the heat source characteristic. The outcome of the study depicts that R1234yf and R1234ze can be considered as the best working fluids for low-grade heat which varies between 120℃ and 150℃.

On the study of (Molés et al., 2014) another fourth generation working fluid, HCFO-1233zd-E was evaluated to be an alternative to HFC-245fa in terms of low temperature waste heat recovery. As a result, this organic fluid was estimated to be substitute for ORC applications. In terms of net cycle efficiency, R1233zd-E gave the highest result of 10.6%.

Further investigations have concluded that in the terms of electrical efficiency of HCFO-1233zd-E and HFC-245fa, the latter is 5% and the former 9.7%(W. Liu et al., 2014).

For high temperature ORC applications, alkanes as the working fluid seem an attractive option. Cyclic and linear alkanes were examined as possible working fluid for biomass applications (Algieri & Morrone, 2012). Beside that study, (Siddiqi & Atakan, 2012) compared three different used working fluids' performances on ORC with the alkanes'. On the work of (Shu, Li, et al., 2014), alkane-based working fluids were

evaluated systematically, with regard to use the diesel engine's exhaust gases as a heat source for ORC. As a result of this research, cyclic alkanes performed well in terms of thermal efficiency and power output.

Another candidate working fluid for high temperature waste heat recovery applications is siloxanes. In (Fernández, Prieto, & Suárez, 2011), simple linear siloxanes applied on saturated regenerative configuration gave convincing results in terms of cycle efficiency and thermal stability of the organic fluid. Siloxanes are simply linear or cyclic polymers composed of alternating silicon-oxygen atoms with methyl groups attached to the silicon atoms (Fernández et al., 2011). Due to its long names, the shortcuts are used in order to identify the fluids. For instance, Dx depicts the cyclic molecules and MDx-$_2$M are linear molecules.

In order to expand the knowledge of the different chemical classes' behaviour on ORC application with waste heat recovery, an alcohol is also going to be investigated.

2.3. The Market Scenario of ORC Applications

The OPEC oil embargo in 1970's led researchers to investigate alternative energy resources and techniques to use sources beneficially. Therefore, ORC systems producers have been taken their places in the market regarding this reason. The leading manufacturers can be named as, Turboden, ORMAT, Enertime and Tri-o-gen. In addition, the rise of importance of environmental issues regarding global warming and ozone depletion problem triggers the increase of the ORC market.

Previous studies reveal that ORC applications have been applied widely around the world. In the work of (Nasir, Jones, Buchanan, & Posner, 2004) they presented an Energy Converter (OEC) producing electricity by the application of an ORC system to convert residual waste heat to useful energy with the help of gas turbines at a Natural Gas Processing Plant . N-pentane is chosen to be the working fluid for the plant which was the first of its kind in the USA.

Furthermore, (LEGMAN & Citrin, 2004) presented a study on the application of the ORC for the conversion of low-temperature waste heat from the clinker cooler air of the Heidelberg –Cement manufacturing plant into electricity. The plant which is located in

Lengfurt, Germany, meets the criteria not only for the cement production but also compatible for other types of industrial processes.

Additionally, ORC technology has also been integrated marine engines to recover waste heat. For instance, Siemens and United Arab Shipping co-operation provided waste heat recovery system for the latter's ships (SIEMENS, 2014).

Regarding geothermal power plant, Chena which is located in Alaska can be given as an example. The plant's capacity is 200 kW and the working fluid is R-134a. It is stated that the application of ORC on Chena displaced around 44,400 gallons of diesel, which was used for power generation formerly (Chena Power, 2007).

Table 2.1. The list of ORC system producers and their applications in the world (Source: Quoilin & Lemort, 2009)

Manufacturer	**Applications**	**Power Range (kWe-MWe)**	**Heat Source Temperature (℃)**	**Technology (working fluid)**
ORMAT, US	Geothermal, WHR, Solar	200 kWe-72 MWe	150-300 ℃	Fluid: n-pentane
Turboden, Italy	CHP, Geothermal	200 kWe-2 MWe	100-300℃	Fluids: OMTS, Solkatherm Axial turbine
Adoratec, Germany	CHP	315 kWe-1.6 MWe	300℃	Fluid: OMTS
GMK, Germany	WHR, Geothermal, CHP	50 kWe- 2MWe	120-350℃	300 rpm multi-stage axial turbine (KKK) Fluid: GL 160 (GMK patented)
Koehler-Ziegler, Germany	CHP	70-200 kWe	150-270℃	Fluid: Hydrocarbons Screw Expander
UTC, US	WHR, Geothermal	280 kWe	>93℃	Pure Cycle
Cryostar	WHR, Geothermal	n/a	100-400℃	Radial inflow turbine Fluids: R-245fa, R134a
Freepower, UK	WHR	6 kWe- 120 kWe	180-225℃	-
Tri-o-gen Netherlands	WHR	160 kWE	>350℃	Turbo-expander
Electratherm, US	WHR	50 kWe	>93℃	Twin screw expander
Infinity Turbine, US	WHR	250 kWe	>80℃	Fluid: R134a Radial turbo expander

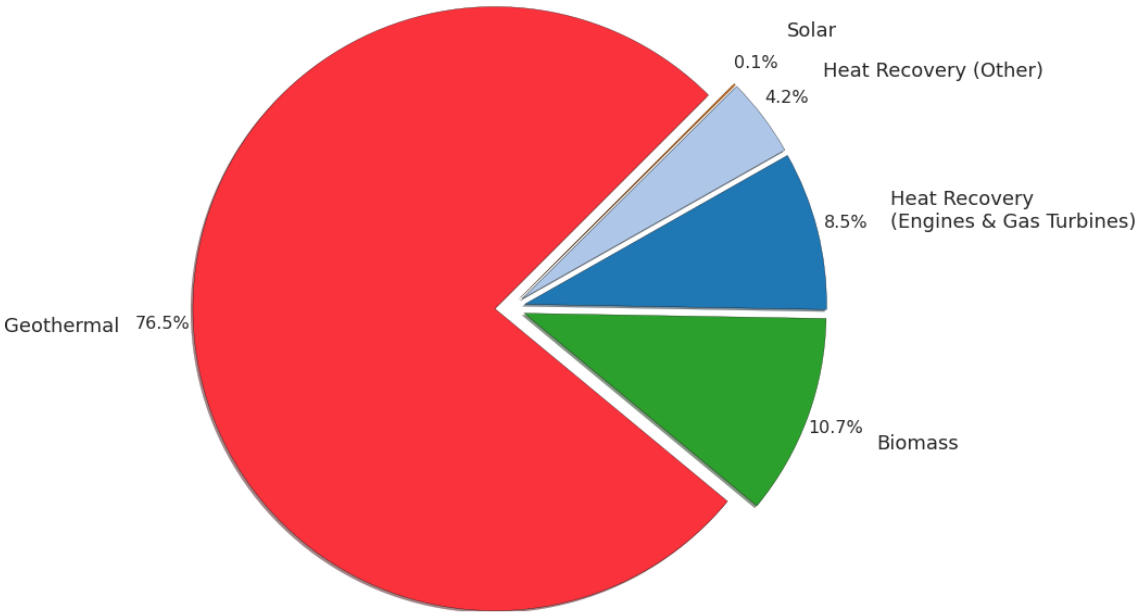

Figure 2. 3. The ORC applications in the World (Source: Tartière, 2015)

Figure 2.3 portrays that ORC systems on geothermal applications are ruling the market 76.5% respectively. Biomass power plants trace geothermal applications with 10.7%.

The ORC applications for geothermal power plants are fairly common in terms of waste heat recovery processes. Developments on the working fluids lead the ORC systems to be more applicable for waste heat recovery for the high temperature heat sources such as internal combustion engines.

Furthermore, as it is depicted on Figure 2.3, the ORCs are also suitable for solar energy productions systems. From the environmental point of view, raising the efficiency of the systems with the environmentally friendly application seems very satisfying due to the environmental systems.

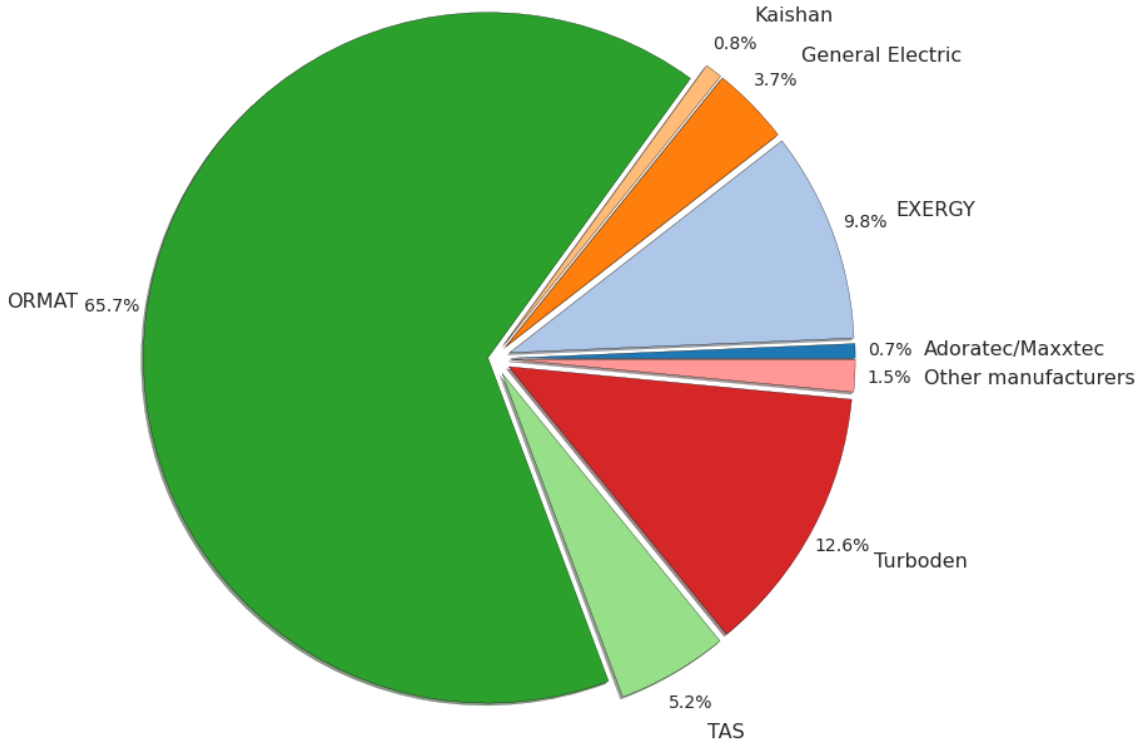

Figure 2. 4. The market share regarding the companies (Source: Tartière, 2015)

As Figure 2.8 illustrates the leader of the production of ORC is ORMAT with 65.7% installed capacity. It is followed by Turboden which is an Italian company.

The market potential and the application of the waste heat recovery systems with the Organic Rankine Cycle rises with regard to the graphs and the charts on the above.

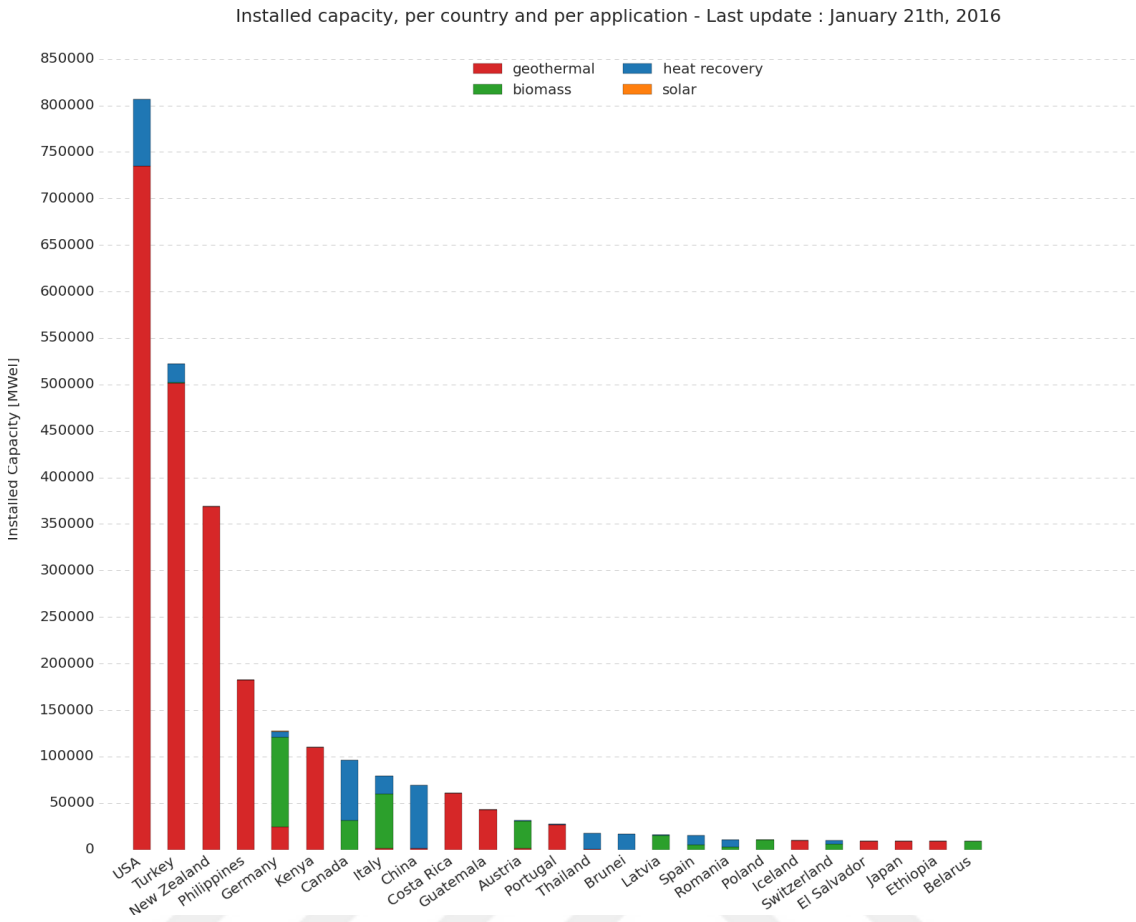

Figure 2. 5. The installed capacities in the World (Source: Tartière, 2015)

The USA has the largest installed capacity all over the world. It is traced by Turkey with fairly high installed geothermal power plants. The first four countries in the Figure 2.5, benefit from the high potential residual geothermal resources. Meanwhile, Germany and Italy are mostly applied ORC technology on biomass power plants.

2.4. The Diesel Engine on Organic Rankine Cycle Applications

Increasingly limiter environmental regulations and legislations influence researchers and industries to raise the power efficiency of engines. A cursory heat balance at the internal combustion engine can be divided into three parts: energy converted to useful work, energy losses through exhaust gases and energy transferred to coolant (Dolz et al., 2012). In power plants and industrial processes, the RC and ORC systems have been employed to enhance the total efficiency. Moreover, waste heat recovery applications on marine diesel engines have been utilised since the 1980s (Teng, 2010a). The success on the marine engines triggered the industries to apply WHR systems on possible processes. Apart from other waste heat recovery applications for instance, thermoelectric generators, the Organic Rankine Cycle assures high efficiency. The well installed applications such as geothermal, solar and biomass plants approve the high potential (Bredel et al., 2011; Tchanche et al., 2011).

Even though, the advanced engine technologies have arisen the greatest efficiency of modern ICE in the passenger cars cannot go beyond 43% (Pischinger et al., 2009). Within the development of waste heat recovery systems, it is claimed that the implementation of WHR can improve the efficiency of the vehicles (Boretti, 2012). On the other hand, in accordance with the (ACTION), passenger vehicles produce 12% of CO_2 emissions in the EU. The increment continues without any drop in terms of the emissions. Due to this reason, the European Commission has put into force new emissions performance standards for passenger cars in order to decrease the greenhouse gas emissions from light duty vehicles. In the literature, the ORC applications on heavy duty engines have contributed excessively (Peralez et al., 2013; Vaja & Gambarotta, 2010). Recently, investigations have focused on the implementation of the ORC systems on passenger cars (Briggs, Wagner, Edwards, Curran, & Nafziger, 2010; Horst et al., 2014).

One of the solid work for integration of WHR systems on passenger is developed at BMW Research and Technology. One of the main targets of the study is to predict fuel saving potential with the implementation of WHR systems (Horst et al., 2014). Consequences of the study can be summarised as, if the integration effects were neglected the current BMW 5 series electrical demand which around 750 W could be supplied by the WHR systems with the benefit of 3.4% fuel saving potential. However, if the side effects of the implementation were taken into account, the fuel saving might be slightly

lower than the first case, 1.3% respectively. Hence, it is clear that WHR systems play a vital role to defeat the problems regarding the increment electric power demand in future automobiles.

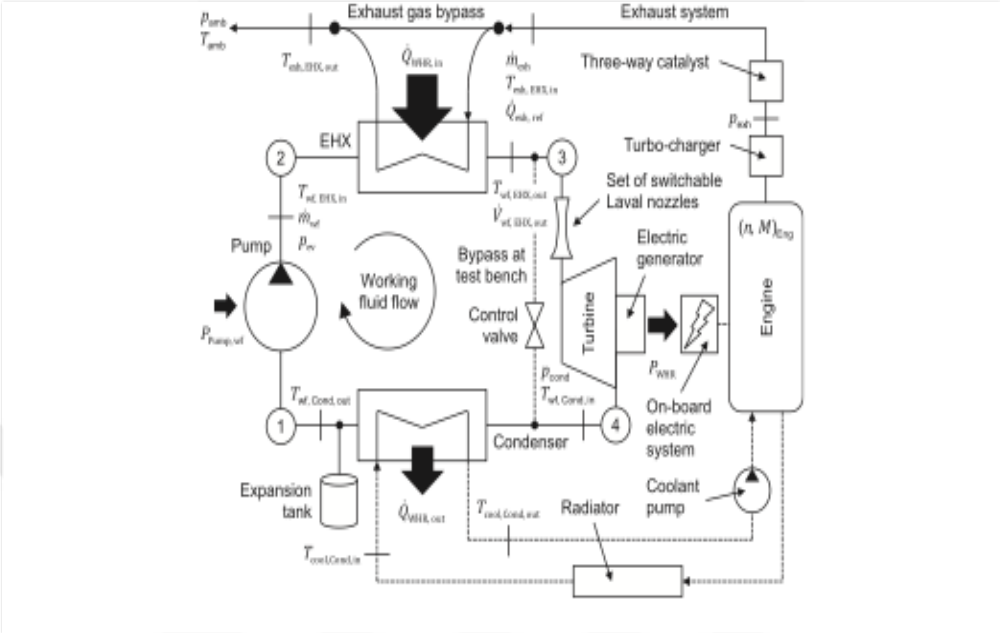

Figure 2. 6. Schematic of automobile exhaust heat recovery systems and main operating variable (Source: Horst et al., 2014)

In addition to the reduction in emissions, Rankine and Organic Rankine Cycle systems are promising approach for achieving decrease in fuel consumption in passenger cars. Despite the fact that WHR systems are not generally included in today's car design, for implementing the systems, they are one of the hot topic of this field. In order to prevent side effects of integration of WHR such as vehicle weight, engine backpressure and cooling demand, special attention must be given in terms of dynamics of the car (Horst et al., 2014). The first application of ORC system for vehicles was endeavoured by Patel and Doyle in 1970s (Patel & Doyle, 1976). The model engine model, Mack 676 was installed in a long heavy duty track. The improvement on fuel consumption was around 12.5%. Despite the satisfied results, during the 90s the importance of the waste heat recovery systems were ignored due to the fact that the higher efficiency of the engine could have been reached by cheaper and easier solutions. However, the rise of the environmental consciousness leads researchers and the industry to develop this technology. Within the application of ORC systems for vehicles, it is expected to reduce

the CO_2 emissions approximately between 3-8% (Arsie, Cricchio, Pianese, Ricciardi, & De Cesare, 2016).

Throughout this study, three different types of diesel generators will be investigated in terms of their suitability for the ORC applications. The ten generators are located in the Izmir Institute of Technology Campus. They are divided into three main groups in terms of their exhaust temperatures. Table 2.3 illustrates the specifications of the generators that are inquired into this study.

In the campus, four different and main generator brands are under operation currently. The generators can be distinguished with the number of cylinders and their power. However, they are all the turbocharged generators running at same and constant speed. . The main purpose of examining different diesel engines is to comprehend their behaviours and compatibilities with the ORC. Furthermore, three types of DE give the opportunity to analyse the effects of the size of the engine, number of cylinders and exhaust temperature with the application of the ORC. Besides that, the comparison between the engines' performance with the ORC will guide the following applications. Consequently, it will be straightforward to choose the engine type which is the most appropriate for further ORC applications and researches.

2.5. Purpose of the Thesis

Through this study, the author intends to develop an optimum Organic Rankine Cycle set up for stationary diesel generators which are located in the Izmir Institute of Technology Campus area, in order to reach the possible maximum efficiencies with reducing the fuel consumption, while concerning the sustainability in the campus.

In order to comprehend the behaviours of the generators, three different diesel generators are going to be investigated. The engines are divided into three groups with regard to the exhaust gas temperatures. One representative engine is chosen for each group due to the alignment, size and power. While the engines are being chosen for each category, the largest size and power percentages are taken into account. As a consequence, the exhaust gas temperatures of the generators are chosen to be the fundamental heat source for this research. However, the cooling water of one of the engines is going to be applied as the second heat source for the third type of Organic Rankine Cycle configuration.

The outcome of the literature survey, three diverse ORC configurations are going to be applied through the study. The first design is the Simple Organic Rankine Cycle. The second is the Regenerative ORC and the last one is the combination of Pre-Heating and Regenerative ORC. As it is stated on the previous paragraph, the additional heat source, the cooling water is employed solely for this configuration.

It is declared on the former sections that one of the vital points for the Organic Rankine Cycle is the working fluid. During the research, from the five different chemical classes, eight organic fluids are going to be applied. The outstanding reason endeavouring various organic fluids is to acquire the most suitable and environmentally friendly working fluid for this type of applications.

Since this study is numerical, in order to assess this study, Matlab and Refprop are going to be applied actively. A set of thermodynamic equations are going to be prepared and evaluated with the Matlab application.

In the present work, taking into the consideration the steps of the working fluid selection procedure, from five different chemical classes, the working fluids are obtained. With regard to the literature survey and all the environmental and safety issues and the performances of the working fluids on ORC applications, the organic fluids are investigated in three varied configurations. Even though, the universal and suitable working fluid for this type of application have not been obtained yet, the researches have a great focus on this area.

Eventually, three different diesel generators' performances can be inquired within the integration of the most desirable ORC with the proper organic working fluid. For the further investigations, the comparison of the three diesel generators with different size and power is going to be fairly helpful to integrate which ORC configuration is compatible with which type of engine. Meanwhile, the chance of increase sustainability of the campus will be one of the outcomes of this study. A minor economic feasibility for the possible application of ORC system on one of the generators is going to be studied.

CHAPTER 3

METHODOLOGY

Chapter three consists of a detailed thermodynamic analysis of the three Organic Rankine Cycle designs. The Simple, Regenerative and Pre-Heating Regenerative Organic Cycle configurations are going to be examined by states. The states are going to be explained and the phases are going to be indicated plainly. The thermodynamic equations are also declared on the section for each configuration.

In the Design and Simulation part is formed by the application of Matlab and Refprop. Through the section, the inputs and the assumption, are applied on the simulation are going to be asserted clearly. In addition, the candidate working fluids and the engines' characteristics are going to be demonstrated extensively.

3.1. The Conventional Rankine Cycle

A Rankine cycle is a closed thermodynamic cycle where a working fluid circulates through four main components in order to produce mechanical energy via a turbine. Water is the working fluid for the conventional Rankine Cycle. Hence, it is named as the standard vapour cycle. The name of the cycle refers to William John Macquorn Rankine (1820-1872) , a Scottish engineer and physicist who is also credited for the "Rankine Temperature" scale (Bamgbopa, 2012). The Rankine cycle consists of a feed pump, an evaporator, a turbine and a condenser.

The transformations of the cycle can be summarized as follows:

Process 1-2s: Saturated water which is at initial condition (low pressure and temperature) is compressed to the high pressure and temperature. The work per unit of mass is calculated by the enthalpy differences on the two states. Throughout this study, isentropic efficiency of the pump is taken into consideration. Hence, the states are obtained accordingly.

Process 2s-2': The compressed water is heated up at constant pressure until the saturation point of the water.

Process 2'-3: Saturated liquid water is vaporised at constant pressure and temperature inside the evaporator or boiler.

Process 3-4s: The water vapour at high pressure expands to low pressure. In accordance with the isentropic efficiency of the turbine, the calculation and the state are specified.

Process 4s-1: The low pressure vapour condensate at constant pressure and temperature to the initial conditions.

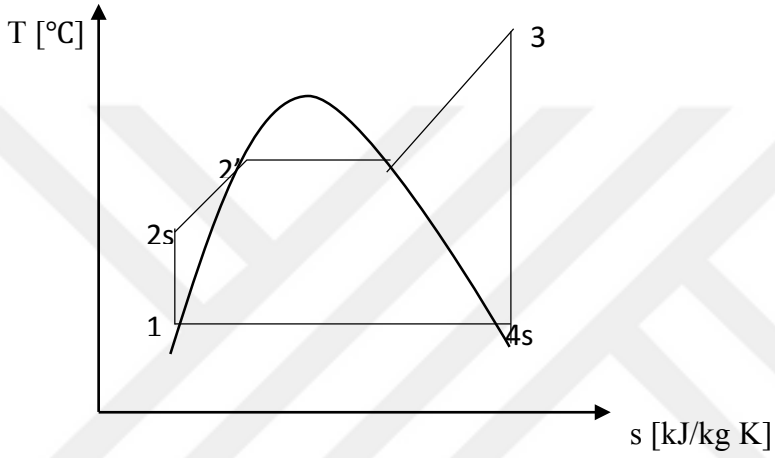

Figure 3. 1. T-s Diagram of the Conventional Rankine Cycle

Since Figure 3.1 depicts the T-s diagram, the state 3 is on the superheated region. This circumstance provides two advantages regarding the increment on the efficiency. Firstly, it is useful avoiding the potential damages on the turbine blades. Because of the fact that, on the state 4 it is not likely possible to face the wet expansion. The second one is that, the cycle efficiency rises evenly with the turbine inlet temperature (T_3) (Hung, Shai, & Wang, 1997).

In terms of the Rankine Cycle, subcritical and supercritical layouts can be discussed. The critical refers to the critical temperature and the pressure of the circulating working fluid. The critical points of the working fluid limit the temperatures and the pressures of the cycle. For instance, the subcritical cycle might occur in two different ways, subcritical superheated or subcritical saturated cycle.

Throughout the study, the subcritical superheated Organic Rankine Cycle is going to be taken into consideration for all the configurations and the candidate working fluids.

3.2. The Organic Rankine Cycle

The Organic Rankine cycle is simply a thermodynamic cycle which uses a circulating organic working fluid pumped around the circuit and heated up by the exhaust gases from an engine in the evaporator in order to produce mechanical power (Qiu & Hayden, 2012). The idea behind the ORC is akin to the conventional RC. However, the only difference occurs in terms of the working fluid. As the name refers, for the ORC applications, an organic component is applied as the working fluid. For waste heat recovery applications, ORC applications are preferred widely regarding the low/medium temperature heat sources (Bianchi & De Pascale, 2011).

In Chapter 2, the applied simulations and research on ORCs were mentioned in detail. Apart from these, commercially ORCs are under operation at the different part of the world with regard to waste heat recovery or geothermal applications.

As shown in Chapter 2, the efficiency of the ORC is highly relied on the cycle configuration. In order to reach the possible highest efficiency on the application, the design of the cycle, the working fluids, the engines' characteristics and the heat sources are going to be varied accordingly. Through this study, in order to distinguish the differences between the cycle configurations in terms of thermal efficiency, three cycle configurations will be investigated, the Simple, the Regenerative and the Pre-heating and Regenerative ORC respectively. The first two designs are thermally powered by the engine exhaust gases. Meanwhile, the pre-heating and regenerative is slightly diverse from the first two configurations regarding the heat source. For the last design, the engine jacket cooling water will be applied on the systems.

3.2.1. The Simple Organic Rankine Cycle

The Simple Organic Rankine Cycle (SORC) is the basic configuration applied for waste heat recovery applications. In Figure 3.2, the T-s diagram of the SORC with superheated is depicted clearly. It solely requires the minor components. Meanwhile, the transformation of the SORC is not different from the conventional RC. On the other hand, in order to vaporise the circulating working fluid, the needed heat is provided only by the exhaust gases of the ICE. The temperature of the exhaust gases varies depending

on the type of engine. However, assuming constant load operation, the generators tend to work already at constant speed.

Inside the evaporator, the mass flow rate of the working fluid can be obtained from the energy balance;

$$\dot{m}_{wf1} = \frac{\dot{m}_{exhuast} \times Cp_{exhuast} \times (T_{exh,in} - T_{exh,pp})}{h_3 - h_{2'}} \quad (3.1)$$

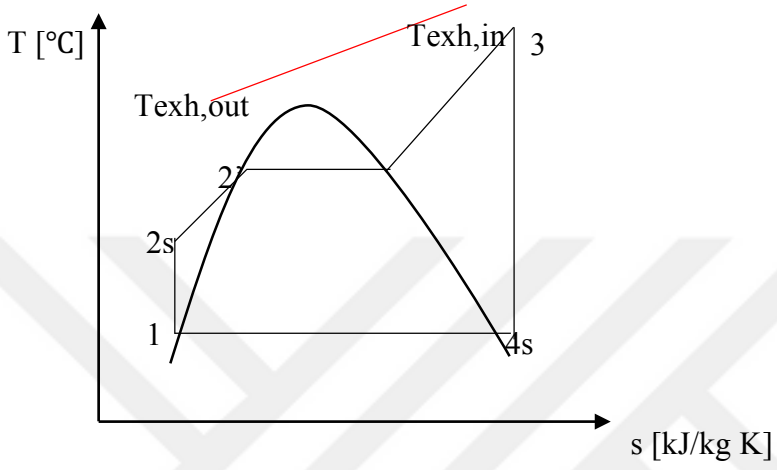

Figure 3.2. The SORC T-s Diagram

The pinch point is an approach to calculate the heat transfer between the exhaust gas and the working fluid. The concept relies on predicting thermodynamically feasible energy targets by recovering and reusing the heat energy with a process until the process is constrained or 'pinched' a lower temperature approached is reached (Oluleye et al., 2016). The pinch point between the exhaust gas and the working fluid restricts the amount of heat recovered. Additionally, the Pinch Point may appear at either the initial point of preheating or the starting point of vaporisation (Yu, Feng, & Wang, 2015). The Pinch Point approach will be applied for three cases.

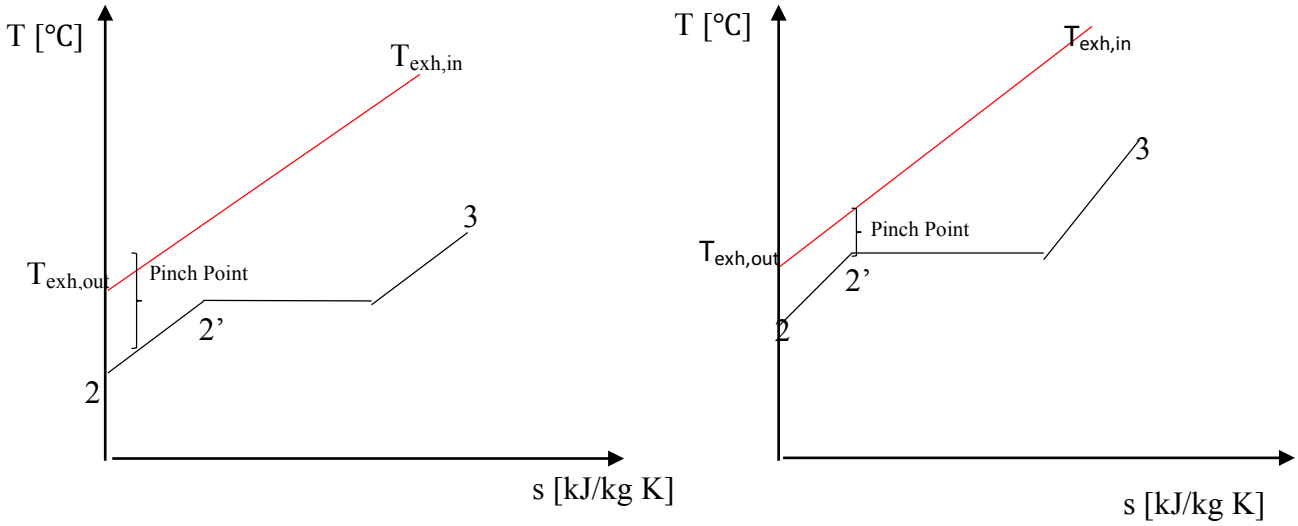

Figure 3. 2. The Possible Pinch Point Positions (Source: Capano, 2014)

A minimum gas pinch point temperature T_{exhpp} is considered as $T_{exh,pp} = T_{2'} + \Delta T_{pp}$. ΔT_{pp} is approximated 30K at the Pinch Point to meet the exhaust and working fluid heat exchanger (evaporator) performances (Vaja & Gambarotta, 2010). The enthalpies of the working fluid are the function of evaporator pressure.

$$T_{exh,out} = T_{exh,pp} - \frac{(h_{2'} - h_2) \times \dot{m}_{wf1}}{\dot{m}_{exhuast} \times Cp_{exhuast}} \tag{3.2}$$

Equation 3.2 determines the $T_{exh,out}$ of the system. In accordance with the result of the equation, (either $T_{exh,out}$ is below or above the T_{min}) the second energy balance could be applied. If the $T_{exh,out} < T_{min}$, which is inconvenient for the cycle conditions, the second energy balance is assigned to find the satisfied mass flow rate of the working fluid.

$$\dot{m}wf2 = \frac{\dot{m}_{exhuast} \times Cp_{exhuast} \times (T_{exh,in} - T_{min})}{h_3 - h_{2a}} \tag{3.3}$$

The obtained $\dot{m}wf2$ satisfies the cycle requirements. The cycle efficiency is calculated as follows;

$$\dot{Q}in = \dot{m}_{wf2} \times (h_3 - h_{2a}) \tag{3.4}$$

$$\dot{W}turbine = \dot{m}_{wf2} \times (h_3 - h_{4a}) \tag{3.5}$$

$$\dot{W}pump = \dot{m}_{wf2} \times (h_{2a} - h_1) \quad (3.6)$$

$$\dot{W}net = \dot{W}turbine - \dot{W}pump \quad (3.7)$$

$$\eta cycle = \frac{\dot{W}net}{\dot{Q}in} \quad (3.8)$$

The equations are applied for three types of engines, three different evaporator pressures and the candidate working fluids to distinguish the performances and the thermal efficiencies for simple ORC.

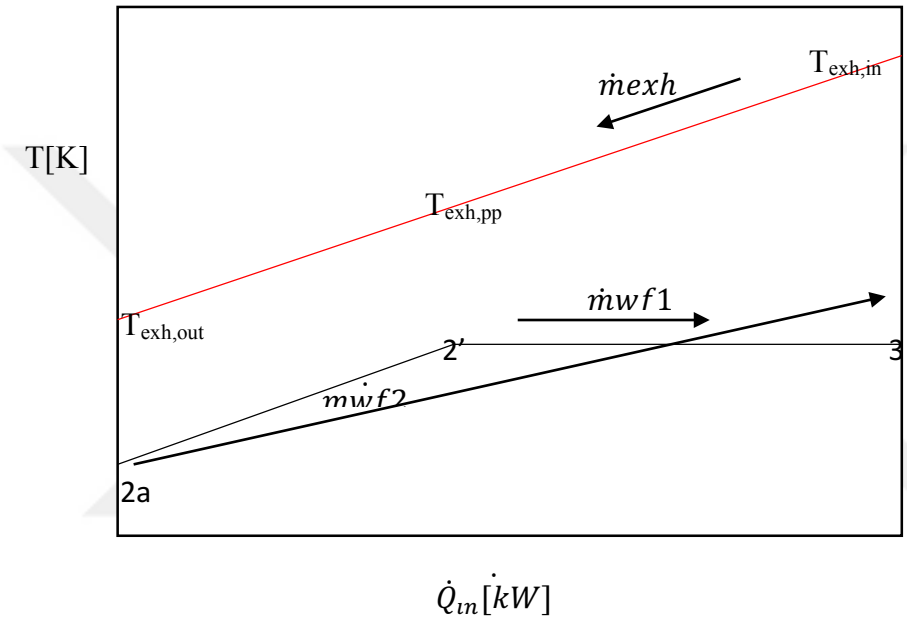

Figure 3.4. T-$\dot{Q}$ diagram of the evaporator for a ORC heated by engine exhaust gases

3.2.2. The Regenerative Organic Rankine Cycle

The idea behind the Regenerative Organic Rankine Cycle (RORC)is to develop thermal match using the residual heat from the exit of the turbine or expander to preheat the working fluid. Theoretically, the RORC is akin to the SORC except for the addition of a heat exchanger located after the turbine. The application of RORC is not only beneficial to increase the thermal match, but also helps to diminish the thermal drain in the condenser (Peris et al., 2013).

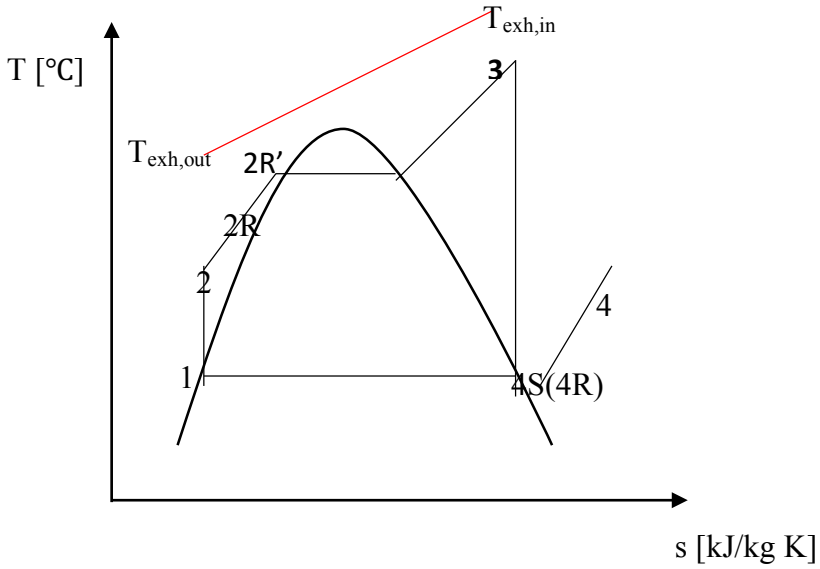

Figure 3.5. T-s Diagram of the Regenerative Organic Rankine Cycle

The equations applied on the former section are adapted to RORC with minor changes.

Process 1-2s: The compression process is same as the SORC. The pump work is forecasted by the same equation on the previous design.

Process 2-2R: The working fluid, compressed by the pump is heated up in the heat exchanger at the constant evaporator pressure.

Process 2R-2R': Inside the evaporator, the working fluid is kept heating by the exhaust gas of the diesel engine. The state 2R' represents the saturation point of the organic working fluid.

Process 2R-3: The circulating organic fluid exchanges heat with the high temperature heat source which in this case the exhaust gases of the DE.

Process 3-4-4s(4R): The expansion process in the turbine takes place. The generated work is calculated with the 5th equation.

Process 4-4s(4R): The high temperature and low pressure working fluid in the form of the superheated vapour is cooled down in the heat exchanger while, it heats up the the compressed liquid.

Since for the sake of the system, the state 4S is estimated equal to the 4R.

$$h_{2R} - h_2 = h_4 - h_{4R} \quad (3.9)$$

Process 4s(4R)-1: The organic working fluid discharges heat to the sink in order to regain the initial conditions.

It is deliberated that the regenerative heat exchanger demands a $\Delta T_{approach} = 15\,K$. Furthermore, the type of the heat exchanger is considered as counter flow. With regard to these hypothesis, the temperature at the outlet of the heat exchanger can be calculated:

$$T_{4R} = T_2 + \Delta T_{approach} \tag{3.10}$$

The second assumption is made to adjust the state after the regeneration process. This state is assumed as equal to the isentropic state after the turbine in order to obtain relevant results.

Equivalent to the SORC, first the energy balance inside the evaporator is practised. Therefore, the same procedure is followed in order to obtain and compare the the efficiency values in terms of working fluid and DEs.

3.2.3. The Pre-Heating and Regenerative Organic Rankine Cycle

The third configuration consists of the combination of the pre-heating and regeneration processes. The hypothesis of the Pre-Heating ORC is to employ the engine jacket cooling water to partially heat up the circulating working fluid. While, the water is cooled from 90℃ to 80℃, the temperature difference between the water outlet and the working fluid outlet is defined as 15K ($\Delta T = 15K$). In addition, the mass flow rate of the water is also assumed 1 kg/s. The Pre-Heater is chosen equally to the regenerative which are both counter flow type heat exchangers.

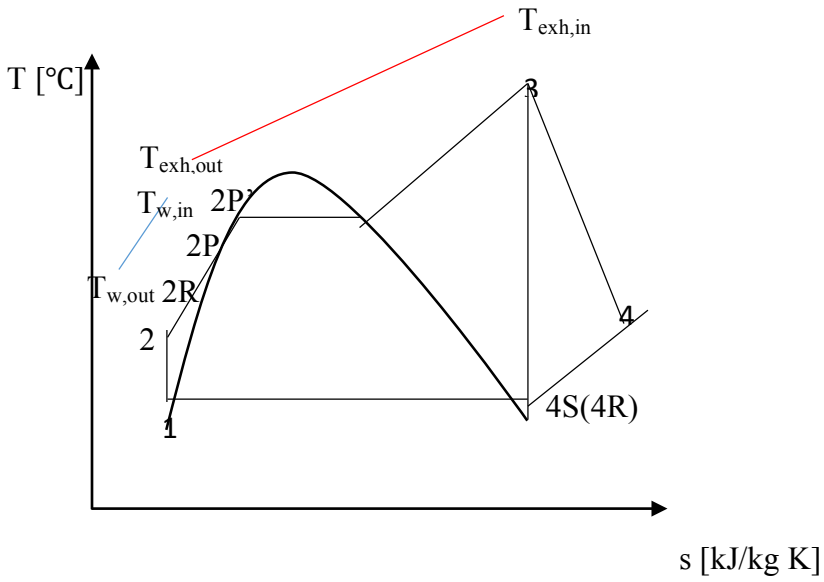

Figure 3. 4. T-s Diagram of Pre-Heating and Regenerative Organic Rankine Cycle

Inside the Pre-Heater, the mass flow rate of the organic fluid is obtained from the 3.11th equation:

$$\dot{m}_{wf} = \frac{\dot{m}_{water} \times Cp_{water} \times (T_{water,in} - T_{water,out})}{(h_{2p} - h_{2R})} \qquad (3.11)$$

If the acquired $\dot{m}wf$ does not satisfy the cycle conditions, the second mass flow rate of the working fluid is calculated from the energy balance inside the evaporator.

After, reaching the accurate $\dot{m}_{wf}$, the same procedure as the previous sections continues to determine the efficiency and performances.

Consequentially, the ORC is an adjustable power generation tool due to its easy modification. Three versatile designs are adopted to the waste heat recovery application. With regard to the flexibility and simplicity, ORC is widely used for waste heat recovery industry (Daccord et al., 2013). In the present work, the friction-heat losses in the evaporator and condenser are neglected.

The reason why the regenerative and pre-heating and regenerative configurations are employed is to reach high efficiencies. In terms of RC, two approaches are proposed to be risen the efficiency on the cycle. The first is to decrease the condenser temperature. However, it does not seem possible due to the fact that the temperature cannot be shrank

below the ambient temperature (Cengel & Boles, 1994). Whilst, the inlet temperature of the turbine can be raised.

The most appropriate approach to comprehend the differences between the Conventional and the Organic Rankine cycle is to compare the working fluids in terms of a saturation curve. Since, the main dissimilarity between two cycles is the circulating organic retardant. Figure 2.1 illustrates, water is a wet fluid due to its negative saturation curve (Chen et al., 2010).

3.3. Design and Simulation

3.3.1. Design and Simulation of the Generators and Organic Rankine Cycle

On the previous sections the importance of Waste Heat Recovery with Organic Rankine Cycle was explained broadly. In this part, the design parameters, the application of Matlab and Refprop will be discussed in detail.

In this study, three different ORC configurations are to be simulated using Matlab. Hence, the thermodynamic equations of the three designs are developed in order to compare the performances with the different working fluids at different operating conditions (Guide, 1998; Lemmon, Huber, & McLinden, 2002).

Since, the one of the fundamental targets of this research is to define the behaviours of the diesel generators with the implementation of the ORC systems, three main diesel generators are going to be applied to be implemented the ORC throughout this study. The analysis of the engines is mostly relied on the exhaust gas temperatures. Therefore, the exhaust gas temperature at the outlet, mass flow rate and the specific heat of the exhaust gas are the input data for the model. As a consequence of simulating three engines, it will be fairly easy to comprehend the differences between the engine types.

In addition to the RC configurations and the engine types, eight dissimilar organic fluids, which belong to five different chemical classes, will be investigated. On the antecedent sections the working fluid procedure was defined fully.

The last parameter to build the simulation model, the ratio between the evaporator pressure and the critical pressure of the working fluid is going to be one of the variables. Within the iteration process, the most suitable evaporator pressure is going to be obtained

for the sake of the cycle. The further calculations are going to be depended on this pressure. Meanwhile, the temperature at the inlet of the turbine is also relied upon the evaporator pressure. Thus, the determination of evaporator pressure plays a vital role for the simulation model.

In order to create a reliable engine-ORC model, the following assumptions are done;

- The specific heat of the exhaust gas is calculated as 1.10 [kJ/kg K].
- For three configurations, state 1 is considered fixed. The condenser temperature is set to 35 ℃. Therefore, the properties of the state 1 are designated via the assumption.
- The isentropic efficiency of the pump is chosen as 75%.
- The isentropic efficiency of the turbine is set to 80% (Vaja & Gambarotta, 2010).
- The minimum temperature difference at Pinch Point to meet the gas and fluid heat exchanger performance is defined as 30 K. ($\Delta T_{pp} = 30\ K$)
- For the regenerative case, $\Delta T_{approach} = 15\ K$ is taken in order to satisfy the demand of the heat exchanger.
- The pressure losses in the heat exchangers and pipes are neglected for the study.
- For all candidate working fluids, dry expansion is assumed. The reason why is to prevent the liquid droplets and damages on the turbine blades.

3.3.2. Methodology and Design Model

The methodology of this study relies on the analytical calculation of the specified configurations with different working fluids and the integration on the diesel engines. For the sake of the thermodynamic calculations, the relevant assumptions were stated clearly on the foregoing section.

The waste heat recovery model with Organic Rankine Cycle simply aims to comprehend the behaviour of the cycle with different working fluids. Moreover, in order to obtain higher efficiencies on the cycle, three different configurations are endeavoured through the simulation.

Before creating the simulation model, one reference working fluid, R-134a was chosen and the set of the thermodynamic equations for the first diesel engine was calculated. In Appendix A, the three cycle configurations with R-134a are presented

plainly with regard to thermodynamic states. The scheme of the study can be summarised as,

- After the accurate calculations, the creating of the Matlab Model for the three configurations
- The application of the Matlab Model on three different engines
- Analysing the result and designate the most applicable working fluid with the configuration and distinguishing the difference between the engines with regard to the mass flow rate and the temperature of the exhaust gas.

Throughout the study, the candidate working fluid properties are depicted in Table 3.1. The thermodynamic properties, safety class and ODP and GWP value are portrayed n details.

The engine characteristics are also summarised in Table 3.2. As it was stated in the previous sections, the engine data are relevant and the main inputs for study.

Table 3.1. The candidate organic working fluids

Working Fluid	**Chemical Class of the Fluid**	**Chemical Formula**	**The Shape of the Slope**	**Critical Temperature [*K*]**	**Critical Pressure [kPa]**	**Ozone Depletion Potential [ODP]**	**Global Warming Potential [GWP]**	**Safety Class**
R-134a	HFC	CH_2FCF_3	Isentropic	374.21	4059	0	1430	B1
R-245fa	HFC	$CF_3CH_2CHF_2$	Isentropic	427.16	3651	0	1030	B1
R-1234yf	HFO	CH_2=$CFCF_3$	Dry	367.85	3382	0	<4.4	A2L r
R-1233zd(E)	HFO	(E)CF_3-CH=CCIH	Dry	438.75	3570	0.00034	7	A1
R1234ze-E	HFO	CHF=$CHCF_3$	Dry	382.51	3634	0	6	A2L/ low flammability
Cyclohexane	Alkane	C_6H_{12}	Isentropic	553.6	4080	0	Very low	Highly Flammable
D4	Siloxane	C_8-H_{24}-O_4-Si_4	Dry	586.5	1332	0	Small(Tian et al., 2017)	Flammable(Falano, Jeswani, & Azapagic, 2014)
Ethanol	Alcohol	C_2H_6O	Wet	514.7	6268	-79.8 to -32(Falano et al., 2014)	-253(Falano et al., 2014)	Severe Flammable

Table 3.2. The Information of the Generators, in IZTECH Campus

Type	**Brand**	**Power**	**No cylinders**	**Volume (L)**	**Bore-Stroke (mm)**	**Compression Ratio**	**Speed/ frequency**	**Exhaust Gas Outlet Temperature (℃)**	**Exhaust Gas Outlet Volume Flow Rate**	**Exhaust Gas Outlet Mass Flow rate (kg/s)**
1st Group	TEKSAN	440 kVA	6 - in line	12.7	130 - 160	16.3 : 1	1500 rpm/ 50 Hz	509	32 kg/min	0.533
2nd Group	TEKSAN	1650 kVA	12 - V Type	45.842	160-190	13: 1	1500 rpm/ 50 Hz	455	320 m3/min	2.595
3rd Group	TEKSAN	550 kVA	6 - in line	12.7	130 - 160	16.3 : 1	1500 rpm/ 50 Hz	563	36 kg/min	0.6

3.4. REFPROP Database

The principal aim of the work is to describe the characteristic of the working fluids, to investigate the applicability with the prescribed systems. The easiest way to implement the thermodynamic properties of the working fluids is to apply REFPROP database/program (Lemmon et al., 2002).

Despite the many other available fluid databases, REFPROP, developed by the NIST (National Institute of Standards and Technology, USA) is chosen for the study. The name of the program comes from the acronym for REFerence fluid PROPerties. The thermodynamic tables and the characteristic of the hydrocarbons, widely used fluids and mixtures in the industry and refrigerants can be obtained easily. The program consists of three models for the thermodynamic properties of pure fluids; equations of state explicit in Helmholtz energy, the modified Benedict-Webb-Rubin equation of state and an enlarged corresponding states (ECS) model. Mixture calculations utilise a model that applies mixing rules to the Helmholtz energy of the mixture components. Viscosity and thermal conductivity are modelled with fluid-specific correlations, and ECS method or in some cases the friction theory method is applied.

Routines are supply to calculate thermodynamic properties at a given (T,h,s) state. One of the reasons to be chosen REFPROP is the compatibility with the Matlab. The function 'refprop.m' is use to call the properties of the organic fluids on the Matlab. The function supplies the required fluid properties given a state point (defined by two specified and known state properties) and given the pure fluid or the fluid mixture composition (if the substance is not a pure fluid) (Lemmon et al., 2002).

3.5. The Simple Organic Rankine Cycle

The fundamental design criteria is the pressure ratio between critical pressure of the working fluid and the evaporator pressure. In order to acquire the optimum evaporator pressure, seven different ratios are tried which range from 50% to 95%. The wide range of the pressure ratios are applied on the model to distinguish the manner of the working fluids on the cycle regarding the evaporator pressure. In accordance with the evaporator pressure, the highest temperature of the cycle is adjusted. In Appendix A, a detailed

SORC with the reference working fluid, R-134a, on the first engine calculation is indicated extensively. The importance of the peak temperature of the cycle directly affects the working conditions. In the following chapter, the effects and the results of the highest temperature of the cycle is going to be explained in details.

On the Matlab code, the condition of the state 1 is given extensively. With regard to the specified temperature, 308 K, the pressure, enthalpy and the specific volume of the organic fluid are calculated. Through the Matlab code, all the states and the thermodynamic equations are articulated in details. Furthermore, the entire assumptions are taken into account cautiously.

The model starts with the 50% pressure ratio with the reference working fluid on the SORC. Matlab Model starts requesting the critical pressure of the working fluid. Within the help of the Matlab function 'refprop.m', the fluid properties on the demand of the state are easily called on the script. Refprop is a program and can be used as a database for ascertain the organic fluids' thermodynamic properties. The function 'refprop.m' works in this way, at a given state, if the two properties are known, the required feature can be calculated.

While the Matlab is on the process, the isentropic efficiencies of the pump and the turbine are provided as an input. Before the calculation of the mass flow rate of the working fluid, the pinch point is calculated ($T_{exh,pp} = T_{2'} + \Delta T_{pp}$). The location of the pinch point is vital for the calculation of the mass flow rate of the organic fluid. The one of the assumptions that is made is the location of the pinch point. Regarding the first premise, the pinch point is assumed to be occurred on the saturation liquid point. After the first energy balance, the outlet temperature of the exhaust gas is calculated. If the assumption of the location of the pinch point is correct, the mass flow rate of the working fluid should satisfy the equation set. Otherwise, a new energy balance must be done to calculate the accurate mass flow rate of the working fluid.

Due to the pinch point between the exhaust gas and the SORC, the energy balance inside the evaporator assists the adjusting the working fluid's mass flow rate. After obtaining the mass flow rate, the outlet temperature of exhaust gas is calculated. The most crucial point after calculation of the outlet temperature of the exhaust gas, the accuracy must be checked. If the exhaust's outlet temperature is above the minimum temperature of the cycle, the calculated mass flow rate of the working fluid can be applied to reach the efficiency of the cycle. Otherwise, the second energy balance inside the evaporator

must be done to calculate the decent mass flow rate of organic fluid. After, prevailing the mass flow rate which satisfies the equation in terms of being above the minimum temperature of the cycle, the results are calculated with regard to the pump and turbine work and heat which is supplied from the exhaust gas.

The same procedure is applied on the three configurations and eight candidate working fluids with slight differences. Moreover, three diesel generators which are considered as the heat source for the waste heat recovery system are applied respectively. The results are going to be defined comprehensively in the subsequent sections.

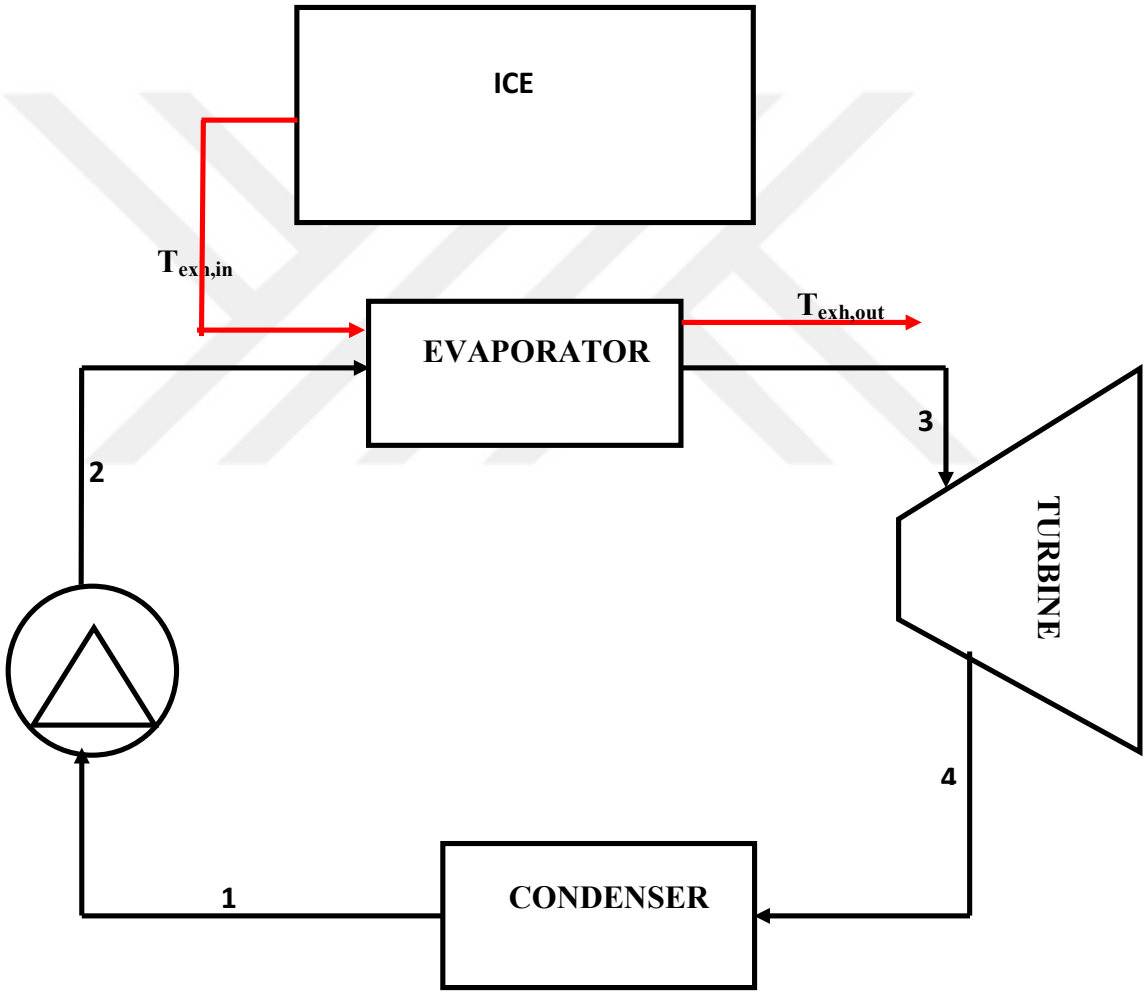

Figure 3. 5. The SORC system layout

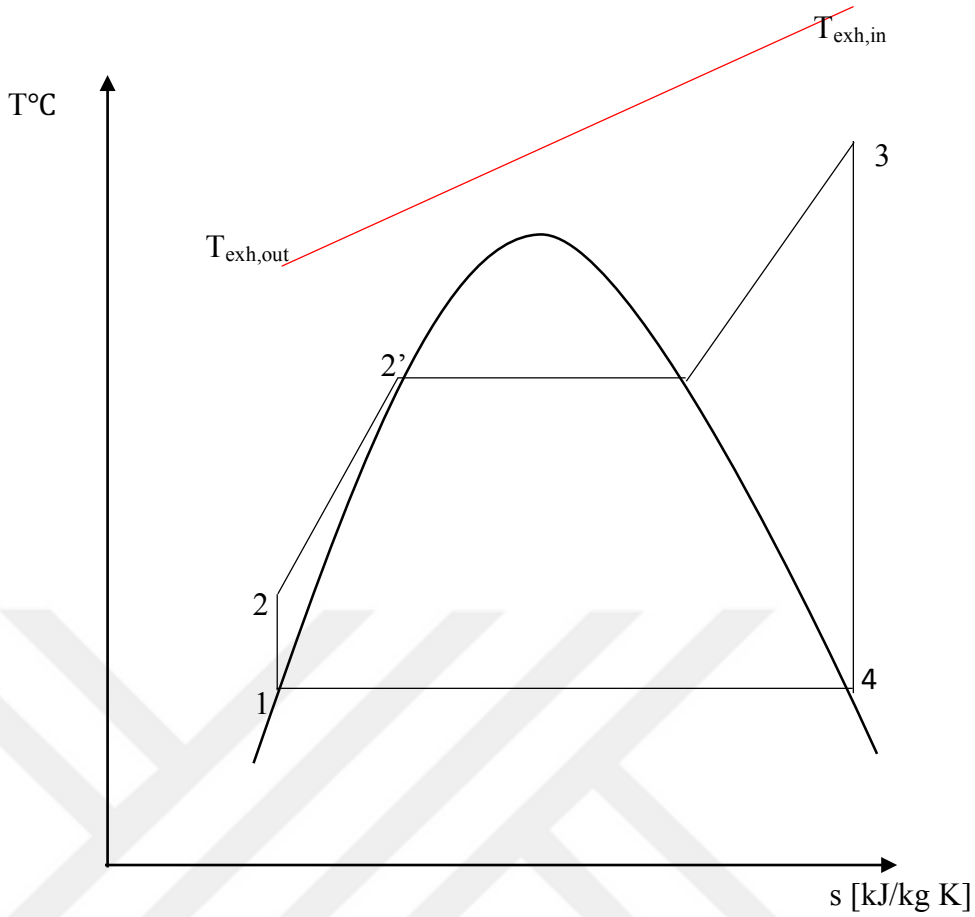

Figure 3. 6. The T-s diagram of SORC

3.6. The Regenerative Organic Rankine Cycle

The second configuration is slightly dissimulated from the SORC. The dominant difference is an additional component which is a heat exchanger. It is implemented right after the turbine. The primary reason adding the heat exchanger is to increase the overall thermal efficiency on the cycle. It is assumed as a counter flow heat exchanger. The working principle is to heat up the circulating working fluid before entering the evaporator. The residual heat from the exit from the turbine heats the working fluid which comes from the pump. Essentially, before entering the evaporator, the working fluid has already reached at a certain temperature. The temperature leads to accomplish higher temperature in the limits of the evaporator pressure inside the evaporator. Additionally, the additional heat exchanger is also beneficial to decrease the thermal drain in the condenser. In Appendix A, the thermodynamic equations of the RORC configuration with

R-134a can be seen plainly regarding the first engine. The states and assumption are indicated distinctly.

Apart from the calculation of the regenerative states, the rest of the calculations are same as the SORC. For the RORC configuration, another Matlab code was constituted with the 'refprop.m' function. The RORC is endeavoured with the three engines and eight working fluids. The results are illustrated in the upcoming section.

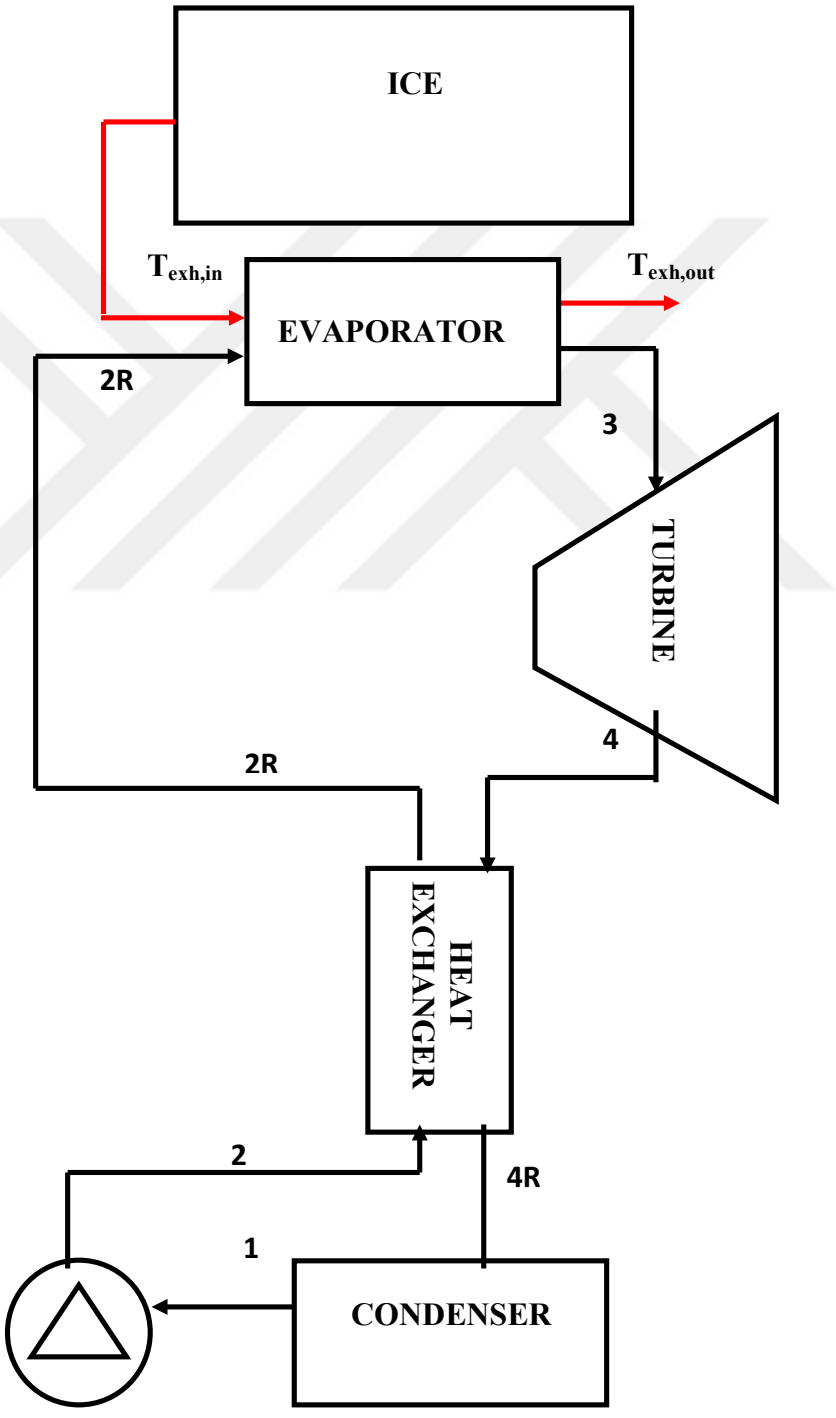

Figure 3. 7. The RORC system layout

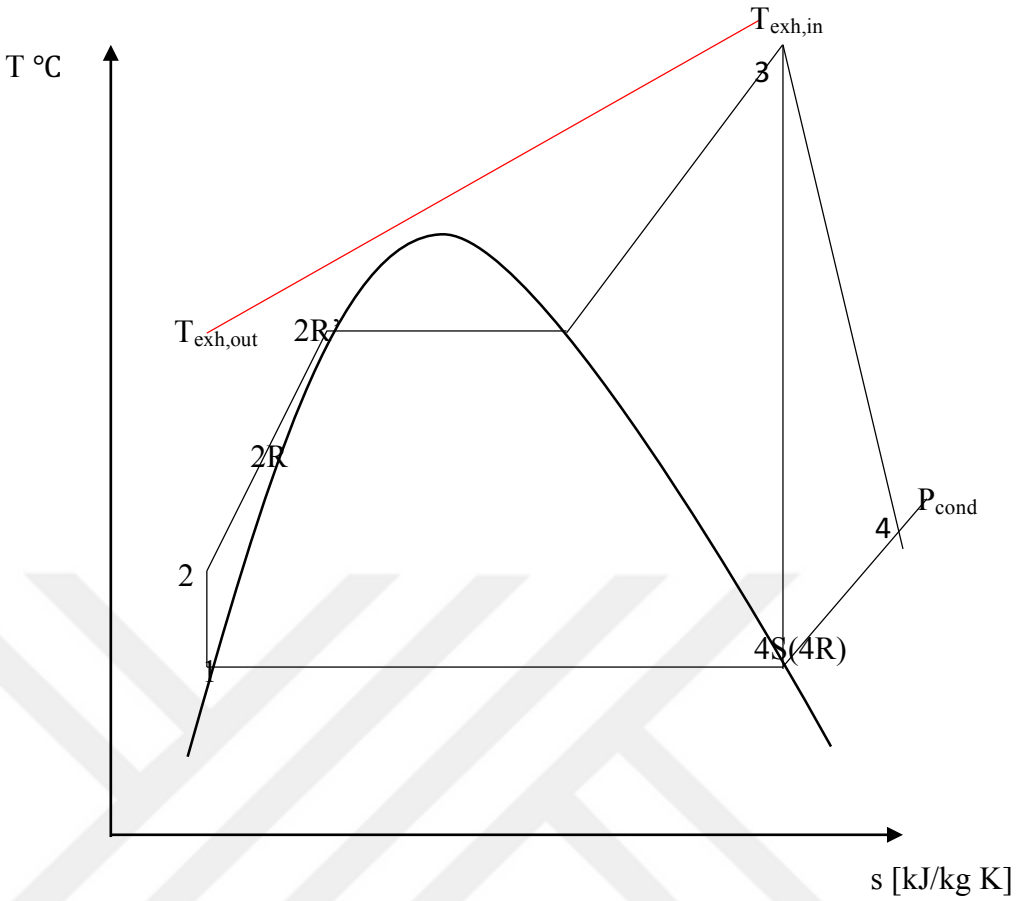

Figure 3. 8. T-s diagram of RORC

3.7. The Pre-Heating and Regenerative Organic Rankine Cycle

The third configuration is an alliance of the pre-heating and regeneration processes. Theory behind the application of pre-heating is to introduce the jacket cooling water as a heat source for the Rankine Cycle. The idea of the pre-heating is akin to the RORC. Instead of using the waste heat from the exit of the turbine, the heat up process is done by the jacket cooling water. While the water is cool downed from 90 ℃ to 80 ℃, the circulating working fluid is received heat from the process. As the component, a counter flow heat exchanger is assumed as the pre-heater. The location of the pre-heater is just before the evaporator. The heat exchanger for the regeneration is located as the RORC case. The concept of applying regeneration part to the pre-heating is to try to obtain higher thermal efficiency with two different heat sources.

Throughout the calculations, one energy balance is done inside the pre-heater. The mass flow rate of the working fluid is acquired and the accuracy of the assumption on the mass

flow rate of the cooling water is checked. In Appendix A, a detailed analysis of the PRORC' states are presented.

The rest of the calculations' procedure is equal to the other two configurations. A specific Matlab Code with the function of 'refprop.m' is also created for the PRORC.

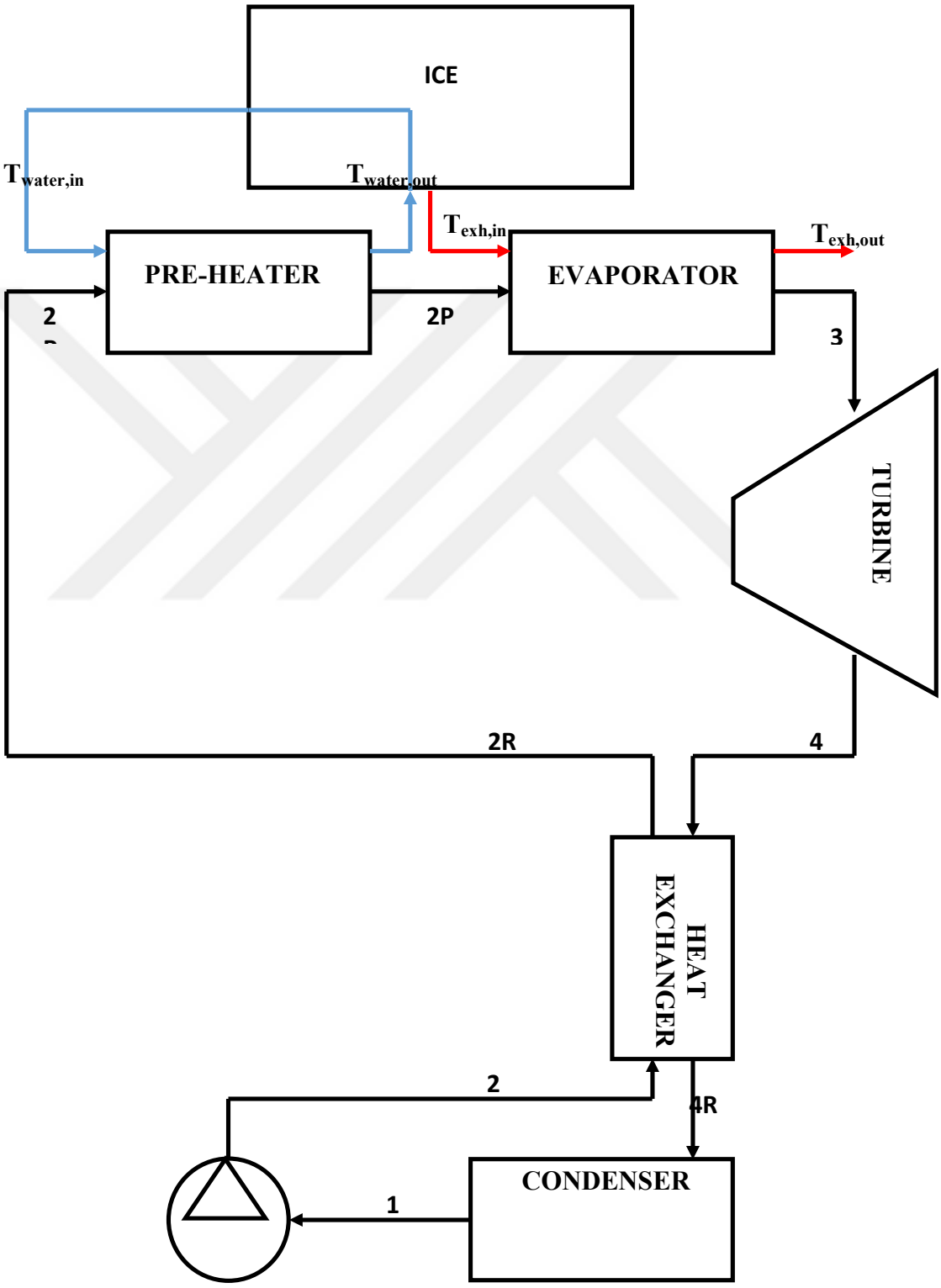

Figure 3. 9. The PRORC system layout

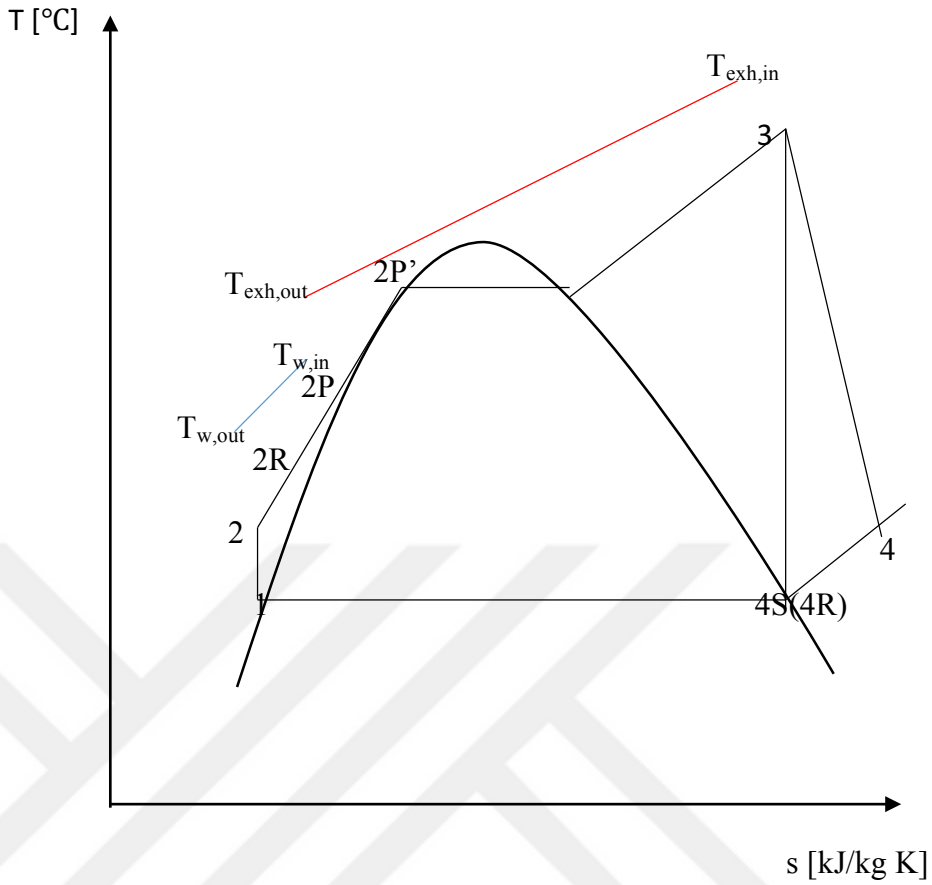

Figure 3. 10. T-s diagram of PRORC

3.8. MATLAB Algorithm

The aim of the study is to investigate the ORC configurations with 8 different working fluids and implementation of the systems on the three diesel engines. In order to examine the possibilities, the numerical method has chosen for the methodology. The simulation model is summarised on the below.

The first inputs are the critical pressure of the candidate working fluid and the pressure ratio between the evaporator and the critical pressure of the applied working fluid. During the Matlab simulation for the three cases regarding the engine types, the isentropic efficiencies of the turbine and the pump.

MATLAB Algorithm

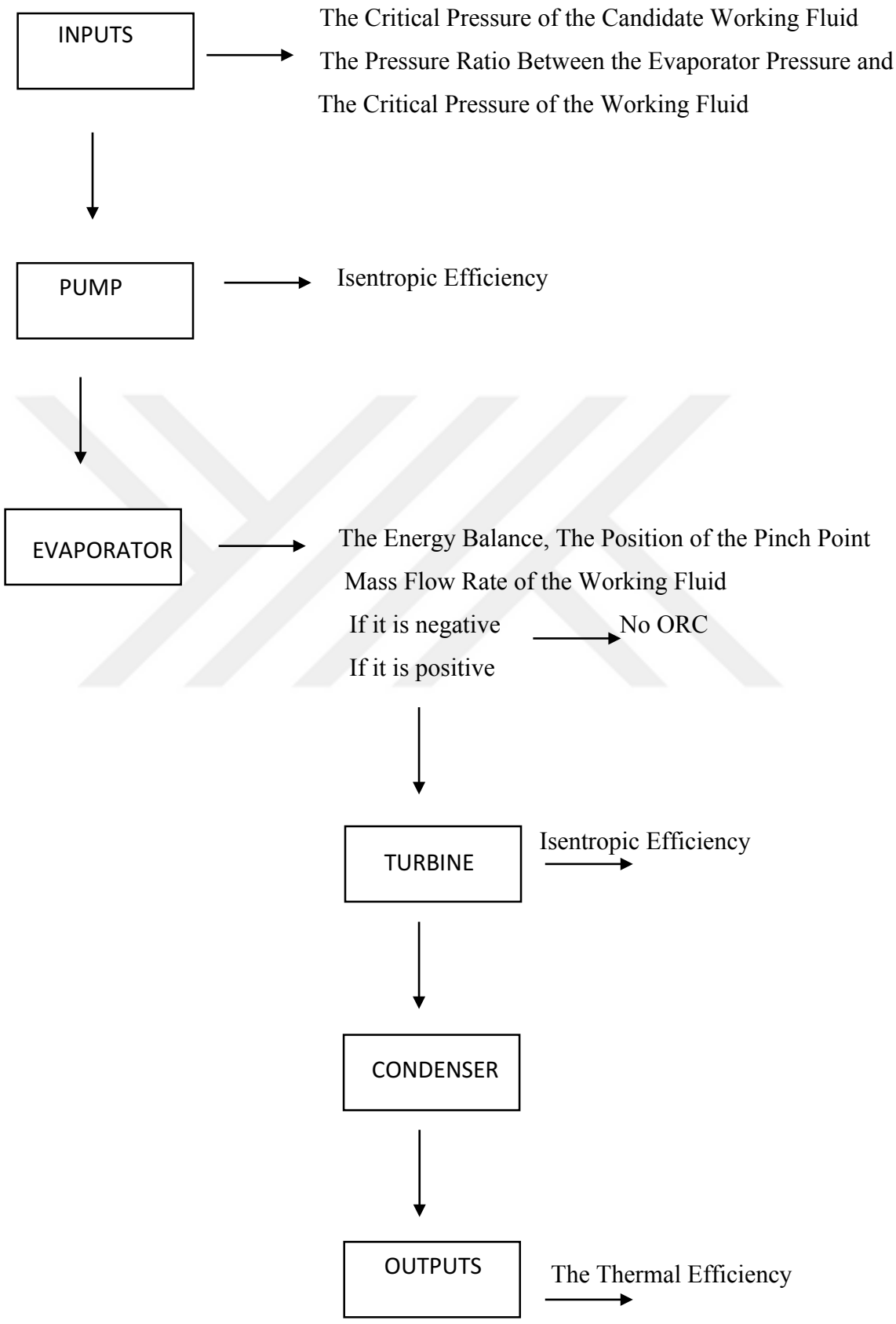

CHAPTER 4

RESULTS AND DISCUSSION

The results will be evaluated in three different sections with respect to the engine type.

4.1. The First Engine Application

The first engine is a six cylinder in line and turbocharged diesel engine. The power of the engine is 550 kVA and located in the Medical Transformer Building in IZTECH campus in Izmir. The exhaust temperature of the engine is 509 ℃ and the mass flow rate of the exhaust gas is 0.533 kg/s. The calculated specific heat capacity is 1.10 kJ/kg K. The mass flow rate, temperature of the exhaust and the specific heat capacity are the fundamental inputs for the first application.

Respectively, the SORC, RORC and PRORC models are applied with the working fluids on Matlab.

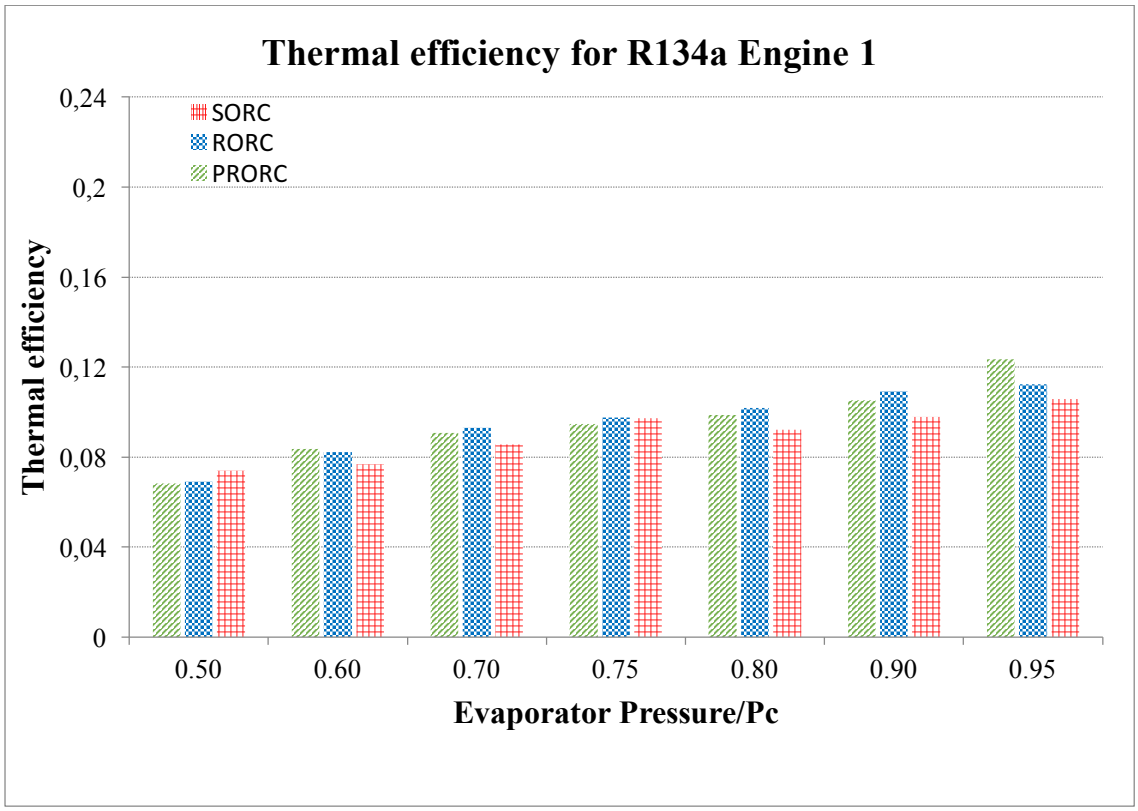

Figure 4. 1. Effect of evaporator pressure on thermal efficiency for R-134a for engine 1

Figure 4.1 illustrates the effect of the pressure ratio representing the pressure of the evaporator over the critical pressure on the thermal efficiency for the three RC configurations with the working fluid R-134a. The base calculation of the cycles is endeavoured with R-134a, since it is one of the most common organic fluids for waste heat recovery applications. The characteristic of the fluid was given in foregoing sections. The critical pressure of R-134a is 4059.3 kPa.

On the SORC case, firstly 0.50 percent ratio is applied to designate the evaporator pressure for the cycle. In accordance with the obtained evaporator pressure, the thermodynamic states are calculated. The first energy balance inside the evaporator is applied to determine the mass flow rate of the circulating organic fluid.

In this case, according to the calculations, the first mass flow rate did not fulfil the thermodynamic equations. Since, the calculated outlet temperature of the exhaust is lower than the minimum temperature of the cycle. At the same time, the pinch point is occurred before the saturation line. Obtaining the accurate mass flow is vital to reach the appropriate pump and turbine work and the heat input.

While the pressure ratio/critical pressure rises, the thermal efficiency of the cycle increases directly proportional. The evaporator pressure is closer to the critical pressure of the R-134a, the thermal efficiency of the SORC is escalated. The thermal efficiency increases from 7.4% at a ratio of 0.5 to a value of 10.6% at the maximum pressure ratio. The only problem with working at high pressures is to control the operating conditions in the turbine. In order to prevent the side effects of the high pressure, the convenience of the turbine should be verified.

For the RORC it can be observed that the thermal efficiency increases with the increase of evaporator pressure over the critical pressure from 6.9% to 11.2%. In comparison to the SORC, the general tendency on the thermal efficiency on the RORC at higher pressure ratios is delicately higher. The reason behind is the additional heat exchanger as regeneration component. On the contrary, while the pressure ratio between the evaporator and critical pressure of R-134a is 50%, the thermal efficiency of the SORC is slightly higher than the RORC's efficiency, 7.40%. This can be due to where the minimum temperature occurs in the cycle. Throughout the RORC calculation, the pinch point is assumed at the saturation liquid point. The most significant point can be said that, the

pinch point occurred on the left side of the saturation point. In order to obtain the relevant mass flow rate of the working fluid, the second energy balance is calculated inside the evaporator. Instead of applying the pinch point, the minimum temperature of the cycle is applied to stay in the cycle limits.

The PRORC is the third configuration shown in Figure 4.1. Similar to the RORC, the increment with the ascent on the pressure ratio between the evaporator and critical can be seen from 6.9% to 12.3%.

It can be seen in Figure 4.1 that the peak efficiency occurs with the PRORC configuration with the highest pressure ratio between the evaporator and the critical pressure of the R-134a with respect to 12.3%. This value is an agreement with previous studies for the waste heat recovery application with R-134a (Peris et al., 2013; Vaja & Gambarotta, 2010).

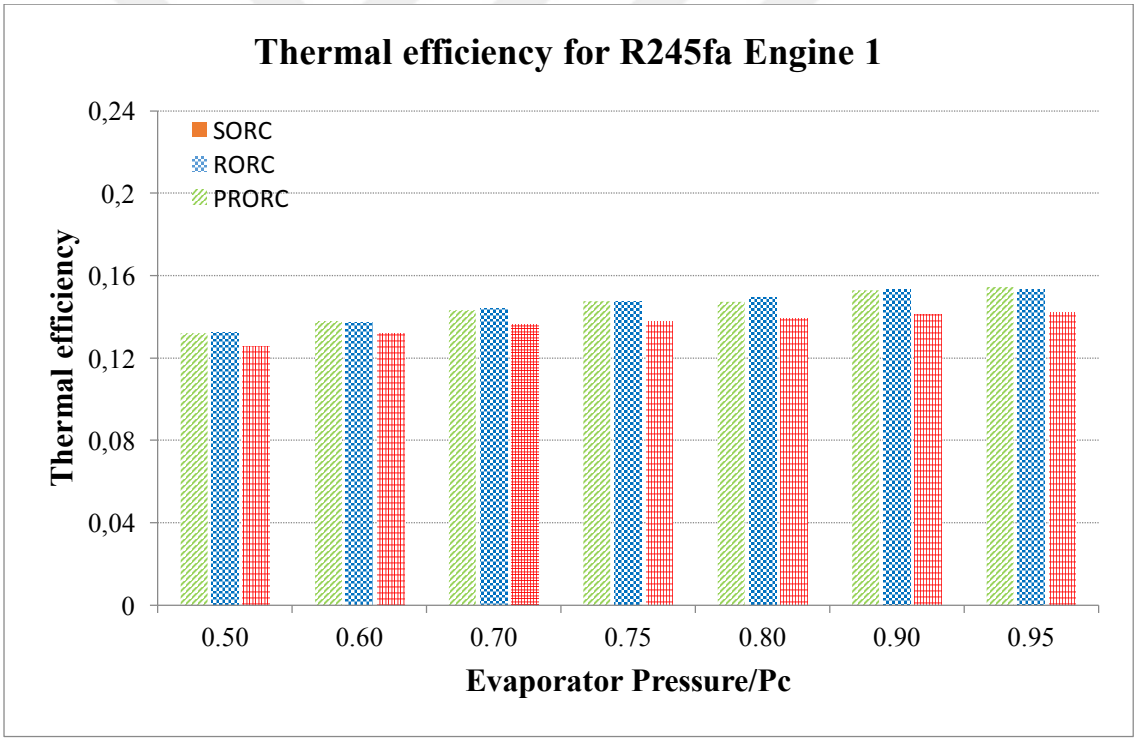

Figure 4. 2. Effect of evaporator pressure on thermal efficiency for R-245fa for engine 1

Figure 4.2 depicts the results for the three cycles with the second candidate working fluid. R-245fa is an organic fluid from the HFC chemical class. The critical pressure of R-245fa is 3651 kPa. The dominant characteristic of R-245fa is to have zero Ozone Depletion Potential, whilst the Global Warming Potential of the fluid is over the

limits. It was stated in the previous chapter that the usage of HFC is intended to be decreased (M. Protocol, 1987). In order to ban HFCs, alternative working fluids are under investigation.

In the SORC, the minimum thermal efficiency is just above the 12.5% at the lowest pressure ratio of the evaporator and the critical pressure of R-245fa. Within the ascent on the ratio between the evaporator and critical pressure of R-245fa, the thermal efficiency rises until reaches around 14.22%. In comparison to R-134a on the SORC, the lowest thermal efficiency is obtained at 50% ratio and the value is around 7.4% which is fairly lower than R-245fa's case. The greatest efficiency of the SORC with R-245fa is obtained as 14.22% at the 95% pressure ratio. The highest efficiency for SORC with R-134a is approximately 10.5%. However, the lowest thermal efficiency with R-245fa, 12.53%, is fairly higher than the highest thermal efficiency, 10.56%, for R-134a for SORC.

In comparison to the application of R-134a, the higher thermal efficiencies are adjusted with R-245fa at the all pressure ratios. Therefore, R-245fa is considered more suitable than R-134a for the medium temperature exhaust gases.

During the calculation, the second energy balance is also applied for this case.

The RORC design results start with 13.21 % thermal efficiency, end with 15.33%. The comparison between the R-134a and R-245fa simulation results at 50% pressure ratio between the evaporator and the critical pressure, can be summarised that R-245fa is almost two times greater than the R-134a case. Even the critical pressure of R-245fa is lower than R-134a, the reason why the thermal efficiency is higher with R-245fa is that this organic fluid is more compatible with waste heat recovery applications with medium and high temperatures. Regarding the studies of (Quoilin et al., 2013), R-134a is mostly used for moderately low temperature WHR systems such as geothermal.

The highest efficiency is achieved with the PRORC case at 95% pressure ratio between the evaporator and critical pressure, with a value of 15.42 %. Additionally, the highest thermal efficiency for R-134a is also obtained on the PRORC. At the lowest pressure ratio of evaporator and the critical pressure of R-245fa is 13.21%, at the highest ratio is adjusted as 15.42%. In R-134a application, the highest thermal efficiency is 12.35%. Even the obtained highest thermal efficiency with R-134a is lower than R-245fa case.

Even though the difference between the 50% and 95% is not enormous, in general the efficiency is considerably higher than the R-134a case.

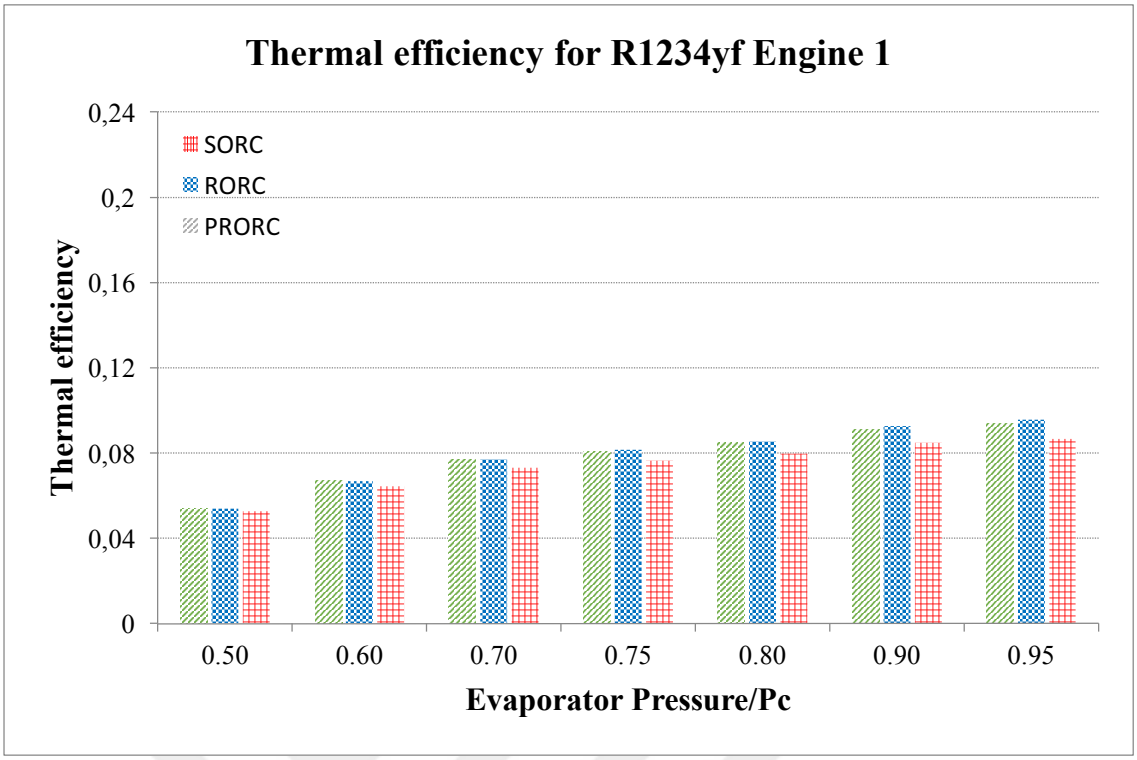

Figure 4. 3. Effect of evaporator pressure on thermal efficiency for R-1234yf for engine 1

The third candidate working fluid is named as R1234yf. The three Rankine cycle configurations are evaluated with this working fluid. R-1234yf is not same as the foregoing two organic fluids. This working fluid is a member of the Hydrofluroroolefins (HFOs) chemical class. This chemical class is assumed as an alternative for HFCs. Since, the HFCs have a great value on GWP, HFOs do not have any side effects related to the global warming. The ODP and GWP values are taken into account, while the comparison is being done between the HFCs and HFOs.

With the SORC, the lowest thermal efficiency is obtained at the lowest pressure ratio between the evaporator pressure and the critical pressure of R1234yf with respect to 5.27%. The maximum thermal efficiency (9.57%) occurs at the maximum pressure ratio. In comparison to the R-245fa case, the thermal efficiency is relatively low in R-1234yf case. The greatest obtained thermal efficiency with R-1234yf is 8.66%. On the contrary, the lowest thermal efficiency of R-245fa are fairly higher than the highest thermal efficiency with R-1234yf, 13.21% and 9.57% respectively.

The critical pressure of R-1234yf is 3382.2 kPa which is slightly lower than first two working fluids. R-1234yf is considered as the alternative for R-134a (Jarall, 2012). The general increase trend on thermal efficiency in Figure 4.3 inclines with the increment of the ratio. However, the thermal efficiencies for the three configurations are below in contrast to the first two cases. While, the thermal efficiencies are calculating for the three designs the pinch point approach is applied. For all the cycles, the pinch point occurred before the saturation liquid point and the mass flow rate of the working fluid is calculated by the second energy balance.

For the RORC and PRORC cases with R-1234yf, the overall efficiencies are under the first two cases' results. The disposition for both cases tends to increase with the rise on the ratio. The peak efficiency is prevailed at 95% ratio of the evaporator and the critical pressure of R-1234yf on the RORC which is approximately 9.57%.

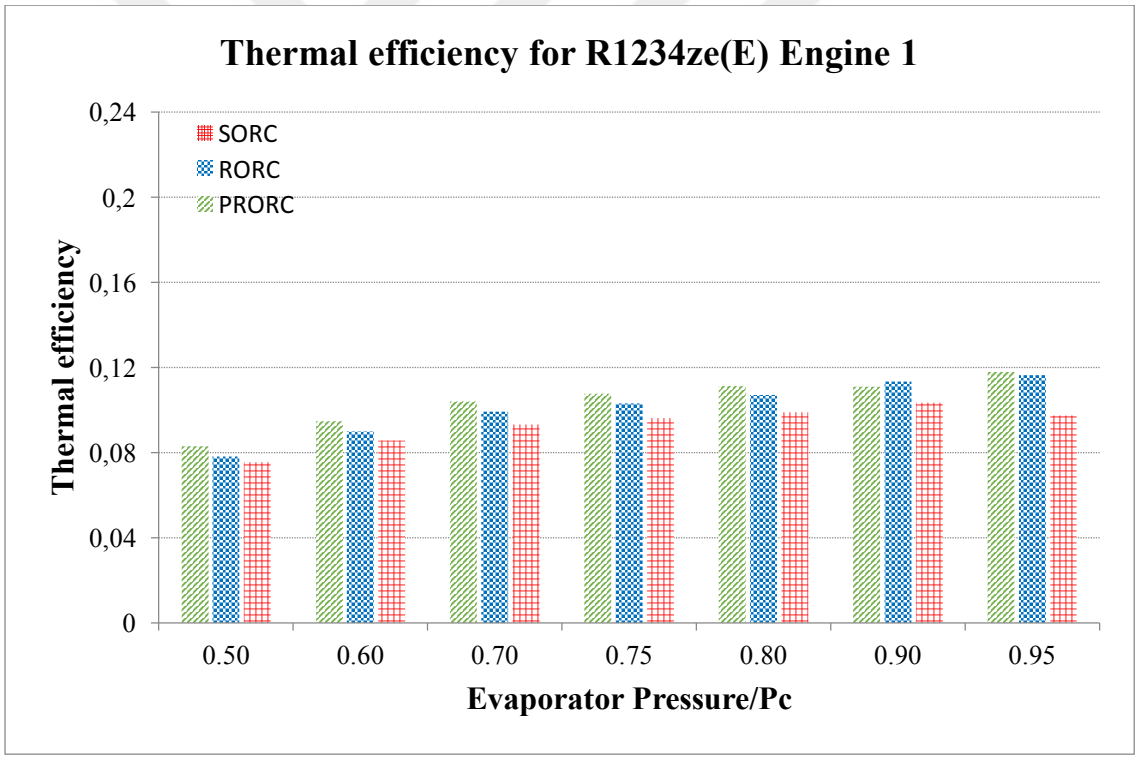

Figure 4. 4. Effect of evaporator pressure on thermal efficiency for R-1234ze(E) for engine 1

The fourth simulation model is applied with R-1234ze(E). The candidate working fluid is also identified as HFO. The characteristics of R-1234ze(E) are similar to R-1234yf. This working fluid has also zero ODP and more importantly almost zero GWP.

The critical pressure of R-1234ze(E) is 3634.9 kPa. In general, Figure 4.4 is akin to the previous figures. All of the cycles' trends are tended to increase with the ratio between the evaporator and critical pressure.

The highest efficiency is prevailed at 95% ratio on the PRORC configuration which just beneath 12%. Apart from 90% pressure ratio, on the rest of the six ratios PRORC design has the highest efficiency among the other two configurations. At the 90%, the RORC is somewhat above the PRORC 11.33%, 11.08% respectively. The lowest efficiency is not different from the previous cases. On the SORC while 7.5% is the smallest thermal efficiency for R-1234ze(E), 9.74% is the highest thermal efficiency under the same operating conditions. The general increase trend of the graph is akin to the previous cases with some fluctuations on the thermal efficiencies.

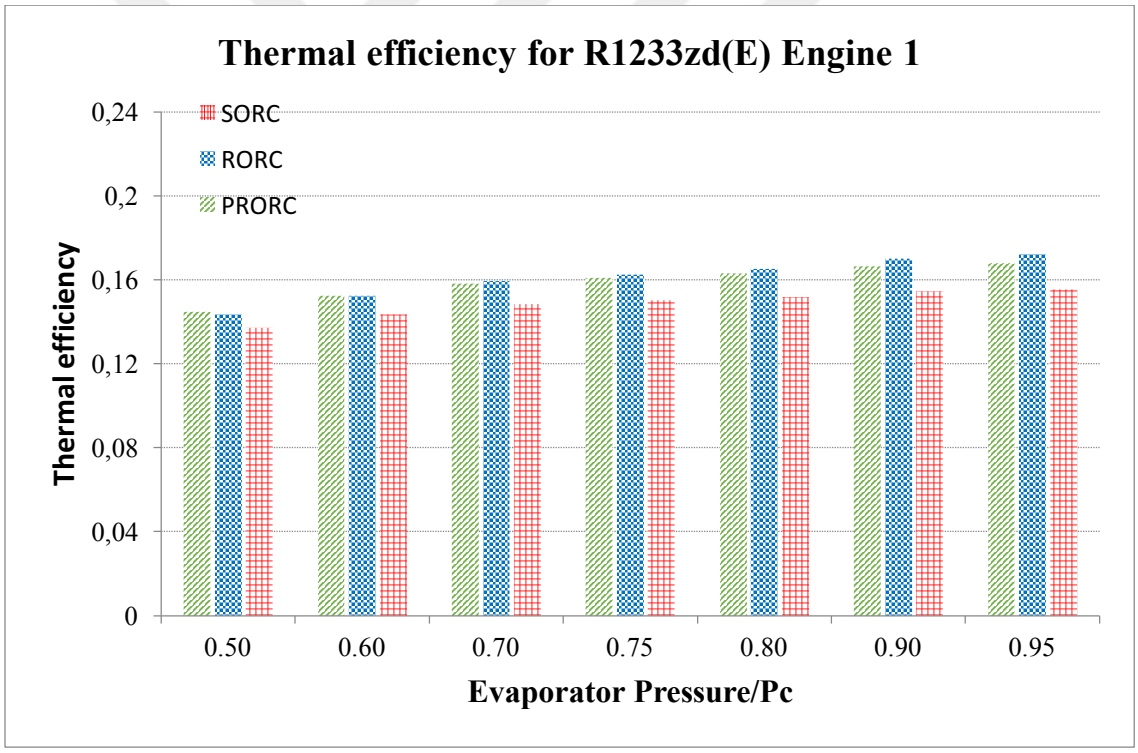

Figure 4. 5. Effect of evaporator pressure on thermal efficiency for R-1233zd(E) for engine 1

The fifth simulation represent the results with R-1233zd(E), shown in Figure 4.5 above. The chemical class of R-1233zd(E) is also HFO which is the fourth generation

working fluid. The most crucial feature of this working fluid is to have zero ODP and GWP similar to R-1234yf and R-1234ze(E). The critical pressure of the organic fluid is 3507.9 kPa. The critical pressures of the applied working fluids are fairly close to each other.

In general, the simulation results seem better than the previous working fluid applications. The SORC design starts with 13.72% thermal efficiency, and resulted around 15.58% thermal efficiency at the 95% pressure ratio between the evaporator and critical pressure of R-1233ze(E). At the 50% pressure ratio, the three configurations results are not different from each other. The lowest thermal efficiency is 13.72% on the SORC design. In the previous cases, the lowest thermal efficiency is also obtained on the SORC in different values. The first adjusted mass flow rate of R-1233zd(E) does not give the relevant result regarding the location of the pinch point. The outlet temperature of the exhaust gas is below the minimum temperature of the cycle. After application of the second energy balance, the the accurate mass flow rate is used for calculating the thermal efficiency.

The highest thermal efficiency for PRORC design is obtained on 95% pressure ratio with respect to 16.80%. The closest thermal efficiency with PRORC was adjusted with R-245fa at the highest pressure ratio value respectively, 15.42%. The other working fluid applications on PRORC are slightly lower than these values.

The RORC configuration simulation outcomes for R-1233zd(E) are substantially higher than the last four candidate working fluids. Until now, the greatest thermal efficiency on WHR with Rankine Cycle is obtained for medium temperature exhaust temperature with respect to 17.23%. The closest result is achieved with R-245fa, 15.33%. The importance of the acquiring the greatest outcome on the first engine application with R-1233zd(E) is to spread the usage of HFOs instead of HFCs. From the environmental point of view and considering environmental regulations, the outcome seems promising.

The PRORC design at 50% pressure ratio between the evaporator and the critical pressure of R-1233zd(E) results the highest efficiency with respect to 14.46%. The increase of the thermal efficiency continues linearly until the last value of the ratio. Even though two different heat sources are applied on PRORC configuration, the highest efficiency is obtained on the RORC layout.

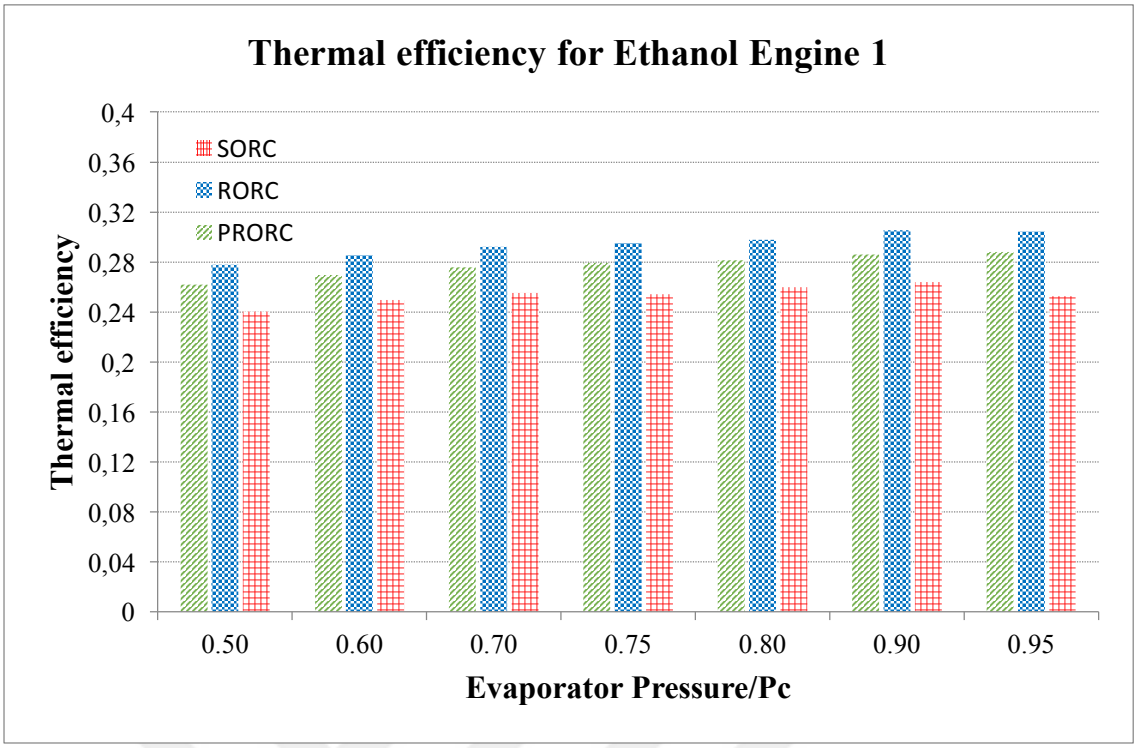

Figure 4. 6. Effect of evaporator pressure on thermal efficiency for Ethanol for engine 1

Figure 4.6 depicts the outcome of the application of ethanol as the working fluid on the three layouts. Ethanol is in the chemical class of alcohol and the critical pressure of ethanol is 6268 kPa.

At 50% pressure ratio of evaporator and the critical pressure of Ethanol, for SORC the lowest thermal efficiency is 24.03%. The highest thermal efficiency is adjusted 26.39% at 90% pressure ratio. In comparison to the previous SORC applications, the calculated efficiencies are virtually beneath the values. The highest obtained thermal efficiency with SORC was approximately 15.53% with R-1233zd(E).

All the designs at seven pressure ratio of the evaporator and the critical pressure of ethanol results rather high thermal efficiencies in contrast to the HFCs and HFOs. As it is stated on the previous paragraph, the critical pressure of ethanol is very high in comparison to the other applied working fluids. This pressure is an effect on the high efficiencies but the dominant reason is related to the type of the cycle. In this study Organic Rankine Cycle design is considered as subcritical superheated. However, in some cases with regard to the obtained evaporator pressure and the temperature superheated state might be over the limits of the cycle or irrelevant temperatures might occur on the cycle. In this case, the temperature at the inlet of the turbine and the temperature at the inlet of the

evaporator are compared. If the temperature at the beginning of the evaporator is higher than the temperature at the third state (superheated vapour phase) regarding the limits of cycle, it is not a relevant case. In this case, the highest temperature of the cycle is obtained at the inlet of the evaporator. In order to prevent this phenomena, the subcritical saturated cycle design can be proposed. Therefore, if the type of the cycle was changed from subcritical superheated to subcritical saturated cycle which leads to the limit the temperature at the inlet of the turbine, the ORC could have worked but in a different way.

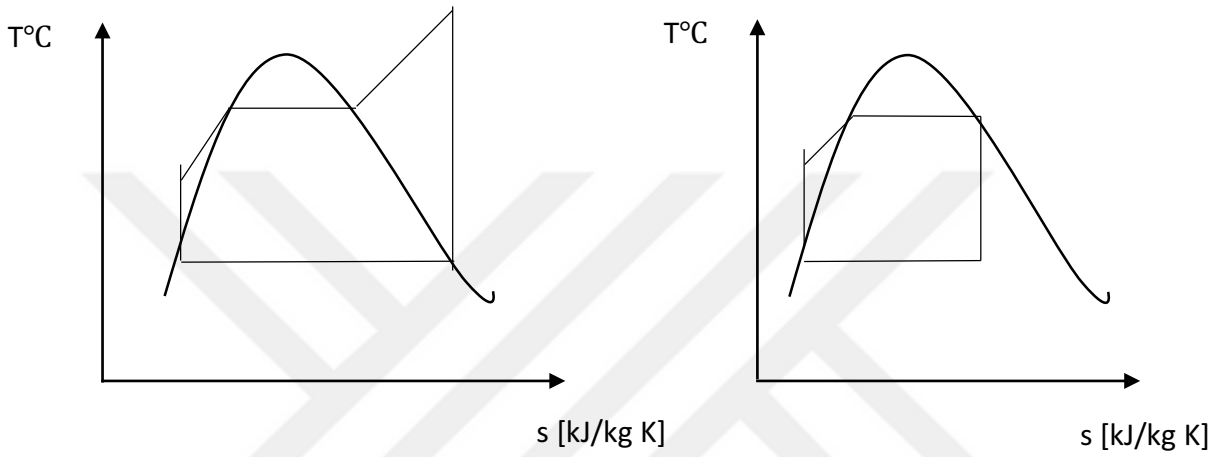

Figure 4. 7. Subcritical superheated and saturated SORC T-s diagrams

Figure 4.7 reveals the differences between the subcritical superheated and saturated SORCs' T-s diagrams. Throughout the study, the subcritical superheated configuration is taken into account. In the further studies, the subcritical saturated case can be investigated in details.

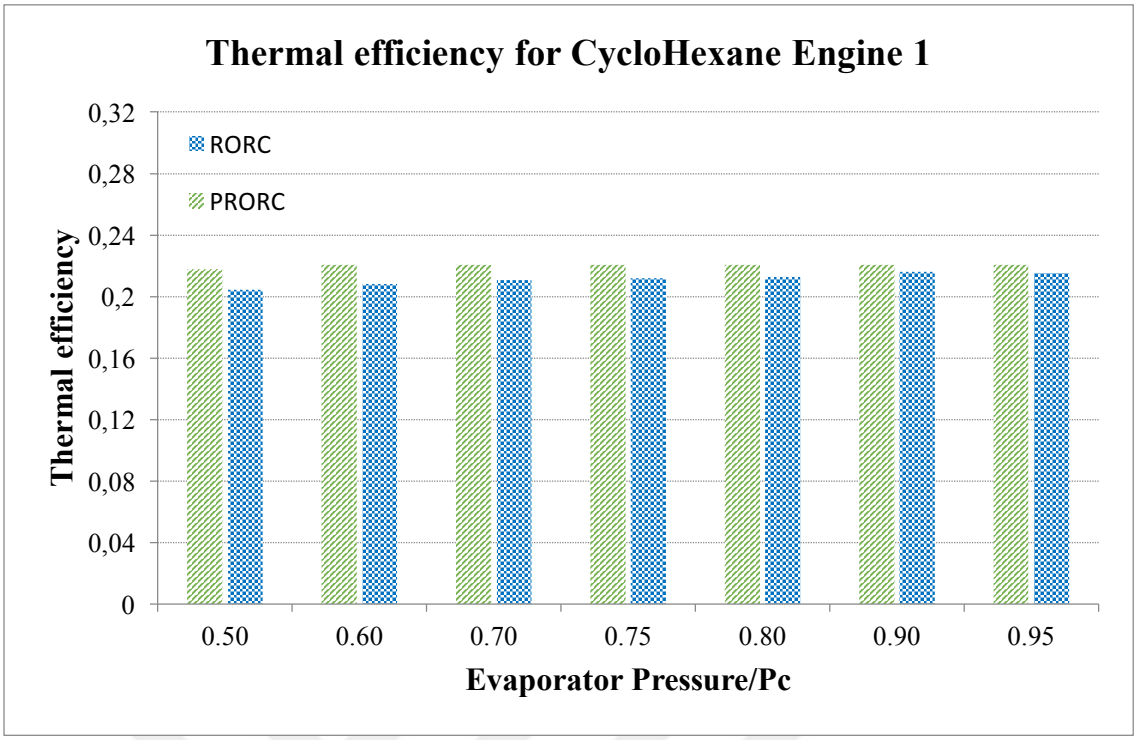

Figure 4. 8. Effect of evaporator pressure on thermal efficiency for cyclohexane for engine 1

Figure 4.8 shows the thermal efficiency of cyclohexane for a range of evaporator pressure using the RORC and PRORC. Cyclohexane is in the chemical class of alkanes. The structure of this organic fluid is cyclic. In the working fluid section, the reasons why a cyclic alkane is tried as candidate working fluid for WHR with ORC were explained in detail. The critical pressure of the fluid is 4080 kPa.

Figure 4.8 does not depict the the SORC configuration for cyclohexane. Through the simulations and the calculations, while the energy balance inside the evaporator is applied, the mass flow rate of the circulating organic fluid is obtained as a negative value. This outcome relies on the same explanation as with the ethanol case. The temperature at the beginning of the evaporator which is State 2' is higher than the State 3. The State 3 is taken into account as the superheated vapour phase. The State 2' is the saturation phase on the evaporator pressure. The state 3 thermodynamic properties are adjusted by the evaporator pressure and entropy value of the vapour phase of the initial conditions. The superheated vapour phase does not compromise the cycle. Therefore, the SORC with cyclohexane does not give any proper results.

For the RORC and PRORC configurations, the obtained thermal efficiencies are fairly high, which are approximately 20%. The greatest thermal efficiency is o as 22.07% on the PRORC design. Meanwhile, the highest efficiency for RORC is obtained as 21.63% at 90% pressure ratio of the evaporator and the critical pressure of cyclohexane. Through the simulations, the negative mass flow rate of the working fluid is not concluded for RORC and PRORC configurations. On the contrary, the negative values determined through the calculations for SORC case. Hence, thermal efficiencies at different pressure ratios are resulted for subcritical superheated ORC layout, apart from SORC design. However, for the sake of the cycle design, the application of the subcritical saturated layout might work in the case of using cyclohexane and derivatives.

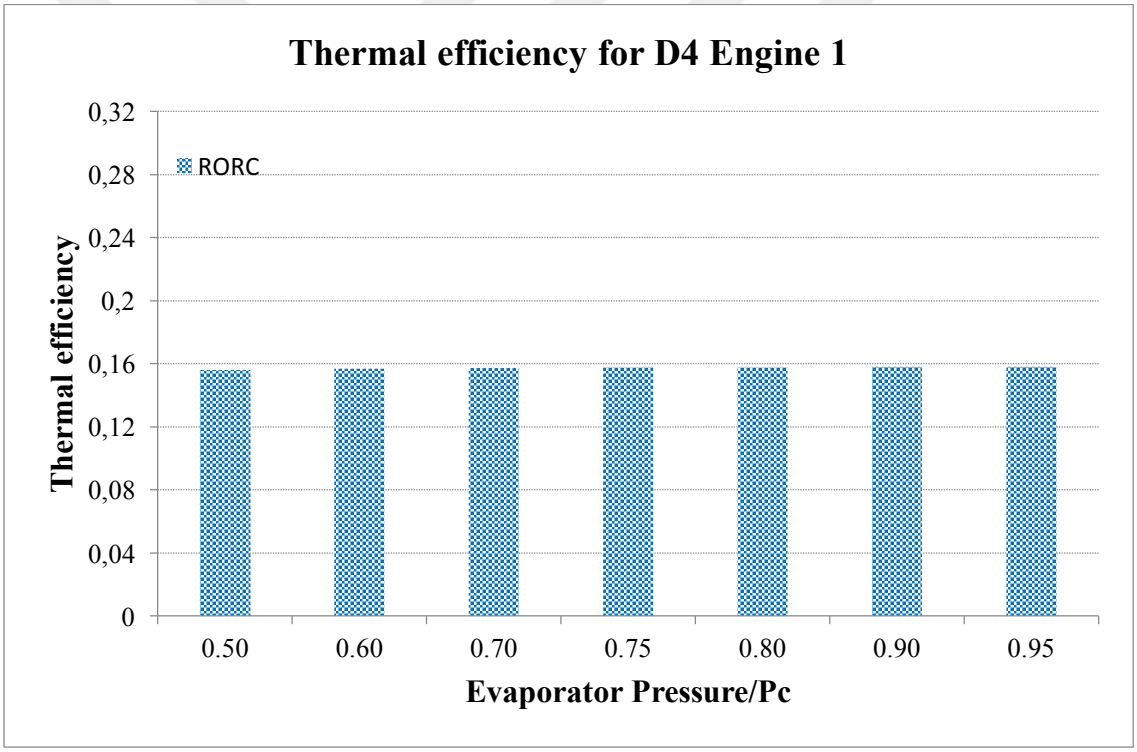

Figure 4. 9. Effect of evaporator pressure on thermal efficiency for D4 for engine 1

D4 is from the chemical class of siloxane. The critical pressure of D4 is 1322 kPa. The critical pressure is not as high as the HFCs and HFOs. Siloxanes are linear or cyclic polymers composed of alternating silicon-oxygen atoms with methyl groups combined to

the silicon atoms. The details of the chemical group were stated clearly in the working fluid section.

As illustrated in Figure 4.9, the thermal efficiency outcomes according to the pressure ratio between the evaporator and critical pressure of D4 are calculated regarding the only RORC configuration. For the SORC, D4 is endeavoured similar to the previous working fluids. During the simulation attempt, a negative mass flow rate of the working fluid is obtained. The thermodynamic properties are over the limits of the cycle. The saturation temperature at the specified evaporator pressure is found higher than the temperature at the superheated state. The reason why the subcritical superheated cycle is applied on the study is to reach higher temperature at the inlet of the turbine. However, for the SORC and PRORC designs with D4 require the subcritical saturation cycle layout akin to the ethanol case.

With regard to the RORC, D4 as the circulating working fluid gives the thermal efficiency outcomes. Inside the evaporator, the energy balance is applied in order to calculate the mass flow rate of D4. In accordance with the calculation of the second energy balance, the position of the Pinch Point recalculated and the result of the thermodynamic equations are calculated. The greatest thermal efficiency of the RORC is achieved at the maximum pressure ratio of the evaporator and the critical pressure of D4 with respect to 15.81%.

For the further studies, in order to obtain better results, the subcritical saturation cycle had better be applied.

Consequently, eight working fluids were employed to run the three ORC configurations at medium exhaust temperature. The HFCs and HFOs give accurate results in terms of the cycle limits.

The most promising outcome is acquired with R-1233zd(E) for the first engine. It is extremely crucial that the greatest thermal efficiency is obtained with an HFO. One of the main purpose of the study is to investigate the behaviours of new generations organic fluids which are much more environmentally friendly. Hence, for medium exhaust temperature waste heat recovery applications, HFCs can be replaced by HFOs. For instance, the obtained greatest efficiency with R-1234yf was not as high as R-1233zd(E), 9.57% and 17.23% respectively. However, 9.57% of thermal efficiency is not inadequate in terms of waste heat recovery potential. Additionally, the advantage of the zero ODP and low GWP cannot be disregarded. Similar to R-1234yf, R-1234ze(E) is also considered as applicable working fluid with regard to the thermal efficiency. In

comparison to the first applied HFC, R-134a the obtained thermal efficiencies do not vary from each other, with respect to 12.35%, 9.57%. The low environmental side effects play a crucial role during the working fluid selection on ORCs. In addition, the application of R-245fa is fairly substantial in terms of thermal efficiency with respect to 15.42%. On the other hand, the GWP of R-245fa is above 1000 (EPA, 2014). Hence, the employment of R-245fa is not convenient when the environmental issues are taken into consideration. Therefore, the satisfied efficiencies regarding waste heat recovery potential, are reached by the employment of the environmentally friendly working fluids.

The last three organic fluids, ethanol, cyclohexane and D4 are slightly different from the HFCs and HFOs. The fundamental reason why these working fluids are not convenient is the determined cycle layout. Due to the cycle limits, these working fluids do not work efficiently. The subcritical saturated ORC layout is much more appropriate for ethanol, cyclohexane and D4. With regard to the environmental concerns, the ODP and GWP values of cyclohexane, ethanol and D4 are unknowns. On the other hand, cyclohexane and ethanol are labelled as highly flammable organic fluids. Hence, the application of these fluids on high temperatures might cause severe problems. Meanwhile, in terms of environmental and safety concerns, D4 seems unproblematic.

4.2. The Second Engine Application

The second engine is a twelve cylinders v type and turbocharged diesel engine. The power of the engine is 1650 kVA and located in the Civil-Food-Electrical Engineering Building's Transformer Building in IZTECH campus in Izmir. The second engine is the biggest engine of all the diesel generators located in the campus. In order to examine the behaviour of the waste heat recovery with Organic Rankine Cycle on the bigger engine, it is chosen as the second type of engine.

The exhaust temperature of the engine is 455 ℃ and the mass flow rate of the exhaust gas is 2.595 kg/s. The exhaust temperature can be defined as low temperature in comparison to the first engine's exhaust temperature. The calculated specific heat capacity is 1.10 kJ/kg K. The mass flow rate, temperature of the exhaust and the specific heat capacity are the fundamental inputs for the second application.

Respectively, the SORC, RORC and PRORC models are applied with the working fluids on Matlab.

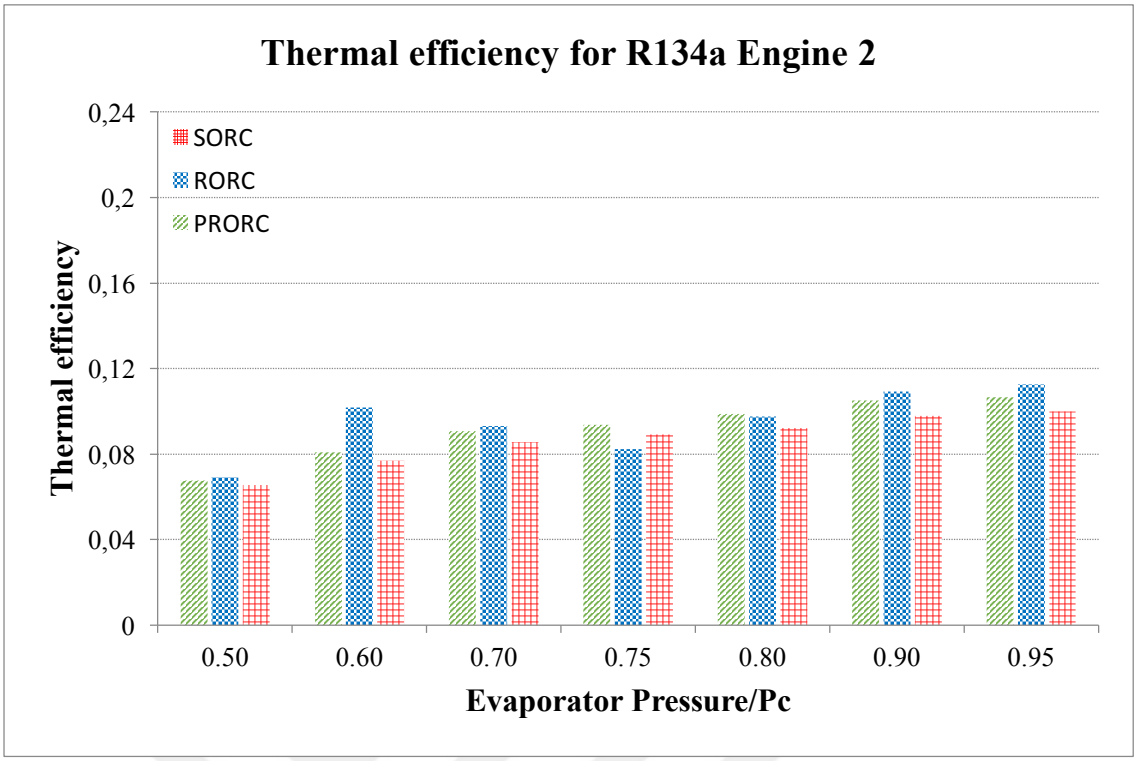

Figure 4. 10. Effect of evaporator pressure on thermal efficiency for R-134a for engine 2

Similar to the first engine application, the reference working fluid, R-134a is applied on the second engine.

At the 50% pressure ratio of evaporator and critical pressure of R-134a, the three configurations' thermal efficiency results are close to each other and below 7%. The SORC layout results around 6.54% at the minimum pressure ratio. On the contrary, for the first engine type, under the same operating conditions, the outcome of SORC was roughly 7.4%. The general increase trend continues for SORC design, whilst the fluctuations can be seen for RORC and PRORC configurations.

The peak thermal efficiency is achieved at 95% pressure ratio of evaporator and the critical pressure of R-134a, on the RORC with a value of 11.26%. However, the highest efficiency of the first engine application with R-134a was obtained on the PRORC, 12.35% respectively. The reason behind this phenomenon is lower exhaust temperature and high mass flow rate of the exhaust. Furthermore, at 60% pressure ratio between the evaporator and the critical pressure of R-134a, thermal efficiency is calculated as 10.71%. The value does not trace the general increase trend of the cycle. The efficiency is akin to

the highest thermal efficiency of the application. On the first engine application, the thermal efficiency at 60% was 8.23%.

Except from the edge ratios, in general the thermal efficiencies on the first and the second engines are not varied from each other for R-134a as the working fluid. The fundamental difference occurs on the values of turbine and pump work and the heat transfer from the exhaust to the working fluid. Due to fact that the second engine is considered as a big engine, the required works and heat input are rather greater than the first engine. It also can be discerned the difference on the mass flow rate of the exhaust gas. The difference is taken into consideration while, the comparison is made between the two engines.

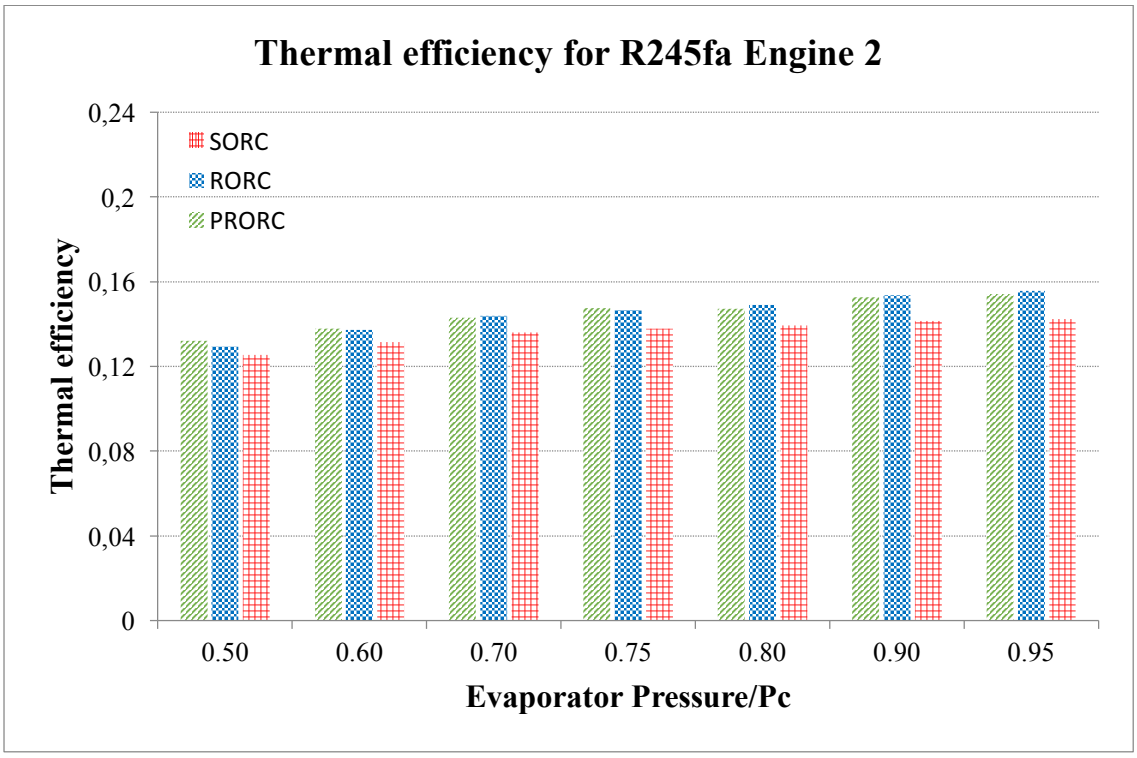

Figure 4. 11. Effect of evaporator pressure on thermal efficiency for R-245fa for engine 2

Figure 4.11 illustrates the thermal efficiency results for R-245fa as the working fluid. The outcomes are not very different from the first engine application's. The primary difference between the two engine is on the turbine work and the amount of heat transferred from the exhaust to working fluid. Due to the high mass flow rate of the exhaust gas and the volume of the engine, these parameters are greater than the first

engine. However, the calculated thermal efficiency ratio between $\dot{W}net$ and $\dot{Q}in$ the outcomes are akin to each other.

All the three cases within the rise on the pressure ratio between the evaporator pressure and the critical pressure, the thermal efficiencies increase at the same time. The SORC starts with approximately 12.5%, ends 14.22%. Similar results for the RORC and PRORC layouts are revealed in Figure 4.11. The peak point of the chart appears on the RORC case at the 95% pressure ratio of evaporator and critical pressure of R-245fa which is rather higher than the first engine application, 15.59 and 15.33% respectively. The outcomes of the PRORC is begun from 13.21% and ended at 15.42%. On the first engine employment, the same results were adjusted.

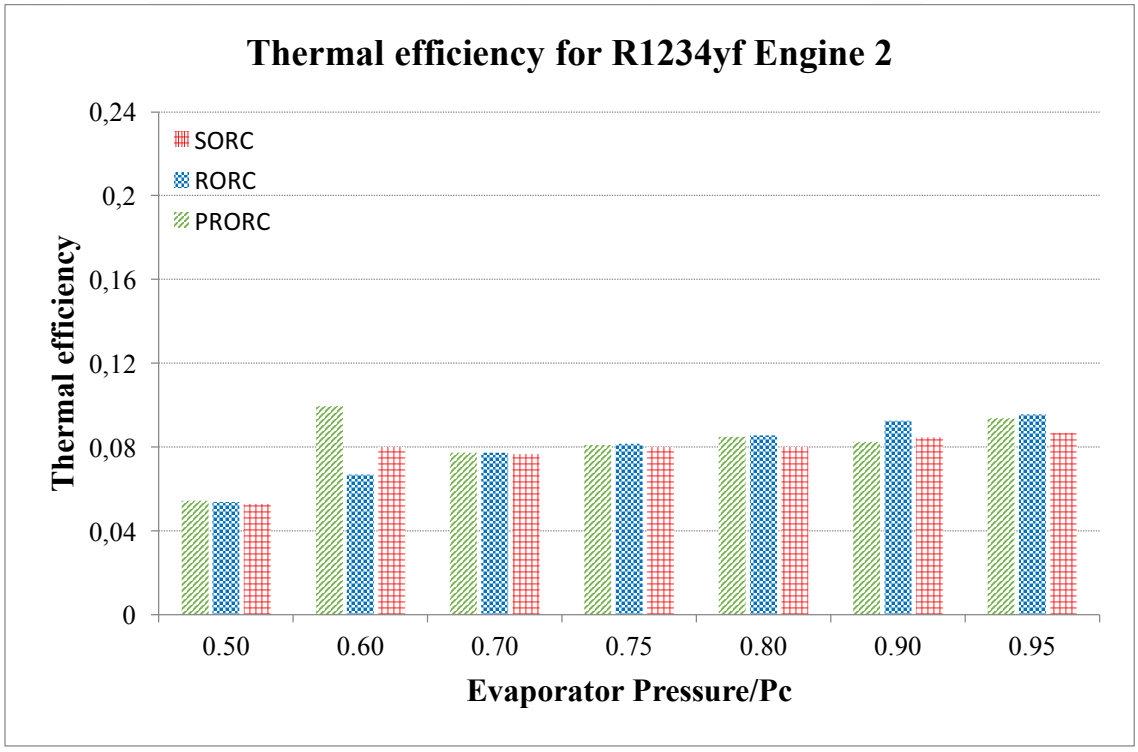

Figure 4. 12. Effect of evaporator pressure on thermal efficiency for R-1234yf for engine 2

From the chemical class of HFOs, R-1234yf is used as the working fluid for the second engine. In comparison to the first engine application, the outcomes are quite similar to each other.

The most unusual aspect in Figure 4.12 is the location of the peak thermal efficiency. On the foregoing operations, the prime efficiency is predominantly acquired at 95% pressure

ratio value. Applying two heat sources on the PRORC design fits very well at the pressure ratio of 60%. Hence, the highest thermal efficiency is obtained at 60% pressure ratio of the evaporator and the critical pressure of R-1234yf with respect to 9.95%. The greatest efficiency of the first engine employment was obtained on the RORC configuration, 9.57%. PRORC design with R-1234yf works better at lower pressure ratios.

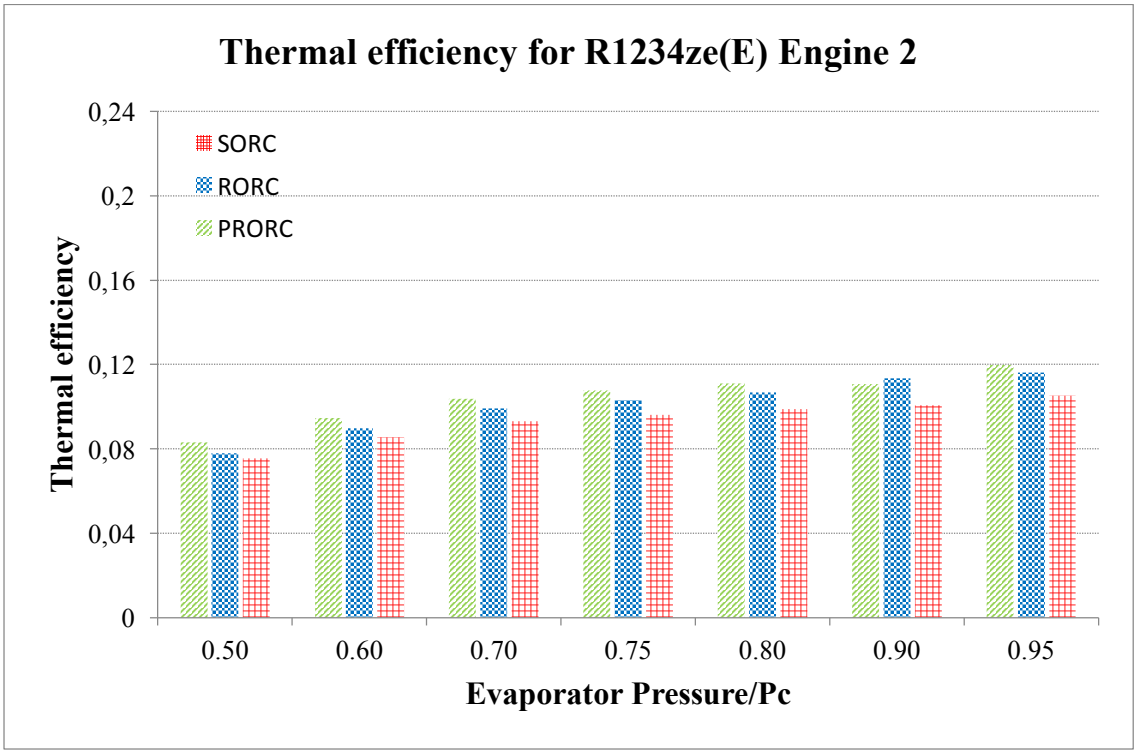

Figure 4. 13. Effect of evaporator pressure on thermal efficiency for R-1234ze(E) for engine 2

Figure 4.13 describes the thermal efficiency outcome for the second engine for R-1234ze(E). As with the previous working fluids, in general, the results are very similar as those for the first engine application, the increase trend can be seen clearly for the three cases. The highest thermal efficiency is adjusted on the PRORC at 95% pressure ratio of evaporator and critical pressure of R-1234ze(E) with respect to 11.98%.

In comparison to the first engine application's greatest thermal efficiency was adjusted as 11.76% at the peak pressure ratio of evaporator and critical pressure of R-1234ze(E) on the PRORC design. For both engine employments starts with the same thermal efficiency, 8.30%, whilst at the highest pressure ratio, the thermal efficiencies are not the same value due to the engine type.

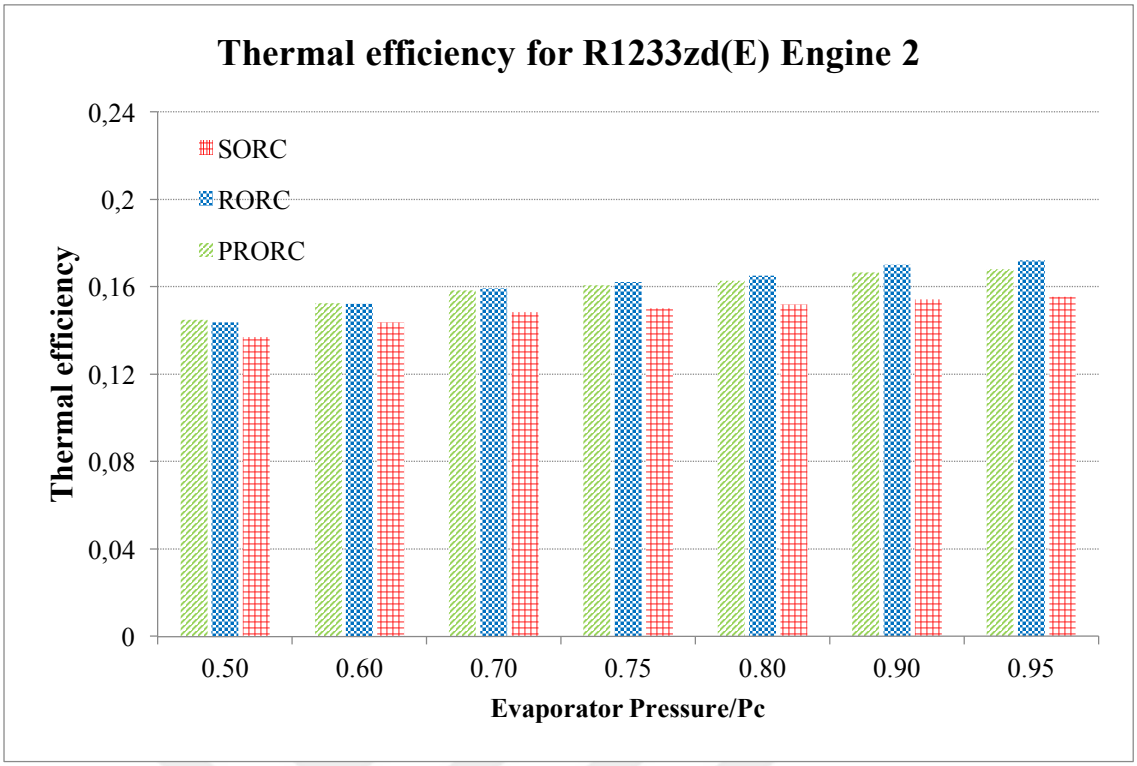

Figure 4. 14. Effect of evaporator pressure on thermal efficiency for R-1233ze(E) for engine 2

Figure 4.14 pictures the thermal efficiency of the three configurations regarding the the pressure ratio of evaporator pressure and the critical pressure of R-1233ze(E). Expect from the engine, the operating and initial conditions are taken same as to the first engine employment.

The low thermal efficiencies are generally obtained for the SORC design. Meanwhile, the outcomes of SORC for R-1233ze(E) are quite higher than the other working fluids' applications. The SORC thermal efficiency value at the lowest pressure ratio is 13.71%, the maximum pressure ratio is 15.53%. On the first engine application, the results were exactly the same as the second one. The engine size does not affect the thermal efficiency on the SORC configuration.

The greatest thermal efficiency is achieved on the RORC at the 95% of the pressure ratio between the evaporator and the critical pressure of R-1233ze(E) with respect to 17.23%. The highest thermal efficiency value is exactly the same on the first engine application.

On the PRORC results are slimly different from the first engine application. The lowest thermal efficiency is obtained as 14.48%, on the contrary, on the first case employment,

the efficiency was 14.46%. The highest thermal efficiencies for both cases are the same with respect to 16.80%.

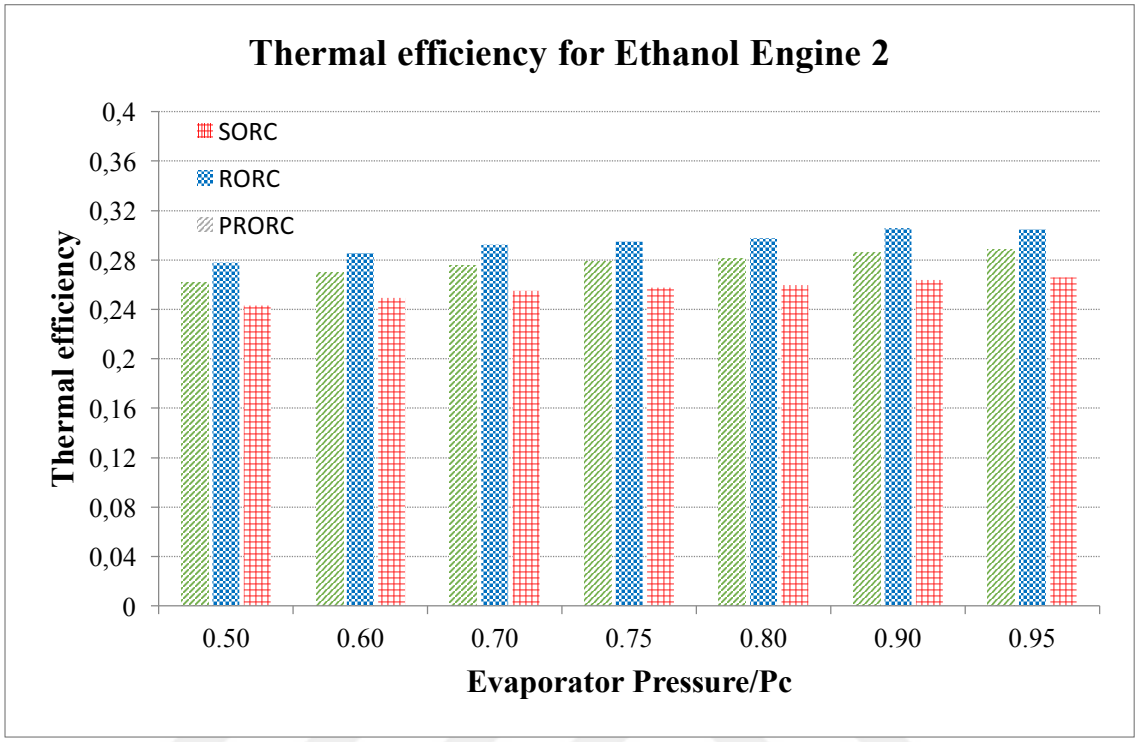

Figure 4. 15. Effect of evaporator pressure on thermal efficiency for ethanol for engine 2

The sixth working for the ORC application chosen is ethanol. Figure 4.15 shows the outcomes of using the ethanol. The highest thermal efficiency is achieved with the RORC design with respect to 30.45%. It is almost same as the first engine's outcomes. The RORC results vary from 27.76% to 30.45%. The efficiency is not only the highest efficiency on the graph, but also the greatest one until it is calculated among the applied working fluids.

However, ethanol is not common organic fluid for waste heat recovery applications. Since, its flammability is profoundly high and hazardous to apply such high temperatures. On the simulation, employing ethanol as a working fluid in order to understand and investigate the characteristic does not cause any problems.

The rest of the results are construed with the first engine application.

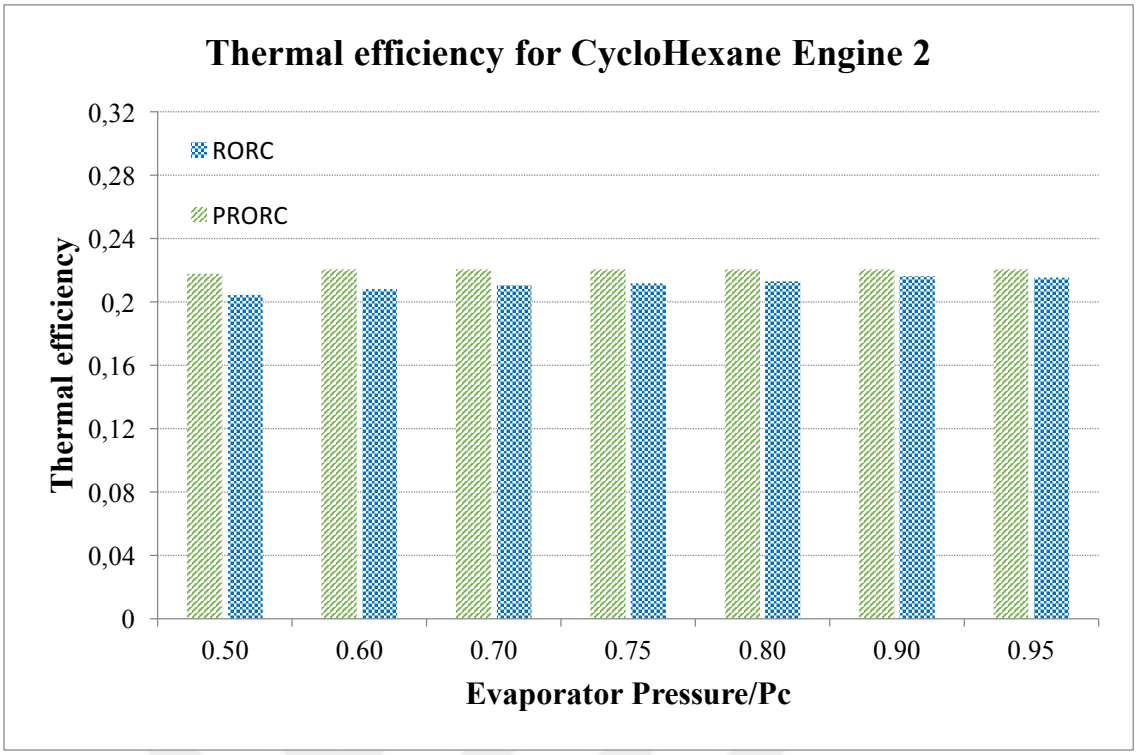

Figure 4. 16. Effect of evaporator pressure on thermal efficiency for cyclohexane for engine 2

Figure 4.16 shows the thermal efficiencies for the two configurations. Through the study, three main ORC layouts are taken into consideration. However, using cyclohexane as the working fluid for the SORC, the outcomes cannot be revealed on the graph. As it is stated on the first engine application, during the simulation process for the SORC the problem occurs on the energy balance as the temperature on the saturation line is higher than the superheated state. As a result of the two issues, the thermal efficiency of the SORC cannot be calculated following the initial assumptions.

On the PRORC configuration, the adjusted thermal efficiency at the lowest pressure ratio of the evaporator pressure and the critical pressure of cyclohexane is around 21.77%. At the 95% pressure ratio, the thermal efficiency is 22.07% which is the peak point the graph. Within the increase on the pressure ration, the thermal efficiency does not vary very much. In comparison to the first engine employment with cyclohexane on PRORC, the exactly the same thermal efficiencies were obtained.

The same phenomenon happens with the RORC configuration. There are no huge differences between the obtained thermal efficiencies at the highest and lowest rations with regard to the pressure ratio between the evaporator pressure and the critical pressure

of cyclohexane 20.44% and 21.53% respectively. The same thermal efficiency percentages were adjusted during the first engine simulation. The PRORC and RORC are not different from each other expect that the PRORC consists of the two heat sources and additional internal heat exchanger. Having the similar outcomes is an expected circumstance.

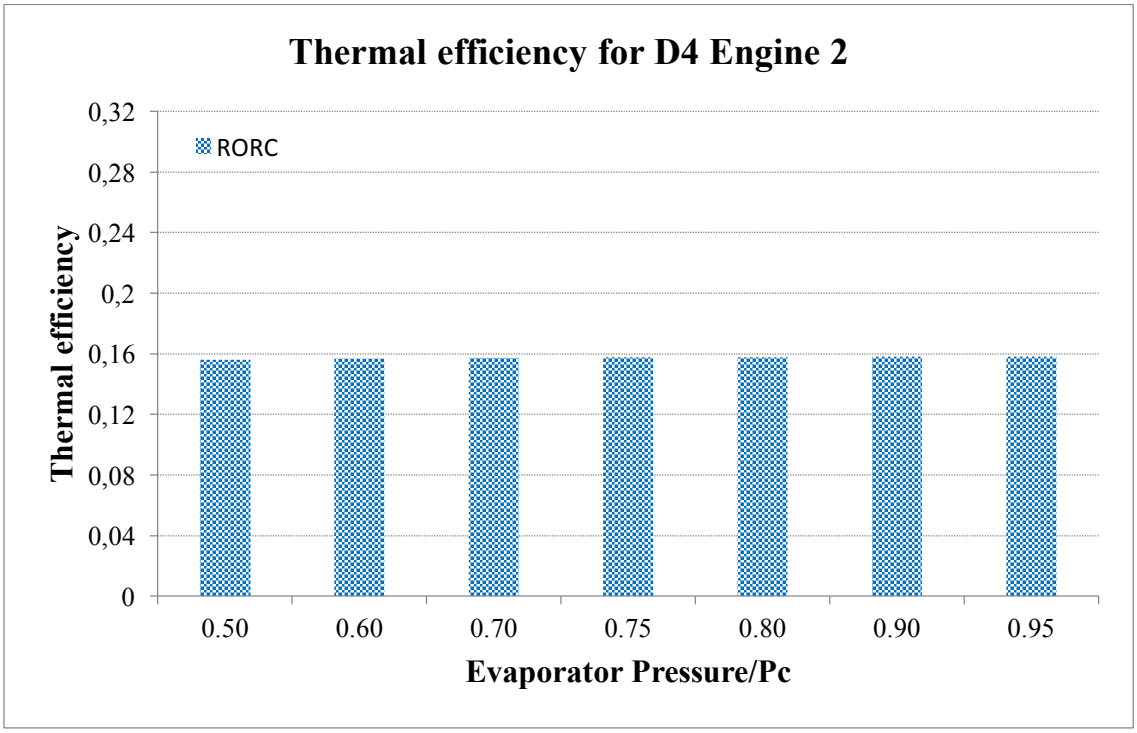

Figure 4. 17. Effect of evaporator pressure on thermal efficiency for D4 for engine 2

As the last working fluid, D4 is applied on the RORC. Similar to the first engine case, the SORC and PRORC cannot be simulated with the organic fluid D4 with regard to the unbalanced on the temperatures and obtaining the negative mass flow rate of D4. For the RORC implementation simulation on the second engine is fairly different from the first engine in terms of the mass flow rate of D4 and the positon of the pinch point. Meanwhile, the thermal efficiency outcomes are almost same as the first engine case. The greatest thermal efficiency is acquired as 15.81% at the 95% pressure ratio between the evaporator and the critical pressure of D4. The same thermal efficiency at the same pressure ratio of evaporator and critical pressure of D4 was determined on the previous engine employment.

At the 50% and 60% pressure ratios, the location of the pinch point changes from the assumed one. At the lower pressures, the pinch point occurs before the saturation point at the evaporator pressure. Whilst, for the higher pressure ratios, the position of the pinch point does not change. Hence, the first mass flow rate satisfies the RORC. This phenomenon happens with the low temperature of the exhaust gas.

In conclusion, the results for the second engine does not vary from the first engine. The fundamental difference between the two cases is the mass flow rate of the exhaust gas. Since, the mass flow of the exhaust gas is high, the turbine and pump works are almost two times as high as the first engine. Moreover, the heat transfer rate inside the evaporator from exhaust gas to the working fluid is rather high in contrast to the first engine application.

In terms of the exhaust temperature, the second engine is considered as relatively low temperature heat source, however this difference (first engine is 509 ℃ and the second one is 455 ℃) was not enough to make an impact on the thermal efficiency. The temperature of the exhaust gas is not the only parameter to construe with the thermal efficiency of the cycle. One of the effects of the high mass flow rate of the exhaust is to be required more mass flow rate of the working fluid. From the economical point of view, the costs of the design will increase regarding the need of the working fluid. Meanwhile, the heat transfer rate between the exhaust and the working fluid rises accordingly. The pump work also arises but the value is not sufficient to consider about the cost. In addition, the turbine work also increases. The increment of the all parameters is relied on the size of the engine. The most vital parameter is the thermal efficiency which is a ratio between the produced net work in the cycle and the heat transfer. Hence, the size of the engine does not affect the thermal efficiency outcomes in comparison to the first engine application.

The applicability of the working fluids, the accuracy of the cycle design, the critical pressure of the organic working fluid should be taken into consideration profoundly.

4.3. The Thirds Engine Application

The third engine is a six cylinder in line turbocharged diesel engine. The power of the engine is 550 kVA and located in Chemical Engineering Building in IZTECH campus in Izmir. The third engine is akin to the first applied engine in terms of power.

However, the exhaust temperature of the third engine is the highest among the the three engines. In order to comprehend the behaviour of waste heat recovery with high exhaust temperature, the third engine is chosen with regard to the exhaust temperature.

The exhaust temperature of the engine is 563 ℃ and the mass flow rate of the exhaust gas is 0.6 kg/s. The exhaust temperature can be defined as high temperature in comparison to the first engine's exhaust temperature. The calculated specific heat capacity is 1.10 kJ/kg K (see Appendix B). The mass flow rate, temperature of the exhaust and the specific heat capacity are the fundamental inputs for the third application as well.

Respectively, the SORC, RORC and PRORC models are applied with the working fluids on Matlab with the function of 'refprop.m'.

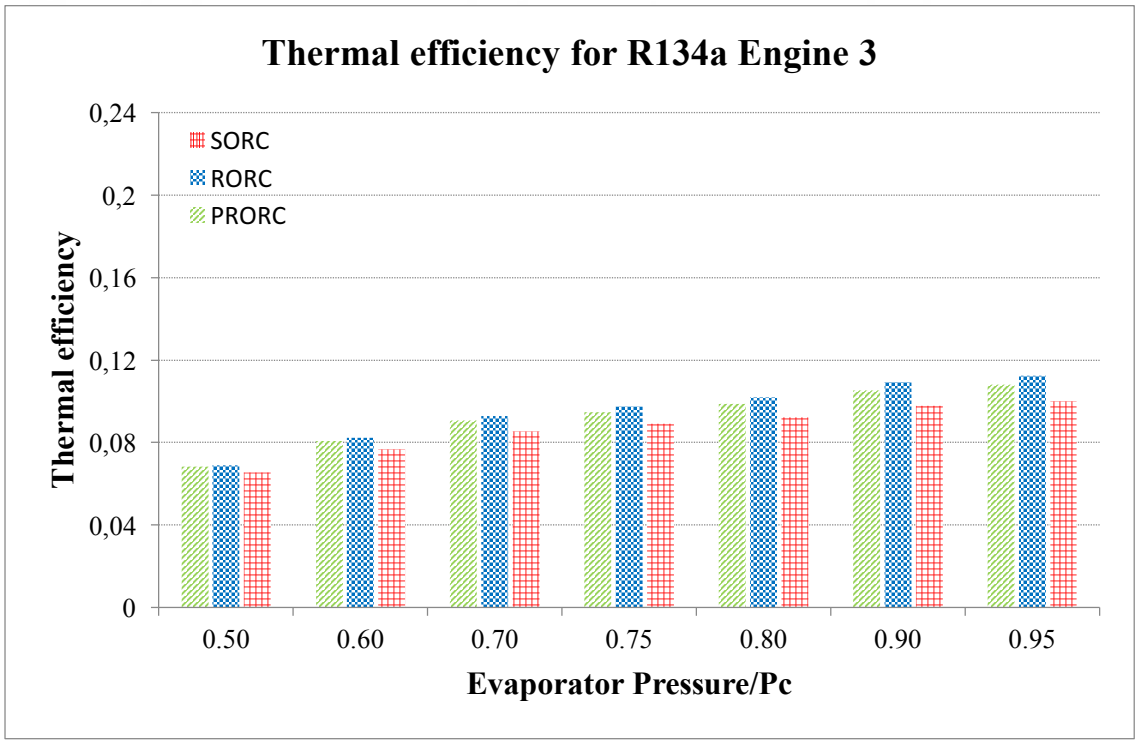

Figure 4. 18. Effect of evaporator pressure on thermal efficiency for R-134a for engine 3

The first working fluid for the third engine is R-134a similar to the previous two engine applications, the increase on the thermal efficiency continues with the rise on the pressure ratio between the evaporator and critical pressure of R-134a. The peak thermal efficiency of the cycle is achieved at the 95% pressure ratio on the RORC configuration with respect to 11.25%. The maximum efficiency for the second engine application was similar to the third engine. However, for the first engine application, the greatest thermal

efficiency is obtained on the PRORC design, 12.35%. The first engine is considered as medium temperature heat source. Hence, the application of R-134a on the medium temperature engine is resulted better than the following two engine employments. At the medium temperature of exhaust gases, the PRORC design with R-134a results slightly better in comparison to the low and high temperature exhaust gases.

Since the temperature of the exhaust gas of the third engine is considered as high, the greatest thermal efficiency outcome is expected to be also higher than the second application. However, the thermal efficiencies of the SORC design vary between the low and high pressure ratios from 6.54% to 10%. Whilst, on the first application the outcomes are slimly satisfied 7.40% and 10.56% respectively.

The effect of the exhaust gas temperature can be stated clearly. With regard to the high exhaust temperatures, the RORC configuration with R-134a fits better.

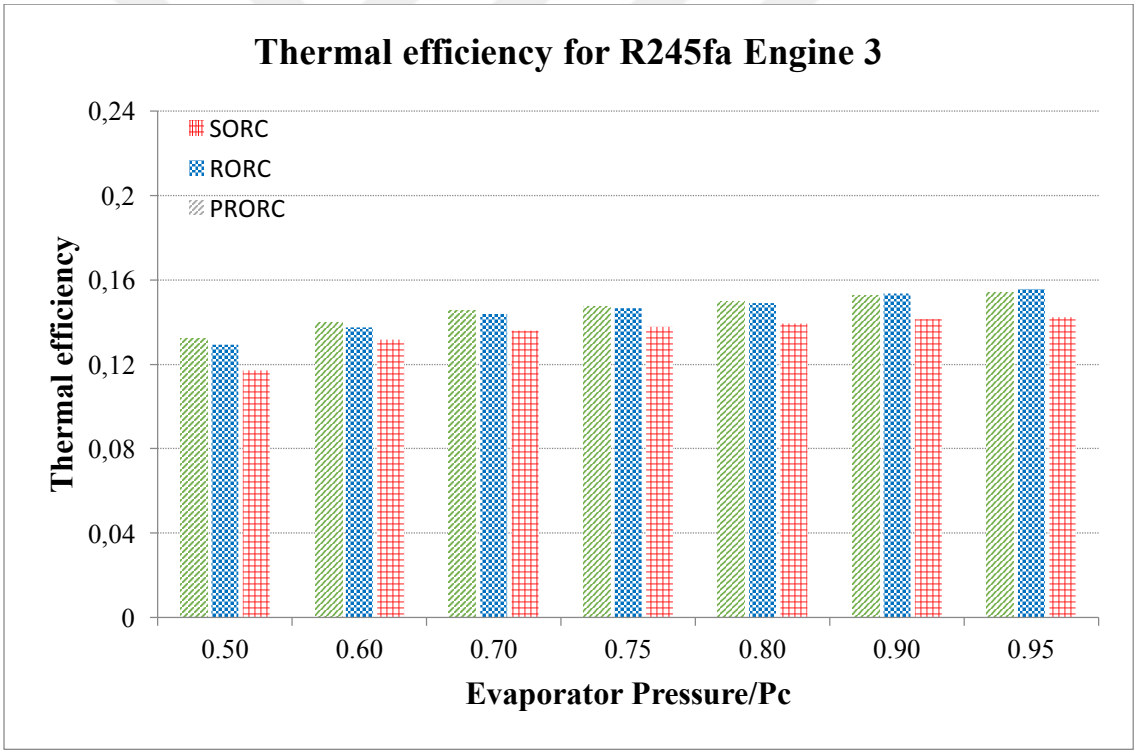

Figure 4. 19. Effect of evaporator pressure on thermal efficiency for R-245fa for engine 3

Figure 4.19 indicates the results of thermal efficiency according to the pressure ratio between the evaporator and the critical pressure of R-245fa. The highest thermal efficiency is adjusted as 15.56% at 95% of the pressure of evaporator and critical pressure

on the RORC. The RORC configuration is generally appropriate for the high temperature waste heat recovery applications (Fernández et al., 2011). The general trend increment on the thermal efficiency persists as the pressure ratio of the evaporator and the critical pressure of R-245fa increases.

The thermal efficiency of the SORC at the lowest pressure is 11.71%. In comparison, on the first engine application, under the same operating conditions, the outcome was 12.53%. In addition, the second engine's result for the lowest pressure ratio was same as the first case, 12.53%.

However, the highest thermal is achieved as 15.42% on the first engine application with the PRORC configuration. The first engine's exhaust temperature is considered as medium temperature. It can be declared that for the medium exhaust temperature WHR applications, PRORC with R-245fa fits more advisedly in contrast to the low and high temperatures of the heat sources. While the research continues to find the best configurations and the working fluid, the exhaust temperatures and the mass flow rate should be examined carefully. Even there is no great difference on the thermal efficiencies results between the second and the third applications, it is still crucial to comprehend the mass flow rate of the exhaust gas, 15.59%, 15.56% respectively.

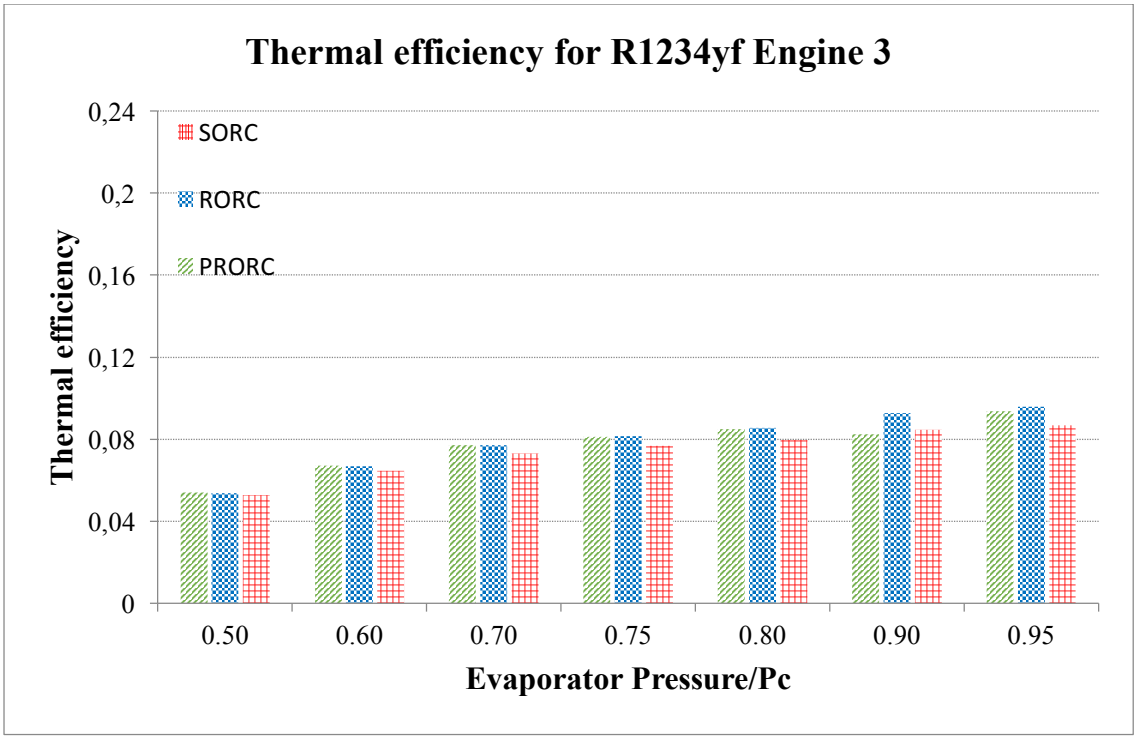

Figure 4. 20. Effect of evaporator pressure on thermal efficiency for R-1234yf for engine 3

As the third working fluid, R-1234yf is utilised on the three configurations. The peak thermal efficiency is found at the 95% pressure ratio of the evaporator and the critical pressure of R-1234yf with respect to 9.57%.

For the three diesel engines applications, the outcomes of the simulations do not vary from each other. The adjusted highest thermal efficiency for the first engine application was 9.57% at 95% pressure ratio, the second engine application resulted 9.95% at 60% pressure ratio of evaporator and critical pressure of R-1234yf. In addition, on the second engine application, the greatest efficiency was adjusted on the PRORC whilst, for the first and third engine cases, the high thermal efficiencies were obtained on RORC configuration. Even though the thermal efficiency results are not as high as the previous two working fluids (HFCs), in terms of the environmental concerns, R-1234yf is an alternative organic fluid to R-134a and R-1245fa.

With regard to the characteristic of R-1234yf, the thermal efficiency is not affected by the engine features in terms of mass flow rate and the temperature of the exhaust gases. At the same time, the usage of R-1234yf as a working fluid for ORC applications is still promising regarding the environmental regulations and problems.

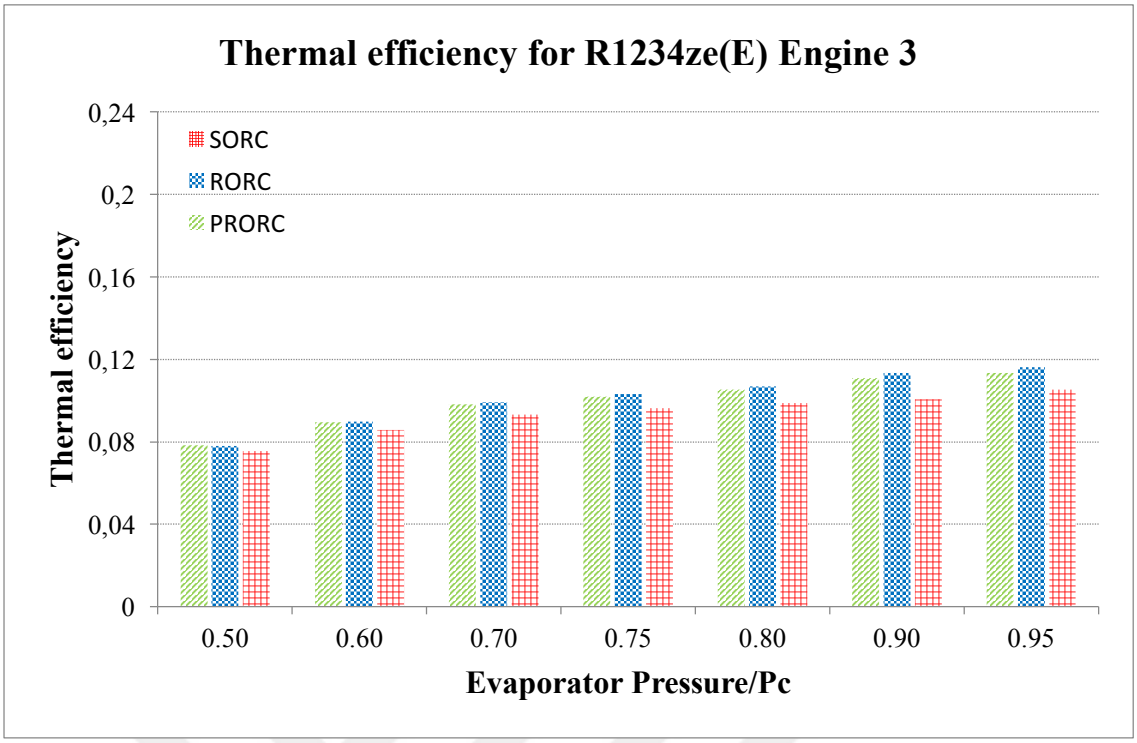

Figure 4. 21. Effect of evaporator pressure on thermal efficiency for R-1234ze(E) for engine 3

Figure 4.21 depicts the thermal efficiency results of the third engine for the three ORC configurations regarding the seven different pressure ratio of the evaporator and the critical pressure of R-1234ze(E). The highest thermal efficiency is achieved at the greatest pressure ratio between the evaporator and the critical pressure of R-1234ze(E) with respect to 11.62%. In comparison to the previous cases, the greatest thermal efficiency was obtained as 11.76% on the first engine employment, the second engine' outcome was 11.98% at 95% pressure ratio. Furthermore, the foregoing applications' greatest thermal efficiencies were adjusted on PRORC configurations. However, the third engine application's highest thermal efficiency was acquired on the RORC configuration. Since, the third engine's most characteristic feature is the high exhaust temperature. The greatest thermal efficiency is obtained on the RORC configuration. Meanwhile, the highest efficiencies for the previous engine applications were acquired on the PRORC layout. It can be claimed that the engines with the low and medium exhaust temperatures are suitable for PRORC with the working fluid of R-1234ze(E). Furthermore, the high exhaust temperature of the engine is much more befitting with RORC configuration.

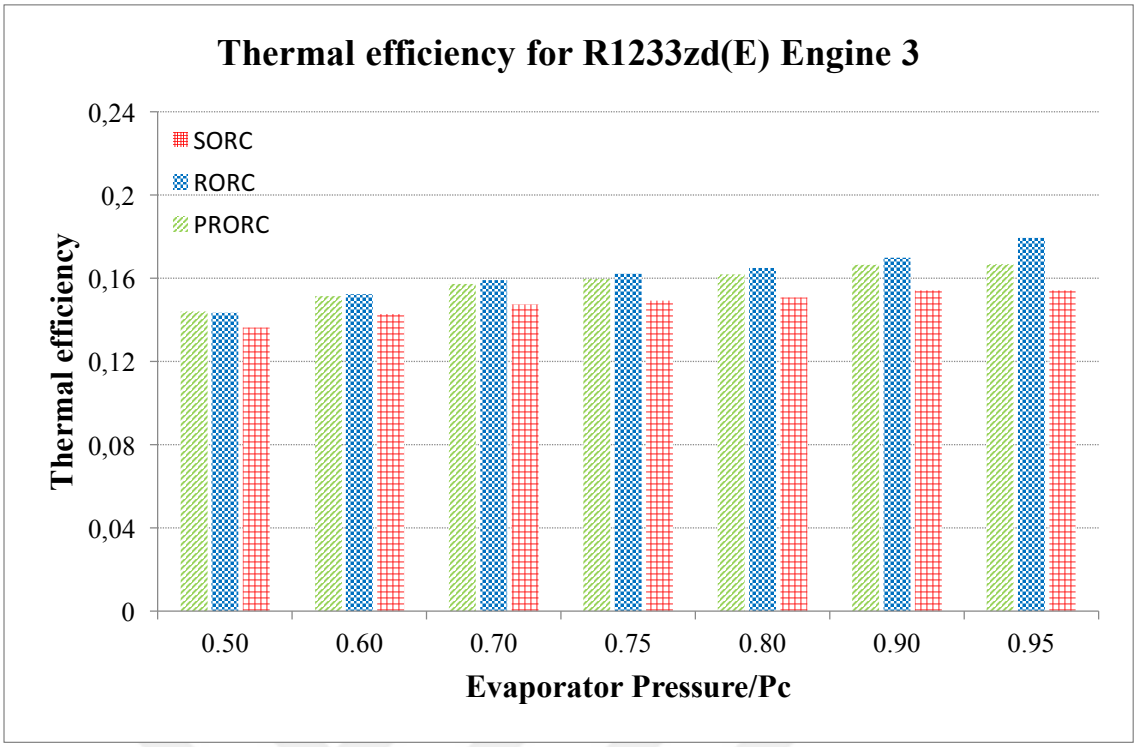

Figure 4. 22. Effect of evaporator pressure on thermal efficiency for R-1233zd(E) for engine 3

The fifth working chosen R1233zd(E) is a member of chemical class of HFOs. For all the configurations' thermal efficiency ratios increase accordingly the increment of the pressure ratio between the evaporator pressure and the critical pressure of R-1233ze(E). The SORC design with R-1233zd(E) at the lowest pressure ratio gives the thermal efficiency as 13.64%, on the first and second applications the thermal efficiencies were adjusted as 13.71%. On the PRORC configuration for the first and second engines, the thermal efficiencies varied from 14.46% and 14.48% to 16.80% respectively.

The lowest thermal efficiency of the application of R-1233zd(E) on the ORC designs is 13.64% which is calculated on the SORC configuration. Whilst, the greatest thermal efficiency is achieved on the RORC layout at the highest pressure ratio with respect to 17.96%. This thermal efficiency is the greatest one among the three diesel engines through the study. The low and medium exhaust temperature on the first and the second engine produce 17.23% under the same operating and initial conditions on the RORC design. Consequently, it can be claimed that the RORC with R-1233zd(E) configuration gives adequate outcomes in terms of thermal efficiency and the waste heat recovery. One of the results can be declared that as a working fluid for RORC

configuration, R-1233zd(E) is implementable for the three engines' exhaust temperatures. Most excellently, one of the HFOs is fairly satisfying with regard to the calculated thermal efficiency. It is extremely crucial to obtain this result due to the environmental issues.

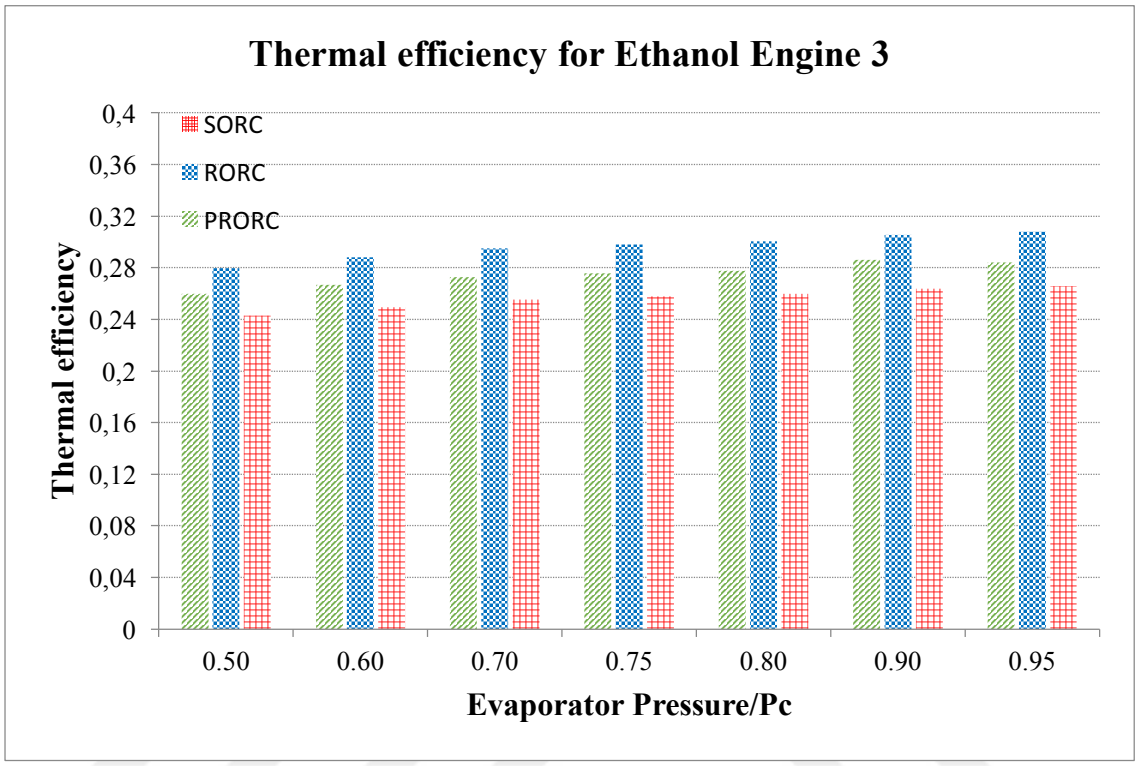

Figure 4. 23. Effect of evaporator pressure on thermal efficiency for ethanol for engine 3

Figure 4.23 illustrates the thermal efficiency ratios on the three different ORC configurations with Ethanol as the circulating organic fluid. Ethanol can be defined one of the problematic working fluid in terms of safety issues and high critical pressure for the designs of the ORC. Despite the high calculated thermal efficiencies, the application of ethanol as the working fluid is not desired for the sake of the turbine and turbine operating conditions. The former reasons were explained in details in the previous sections.

The peak thermal efficiency is achieved on the RORC configuration at the highest pressure ratio between the pressure of the evaporator and the critical pressure of ethanol with respect to 30.79%. The first and second engine applications were resulted under the same operating conditions, 30.46% and 30.45% at the highest pressure ratio of evaporator

and critical pressure of Ethanol respectively. In addition, the thermal efficiency on the third engine is the greatest among the two other diesel engines.

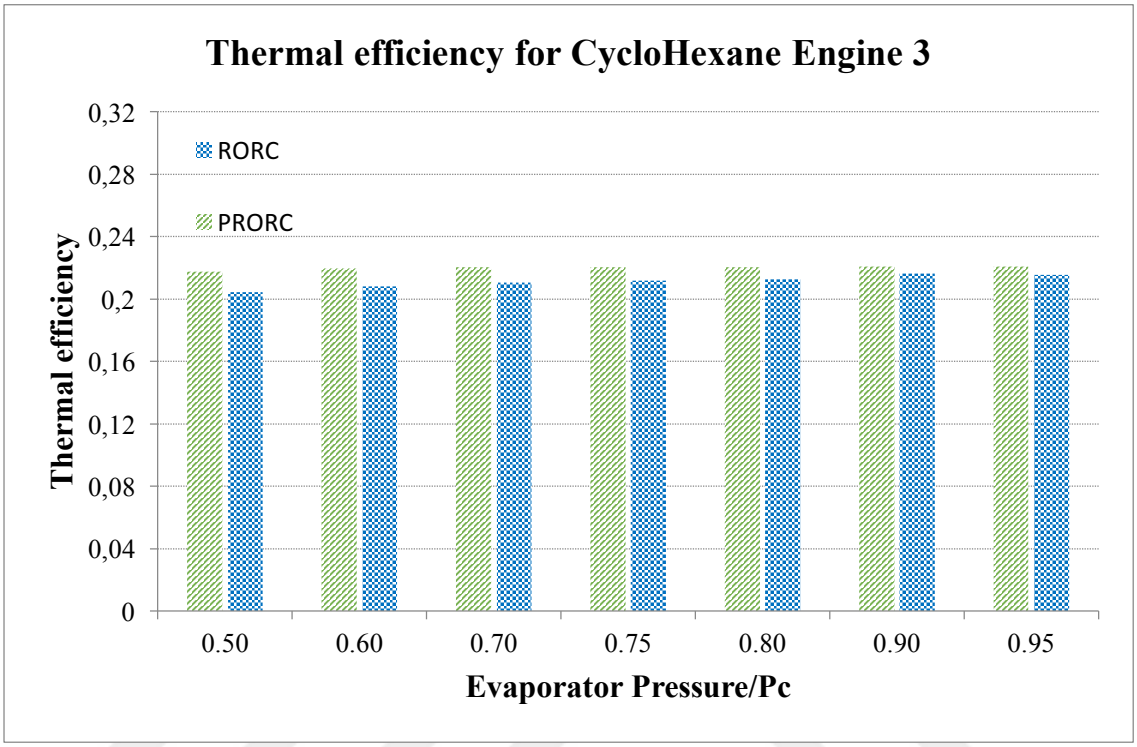

Figure 4. 24. Effect of evaporator pressure on thermal efficiency for cyclohexane for engine 3

From the chemical class of alkanes, cyclohexane is chosen as a candidate working fluid for ORC configurations. On the foregoing engine employments, the SORC could not be calculated regarding the temperature issue of the saturation and superheated states. The saturation temperature at the evaporator pressure is higher than the calculated superheated state. Due to the cycle limits, the mass flow rate of the working fluid cannot be acquired properly. Hence, Figure 4.24 cannot depict any results related to the thermal efficiency of the SORC. For the three engine, the thermal efficiency is acquired as 22.07% on the PRORC at the highest pressure ratio between the evaporator pressure and the critical pressure of cyclohexane. The thermal efficiencies are fairly fulfilled. However, in order to obtain much more accurate outcomes, the subcritical saturated cycle should be investigated during the further studies.

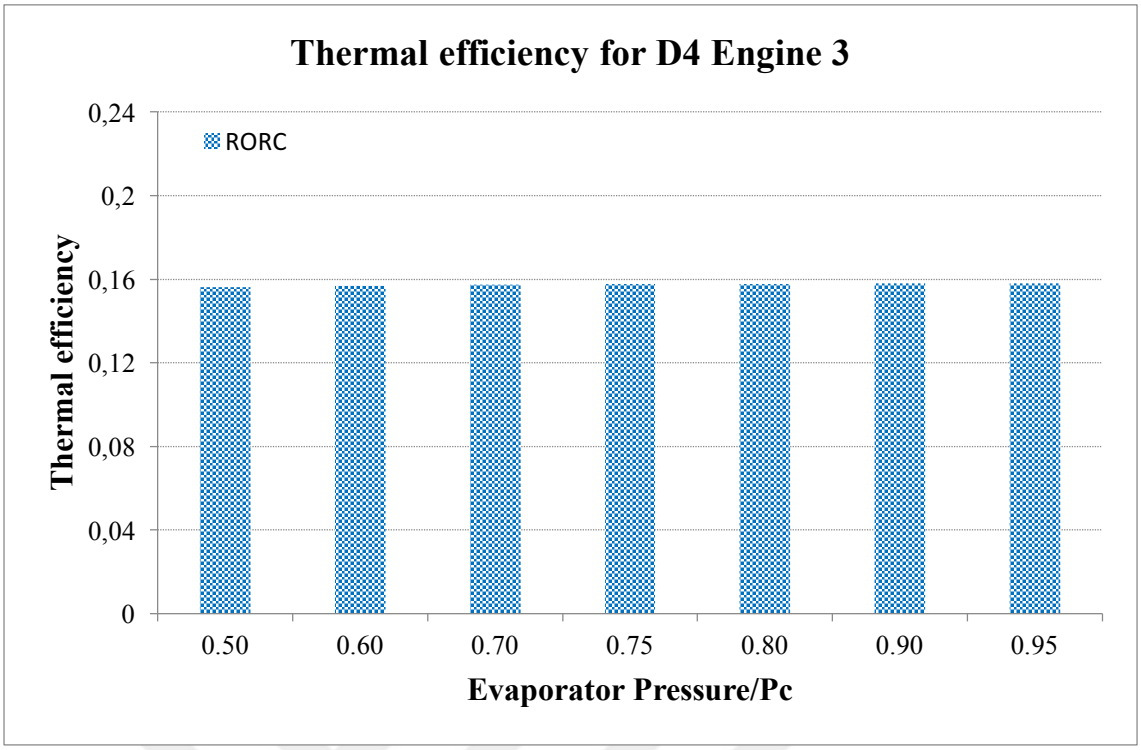

Figure 4. 25. Effect of evaporator pressure on thermal efficiency for D4 for engine 3

The ultimate working fluid, D4 is applied on the RORC. The simulation attempts on the SORC and PRORC fail due to the characteristic of D4 and the limits of the cycle layouts. The peak thermal efficiency is achieved as 15.81% at the highest pressure ratio of the evaporator and the critical pressure of D4. The same thermal efficiency was obtained through the three engine types. The pinch point occurs before the saturation liquid point of the calculated evaporator pressure. Thus, the second mass flow rate is calculated with the second energy balance inside the evaporator.

Table 4.1. The thermal efficiencies for the first engine

Working Fluids	**Cycle Configuration**	**Efficiency**						
R-134a	SORC-1	0,074	0,077	0,085	0,097	0,092	0,098	0,106
	SORC-2	0,075	0,089	0,099	0,103	0,107	0,114	0,117
	RORC-1	0,069	0,082	0,093	0,098	0,102	0,109	0,113
	RORC-2	0,074	0,093	0,105	0,110	0,115	0,123	**0,127**
	PRORC-1	0,068	0,084	0,091	0,095	0,099	0,105	**0,124**
	PRORC-2	0,078	0,092	0,103	0,112	0,112	0,120	0,123

(cont. on the next page)

Table 4.1. (cont.)

Working Fluids	Cycle Configuration	Efficiency						
R-245fa	SORC-1	0,125	0,132	0,136	0,138	0,139	0,141	0,142
	SORC-2	0,143	0,150	0,155	0,158	0,159	0,162	0,163
	RORC-1	0,132	0,137	0,144	0,148	0,149	0,154	0,153
	RORC-2	0,144	0,153	0,160	0,163	0,166	0,171	**0,173**
	PRORC-1	0,132	0,138	0,143	0,147	0,147	0,153	**0,154**
	PRORC-2	0,148	0,156	0,162	0,165	0,167	0,171	**0,173**
R1234yf	SORC-1	0,053	0,800	0,077	0,073	0,080	0,085	0,087
	SORC-2	0,061	0,075	0,085	0,089	0,093	0,100	0,102
	RORC-1	0,054	0,067	0,081	0,077	0,086	0,093	**0,094**
	RORC-2	0,062	0,077	0,089	0,094	0,099	0,107	**0,111**
	PRORC-1	0,054	0,081	0,067	0,077	0,085	0,091	**0,094**
	PRORC-2	0,061	0,075	0,085	0,089	0,093	0,100	0,102
R-1233zd(E)	SORC-1	0,137	0,144	0,148	0,150	0,152	0,154	0,155
	SORC-2	0,156	0,164	0,169	0,172	0,174	0,177	0,178
	RORC-1	0,144	0,152	0,159	0,162	0,165	0,170	**0,172**
	RORC-2	0,160	0,169	0,177	0,180	0,184	0,189	**0,191**
	PRORC-1	0,145	0,152	0,158	0,161	0,163	0,166	0,168
	PROC-2	0,161	0,170	0,177	0,179	0,182	0,186	0,188
R1234ze(E)	SORC-1	0,076	0,086	0,093	0,096	0,099	0,103	0,097
	SORC-2	0,087	0,099	0,108	0,111	0,115	0,120	0,122
	RORC-1	0,078	0,090	0,099	0,103	0,107	0,113	0,116
	RORC-2	0,101	0,101	0,112	0,117	0,121	0,128	**0,131**
	PRORC-1	0,083	0,095	0,104	0,108	0,111	0,111	**0,118**
	PRORC-2	0,086	0,098	0,108	0,112	0,115	0,121	0,124
Cyclohexane	SORC-1	-	-	-	-	-	-	-
	SORC-2	-	-	-	-	-	-	-
	RORC-1	0,204	0,208	0,211	0,212	0,213	0,216	0,215
	RORC-2	0.203	0,208	0,210	0,212	0,213	0,216	0,217
	PRORC-1	0,218	0,221	0,220	0,221	0,206	0,166	**0,221**
	PRORC-2	0,218	0,222	0,220	0,221	0,208	0,177	**0,222**
D4	SORC-1	-	-	-	-	-	-	-
	SORC-2	-	-	-	-	-	-	-
	RORC-1	0,156	0,157	0,157	0,158	0,158	0,158	**0,158**
	RORC-2	0,157	0,159	0,159	0,159	0,160	0,160	**0,160**
	PRORC-1	-	-	-	-	-	-	-
	PRORC-2	-	-	-	-	-	-	-

(cont. on the next page)

Table 4.1. (cont.)

Ethanol	SORC-1	0,240	0,250	0,255	0,254	0,260	0,264	0,253
	SORC-2	0,271	0,278	0,284	0,287	0,289	0,293	0,295
	RORC-1	0,278	0,286	0,292	0,295	0,298	0,306	**0,305**
	RORC-2	0,302	0,311	0,318	0,321	0,324	0,301	0,331
	PRORC-1	0,262	0,270	0,276	0,279	0,281	0,286	0,288
	PRORC-2	0,284	0,291	0,298	0,301	0,303	0,308	**0,310**
Pressure Ratio		0,5	0,6	0,7	0,75	0,8	0,9	0,95

Table 4.2. The thermal efficiencies for the third engine

Working Fluids	**Cycle Configuration**	**Efficiency**						
R-134a	SORC-1	0,065	0,077	0,085	0,089	0,092	0,098	0,100
	SORC-2	0,075	0,089	0,099	0,103	0,107	0,114	0,117
	RORC-1	0,069	0,082	0,093	0,098	0,102	0,109	**0,113**
	RORC-2	0,078	0,093	0,105	0,110	0,115	0,124	**0,127**
	PRORC-1	0,068	0,081	0,091	0,095	0,099	0,105	0,108
	PRORC-2	0,078	0,092	0,103	0,108	0,120	0,120	0,123
R-245fa	SORC-1	0,117	0,132	0,136	0,138	0,139	0,141	0,142
	SORC-2	0,143	0,150	0,158	0,158	0,159	0,162	0,163
	RORC-1	0,129	0,137	0,144	0,147	0,149	0,154	**0,156**
	RORC-2	0,144	0,153	0,160	0,163	0,166	0,171	**0,173**
	PRORC-1	0,132	0,140	0,145	0,147	0,149	0,153	0,154
	PRORC-2	0,148	0,156	0,162	0,165	0,167	0,171	**0,173**
R1234yf	SORC-1	0,053	0,065	0,073	0,077	0,080	0,085	0,087
	SORC-2	0,061	0,075	0,089	0,089	0,093	0,099	0,102
	RORC-1	0,054	0,067	0,077	0,082	0,086	0,093	**0,096**
	RORC-2	0,062	0,077	0,089	0,094	0,099	0,107	**0,111**
	PRORC-1	0,054	0,067	0,077	0,081	0,085	0,083	0,094
	PRORC-2	0,063	0,078	0,090	0,095	0,099	0,107	0,110
R-1233zd(E)	SORC-1	0,136	0,143	0,147	0,149	0,151	0,154	0,154
	SORC-2	0,156	0,164	0,169	0,172	0,174	0,177	0,178
	RORC-1	0,144	0,152	0,159	0,162	0,165	0,170	**0,180**
	RORC-2	0,160	0,169	0,177	0,180	0,184	0,189	**0,191**
	PRORC-1	0,144	0,152	0,157	0,160	0,162	0,166	0,167
	PRORC-2	0,161	0,170	0,177	0,179	0,182	0,186	0,188
R1234ze(E)	SORC-1	0,076	0,086	0,093	0,096	0,099	0,101	0,105
	SORC-2	0,087	0,099	0,108	0,111	0,115	0,120	0,122
	RORC-1	0,078	0,090	0,099	0,103	0,107	0,113	**0,116**
	RORC-2	0,088	0,101	0,112	0,117	0,121	0,128	**0,131**
	PRORC-1	0,078	0,089	0,098	0,102	0,105	0,111	0,113
	PRORC-2	0,086	0,098	0,108	0,112	0,115	0,121	0,124

(cont. on the next page)

Table 4.2. (cont.)

Cyclohexane	SORC-1	-	-	-	-	-	-	-
	SORC-2	-	-	-	-	-	-	-
	RORC-1	0,204	0,208	0,211	0,212	0,213	0,216	0,215
	RORC-2	0,209	0,210	0,211	0,213	0,216	0,216	0,216
	PRORC-1	0,218	0,220	0,220	0,221	0,221	0,221	**0,221**
	PRORC-2	0,220	0,221	0,221	0,223	0,223	0,223	**0,223**
D4	SORC-1	-	-	-	-	-	-	-
	SORC-2	-	-	-	-	-	-	-
	RORC-1	0,156	0,157	0,157	0,158	0,158	0,158	**0,158**
	RORC-2	0,171	0,172	0,172	0,173	0,173	0,173	**0,173**
	PRORC-1	-	-	-	-	-	-	-
	PRORC-2	-	-	-	-	-	-	-
Ethanol	SORC-1	0,243	0,250	0,255	0,258	0,260	0,264	0,266
	SORC-2	0,271	0,278	0,284	0,287	0,289	0,293	0,295
	RORC-1	0,280	0,288	0,295	0,298	0,301	0,306	**0,308**
	RORC-2	0,302	0,311	0,318	0,321	0,324	0,329	**0,331**
	PRORC-1	0,260	0,267	0,273	0,275	0,278	0,286	0,260
	PRORC-2	0,284	0,291	0,298	0,301	0,303	0,308	0,310
Pressure Ratio		0,5	0,6	0,7	0,75	0,8	0,9	0,95

The tables on the above reveal the thermal efficiency values regarding the pressure ratio between the evaporator pressure and the critical pressure for the three configurations and eight organic fluids. The first cases indicate the low isentropic efficiency on the pump and the turbine, 75 % and 80 % respectively. Meanwhile, the second cases reveal the application of high isentropic efficiencies on the pump and turbine regarding 85 % and 90%. In previous sections, the thermal efficiencies were evaluated separately due to the engine operations. The outcomes of the simulations are summarised on the graphs between the pressure ratio and the thermal efficiency. The highest thermal efficiency for each engine are adjusted with regard to the applied working fluid.

Table 4.1 and 4.2 reveal the thermal efficiencies with regard to the applied pressure ratios and the working fluids for the three configurations for engine 1 and 3. Since, the second engine's results are almost equal to the first one, are not revealed on a table separately. On the foregoing parts, the essential comparisons are mentioned in details.

For SORC configuration on the first engine application, the highest efficiency is obtained as 15.5% with R-1233zd(E) at the 95% pressure ratio between the evaporator and the critical pressure of the organic fluid which is a promising result in terms of working fluid.

Even though the application with ethanol is also resulted at a high thermal efficiency, the outcomes with R-1233zd(E) are stable and reliable than the ethanol application. Since, R-1233zd(E) is HFO and known as the fourth generation working fluid and had lower GWP and zero ODP values. Despite the other the configurations resulted higher thermal efficiencies with the same working fluid, the SORC also have some advantages regarding the simplicity. As it is stated on Chapter 3, the SORC is can be easily implemented and operated on the engines.

Similarly, on the second engine, the greatest efficiency on the SORC is achieved with ethanol whilst, the more reliable result with R-1233zd(E) is taken into consideration. The SORC can be chosen with R-1233zd(E) at high pressure ratios on both medium and high temperature heat sources.

One of the most efficient configuration can be mentioned as RORC. On the previous chapters, it can be seen clearly on the figures.

The peak efficiency of RORC is adjusted for the first engine at the maximum pressure ratio with the organic fluid R-1233zd(E) with respect to 17.2%. In terms of thermal efficiency, the outcome also seems promising. Especially, it is satisfying that the greatest thermal efficiency is obtained with an HFO. With regard to the replacement studies with HFCs and HFOs, it is a positive progress for the waste heat recovery applications with ORC. Nevertheless, the layout of RORC is not simple as the SORC, it is still quite applicable with an additional internal heat exchanger. Even with one additional heat exchanger, the thermal efficiency is improved 2% in comparison to the SORC. For the third engine, the highest efficiency with RORC configuration is achieved at 95% pressure ratio of evaporator and critical pressure of R-1233zd(E), 18%. In table 4.2 some higher efficiencies than 18% are revealed regarding the different working fluids. For instance, the application with ethanol resulted with 30.8% thermal efficiency. The same problem occurred similar to the first engine case. The accuracy of the cycle is not sufficient satisfying regarding the issues with the temperatures. Therefore, the high flammability of ethanol is a thorny issue in terms of the temperature waste heat recovery applications. Consequently, the RORC configuration with R-1233zd(E) is an encouraging result with 18% thermal efficiency. Meanwhile, the usage of HFOs is beneficial in terms of emissions and environment.

For the first engine, the high thermal efficiencies are generally achieved with the PRORC design regarding several working fluids. However, the peak efficiency, 28.8% is adjusted

at the highest pressure ratio of evaporator and critical pressure of the ethanol. It is mentioned on the former parts that ethanol is not suitable for high temperature waste heat recovery applications. Hence, with respect to 22.1% which is the thermal efficiency value of the application of cyclohexane as the circulating working fluid. However, it is the greatest efficiency, during the calculations some problems occurred with regard to the cycle limits. Due to the fact that the critical pressure of cyclohexane is fairly high, some problems on the operation of the turbine might occur in practical applications. While the suitable working fluid is choosing for the ORC, the pressure limits of the turbine must be checked and compared with the critical pressure of the candidate working fluid.

In terms of HFOs and HFCs, 15.4% thermal efficiency is obtained with R-245fa. Even though it is widely used organic fluid regarding the high and medium temperature waste heat recovery applications, it is not preferable due to its high GWP value.

The third engine's main characteristic is the high exhaust temperature. In Table 4.2, the high thermal efficiencies are portrayed clearly. The RORC seems promising in terms of the high exhaust temperatures with eight working fluid applications. It can be asserted that RORC configuration is appropriate for the high temperature waste heat recovery applications with ORCs.

In order to make further analysis about the obtained thermal efficiencies, the efficiencies of the three engine are calculated with regard to the full load fuel load consumption. The lower heating value of the fuel is taken as 42000 kJ/kg. The first engine's fuel consumption at 100% load is stated 0.0165 kg/s. Hence, the efficiency of the 1st engine is adjusted as 46%. The second engine's fuel consumption at full load is 0.0731 kg/s, the efficiency is 39%. The last diesel engine's fuel consumption is 0.0217 kg/s and the engine efficiency is adjusted 43%. The loss through the exhaust is estimated approximately 30% for the three cases. For the first engine application, the increment in the total efficiency is approximately 6%. In accordance with the increase of the efficiency, the fuel consumption is reduced 10%. Hence, the university would account for nearly 100,000 TL. Since, the three engine efficiency is akin to each other, the same approximation can be applied for the second and the third engine.

In order to assess the sensibility of the study to the turbine and the pump, the isentropic efficiencies were increased 10% and the systems efficiencies were recalculated. The first case represents when the pump and turbine isentropic efficiency were taken as 75% and 80% respectively, whereas the second corresponds to isentropic

efficiency of 85% for the pump is rose to, and 90% for the turbine. Regarding the increment, the thermal efficiency results for the three configurations are increased approximately between 10 to 15% for both engines. For instance, the application of R-134a on the third engine, the greatest thermal efficiency is obtained as 11.3%, whereas under same operating conditions including the increased isentropic efficiencies are resulted 12.7%. The difference can be also seen on the first engine as well. R-245fa as the working fluid for the system, the highest thermal efficiency is calculated 15.4% with the low isentropic efficiencies. Meanwhile, the high isentropic efficiencies on the pump and turbine is increased the results about 2% which is 17.3% thermal efficiency.

In general, the increment of the isentropic efficiencies for the pump and the turbine is resulted with 13% increased on the thermal efficiency with regard to the three configurations and eight working fluids applications in a similar manner.

Furthermore, the thermal efficiency is not relied on only one parameter. The importance of choosing the suitable working fluid for the appropriate cycle configuration directly effects the results. Furthermore, the engine characteristics with regard to temperature and mass flow rate of the exhaust also play a key role on ORC applications. Due to the exhaust characteristic, the configurations behave in different ways. For instance, for the high exhaust temperatures, the RORC design fits better in contrast to the medium and low exhaust temperatures. However, it is not sufficient to reach higher efficiencies. Within the application of the accurate organic fluid to the cycle directly increases the thermal efficiency of the cycle. It is crucial to state that, the environmental concerns must be taken into consideration, while the working fluid is being selected. Since, the ozone depletion and the global warming are the fact of the today's world and the working fluids are directly the one of the main reasons of these problems. Hence, the third generation working fluids (HFOs) had better being chosen for the ORC applications.

CHAPTER 5 CONCLUSION

5. CONCLUSION

In the present work, three different ORC configurations were modelled with eight different working fluid candidates for three stationary diesel engines. The cycle configuration simulation models were applied numerically to comprehend the suitability of the cycles and the working fluids with respect to the exhaust characteristics of the diesel engines employed in the study. The simulation model was developed on Matlab environment.

The idea of combining a stationary ICE with an ORC was to increase the efficiency and the sustainability of the system. A comprehensive thermodynamic analysis had applied with three different cycle configurations to demonstrate the advantages of the ORC. Meanwhile, having three different engines gave the chance of investigation of the different heat sources of exhaust temperature and exhaust mass flow rate. The influence of the engine characteristics directly affected the thermal efficiency. The one of the goal of the study was to indicate the possible results of the application of ORC on different engines to enhance the overall efficiency and sustainability.

The working fluids played a key role in terms of the cycle efficiency. It was crucial to apply the right working fluid to the suitable design. Meanwhile, the exhaust gas temperature and the mass flow rate were taken into account in terms of heat input for the cycle. The three parameters were employed properly to reach high and efficient result regarding the heat recovery. In terms of working fluid selection, the environmental issues were also taken into consideration due to the global warming problem. Hence, the environmentally friendly working fluids are preferred for WHR applications with ORC.

The three thermodynamic configurations were employed to demonstrate the differences between the designs, the appropriateness to the different heat source and temperatures. The SORC and RORC were designed to use only the exhaust temperature as the heat source, whilst the PRORC used as an additional heat source, the engine cooling water. The additional heat source was used to increase the thermal efficiency and

sustainability of the system. Since, the engine cooling water was also residual heat to recover in terms of waste heat recovery. Additionally, the subcritical superheated cycle was employed for the three designs. One of the future aims of the work was to endeavour various cycle layouts such as subcritical saturated cycle to seek the feasibility of the cycles.

Throughout the study, one of the striking aspects was the behaviours of the working fluids on different engines and cycle configurations. In terms of chemical classes, HFOs gave fairly satisfied outcomes on the thermal efficiency. R-1233zd(E) fitted on the three engines and three configurations. Furthermore, the determined greatest thermal efficiencies for the first and third engines on the RORC are approximately 17.5%. The two HFO organic fluids' outcomes were not high as R-1233zd(E), R-1234yf and R-1234ze(E), are still attractive for ORC applications with regard to zero ODP and low GWP. Additionally, the maximum thermal efficiency with HFOs was acquired on RORC with R-1233zd(E). In general, the greatest thermal efficiencies were procured on the RORC configurations with HFOs, alkane and siloxane. However, in some cases PRORC was given promising thermal efficiency results. SORC design was generally resulted minimum thermal efficiency with the eight different working fluids due its layout. In addition, the SORC configuration did not compute with the working fluids, cyclohexane and D4. Despite the low thermal efficiency and issues with two specific working fluids, the SORC can be still applied as a configuration with the advantage of the simplicity.

The engines were classified with regard to exhaust temperatures. The medium and low exhaust temperature engines' thermal efficiency results were not diverse from each other. However, the size of the low temperature engine was bigger, the heat input and the pump and turbine works were slightly higher in contrast to the first engine. Apart from that, the thermal efficiency outcomes were obtained akin to each other. Generally, the high thermal efficiency values were obtained on both RORC and PRORC designs.

The third engine's primary characteristic was the high exhaust temperature. Hence, the acquired thermal efficiency outcomes were satisfied. On the third engine application, apart from cyclohexane application, the greatest thermal efficiencies were procured on the RORC configuration. As a consequence, RORC design is appropriate for high temperature exhaust gas employments. PRORC can be also employed with the accurate working fluids on low and medium exhaust temperature heat sources.

Since, the present work is analytical and any experimental test has not been applied, for the future work the idea of the study can be applied on a proper test bench. On the practical work, the components of the ORC are investigated profoundly from the economical point of view. During the calculations, the pressure drops are neglected, can be added to before the test bench application.

The working fluids are examined in details with regard to the GWP and ODP. However, the effect of the ORC on the emission has not been studied. One of the future goals is to make a detailed analysis on the emission of the ICE-ORC combine system.

REFERENCES

ACTION, C. *Technical Guidelines for the preparation of applications for the approval of innovative technologies pursuant to Regulation (EC) No 443/2009 of the European Parliament and of the*. Retrieved from

Algieri, A., & Morrone, P. (2012). Comparative energetic analysis of high-temperature subcritical and transcritical Organic Rankine Cycle (ORC). A biomass application in the Sibari district. *Applied Thermal Engineering, 36*, 236-244.

Algrain, M., & Hopmann, U. (2003). *Diesel engine waste heat recovery utilizing electric turbocompound technology.* Paper presented at the DEER Conf., Newport, Rhode Island.

Amicabile, S., Lee, J.-I., & Kum, D. (2015). A comprehensive design methodology of organic Rankine cycles for the waste heat recovery of automotive heavy-duty diesel engines. *Applied Thermal Engineering, 87*, 574-585.

Arsie, I., Cricchio, A., Pianese, C., Ricciardi, V., & De Cesare, M. (2016). *Modeling and Optimization of Organic Rankine Cycle for Waste Heat Recovery in Automotive Engines* (0148-7191). Retrieved from

Auld, A., Berson, A., & Hogg, S. (2013). Organic Rankine cycles in waste heat recovery: a comparative study. *International Journal of Low-Carbon Technologies, 8*(suppl 1), i9-i18.

Bamgbopa, M. O. (2012). *Modeling and performance evaluation of an organic Rankine cycle (ORC) with R245FA as working fluid.* MIDDLE EAST TECHNICAL UNIVERSITY.

Bianchi, M., & De Pascale, A. (2011). Bottoming cycles for electric energy generation: parametric investigation of available and innovative solutions for the exploitation of low and medium temperature heat sources. *Applied Energy, 88*(5), 1500-1509.

Bombarda, P., Invernizzi, C. M., & Pietra, C. (2010). Heat recovery from Diesel engines: A thermodynamic comparison between Kalina and ORC cycles. *Applied Thermal Engineering, 30*(2), 212-219.

Boretti, A. A. (2012). Transient operation of internal combustion engines with Rankine waste heat recovery systems. *Applied Thermal Engineering, 48*, 18-23.

Bracco, R., Clemente, S., Micheli, D., & Reini, M. (2013). Experimental tests and modelization of a domestic-scale ORC (Organic Rankine Cycle). *Energy, 58*, 107-116.

Bredel, D. E., Nickl, I. J., & Bartosch, D.-I. S. (2011). Waste heat recovery in drive systems of today and tomorrow. *MTZ worldwide eMagazine, 72*(4), 52-56.

Briggs, T. E., Wagner, R., Edwards, K. D., Curran, S., & Nafziger, E. (2010). *A waste heat recovery system for light duty diesel engines* (0148-7191). Retrieved from
Capano, G. (2014). Waste Heat Recovery Systems for Fuel Economy.

Cengel, Y. A., & Boles, M. A. (1994). Thermodynamics: an engineering approach. *Sea, 1000*, 8862.

CHANGE, I.-I. P. O. C. (2007). IPCC fourth assessment report: climate change 2007. *Cambridge, 104p*.

Chen, H., Goswami, D. Y., & Stefanakos, E. K. (2010). A review of thermodynamic cycles and working fluids for the conversion of low-grade heat. *Renewable and Sustainable Energy Reviews, 14*(9), 3059-3067.

Chena Power, L. (2007). 400kW Geothermal Power Plant at Chena Hot Springs, Alaska. *Final Report for Alaska Energy Authority*.

Daccord, R., Melis, J., Kientz, T., Darmedru, A., Pireyre, R., Brisseau, N., & Fonteneau, E. (2013). Exhaust heat recovery with Rankine piston expander. *Proceedings of ICE Powertrain Electrification & Energy Recovery, Rueil-Malmaison, France, 28*.

Desideri, A., Gusev, S., van den Broek, M., Lemort, V., & Quoilin, S. (2016). Experimental comparison of organic fluids for low temperature ORC (organic Rankine cycle) systems for waste heat recovery applications. *Energy, 97*, 460-469.

Designation, N. (1993). Safety Classification of Refrigerants. *ASHRAE Standard, ANSI/ASHRAE*.

Dolz, V., Novella, R., García, A., & Sánchez, J. (2012). HD Diesel engine equipped with a bottoming Rankine cycle as a waste heat recovery system. Part 1: Study and analysis of the waste heat energy. *Applied Thermal Engineering, 36*, 269-278.

Domingues, A., Santos, H., & Costa, M. (2013). Analysis of vehicle exhaust waste heat recovery potential using a Rankine cycle. *Energy, 49*, 71-85.

EPA. (2014). Retrieved from https://www.epa.gov/ghgemissions/overview-greenhouse-gases

EPA. (2016, 18/10/2016). Retrieved from https://www.epa.gov/aboutepa

Eyerer, S., Wieland, C., Vandersickel, A., & Spliethoff, H. (2016). Experimental study of an ORC (Organic Rankine Cycle) and analysis of R1233zd-E as a drop-in replacement for R245fa for low temperature heat utilization. *Energy, 103*, 660-671.

Falano, T., Jeswani, H. K., & Azapagic, A. (2014). Assessing the environmental sustainability of ethanol from integrated biorefineries. *Biotechnology journal, 9*(6), 753-765.

Fernández, F., Prieto, M., & Suárez, I. (2011). Thermodynamic analysis of high-temperature regenerative organic Rankine cycles using siloxanes as working fluids. *Energy, 36*(8), 5239-5249.

Gao, H., Liu, C., He, C., Xu, X., Wu, S., & Li, Y. (2012). Performance analysis and working fluid selection of a supercritical organic Rankine cycle for low grade waste heat recovery. *Energies, 5*(9), 3233-3247.

Glavatskaya, Y., Olivier, G., Podevin, P., & Shonda, O. F. (2011). *Heat Recovery Systems within passenger cars.* Paper presented at the International Congress Automotive and environment CAR.

Guide, M. U. s. (1998). The mathworks. *Inc., Natick, MA, 5*, 333.

Hærvig, J., Sørensen, K., & Condra, T. J. (2016). Guidelines for optimal selection of working fluid for an organic Rankine cycle in relation to waste heat recovery. *Energy, 96*, 592-602.

He, C., Liu, C., Gao, H., Xie, H., Li, Y., Wu, S., & Xu, J. (2012). The optimal evaporation temperature and working fluids for subcritical organic Rankine cycle. *Energy, 38*(1), 136-143.

Horst, T. A., Tegethoff, W., Eilts, P., & Koehler, J. (2014). Prediction of dynamic rankine cycle waste heat recovery performance and fuel saving potential in passenger car applications considering interactions with vehicles' energy management. *Energy Conversion and Management, 78*, 438-451.

Hossain, S. N., & Bari, S. (2013). Waste heat recovery from the exhaust of a diesel generator using Rankine Cycle. *Energy Conversion and Management, 75*, 141-151.

Houghton, J., Jenkins, C., & Ephraums, J. (1990). Climate Change: The IPCC Scientific Assessment, report of the United Nations Environment Programme, Intergovernmental Panel on Climate Change (IPCC): Cambridge University Press, Cambridge and New York.

Hountalas, D., Katsanos, C., Kouremenos, D., & Rogdakis, E. (2007). Study of available exhaust gas heat recovery technologies for HD diesel engine applications. *International Journal of Alternative Propulsion, 1*(2-3), 228-249.

Hountalas, D., & Mavropoulos, G. (2010). *Potential for improving HD diesel truck engine fuel consumption using exhaust heat recovery techniques*: INTECH Open Access Publisher.

Hung, T.-C. (2001). Waste heat recovery of organic Rankine cycle using dry fluids. *Energy Conversion and Management, 42*(5), 539-553.

Hung, T.-C., Shai, T., & Wang, S. (1997). A review of organic Rankine cycles (ORCs) for the recovery of low-grade waste heat. *Energy, 22*(7), 661-667.

Invernizzi, C. M., Iora, P., Preßinger, M., & Manzolini, G. (2016). HFOs as substitute for R-134a as working fluids in ORC power plants: A thermodynamic assessment and thermal stability analysis. *Applied Thermal Engineering, 103*, 790-797.

Jarall, S. (2012). Study of refrigeration system with HFO-1234yf as a working fluid. *International journal of refrigeration, 35*(6), 1668-1677.

Jumel, S., Feidt, M., & Kheiri, A. Working fluid selection and performance comparison of subcritical and supercritical organic Rankine cycle (ORC) for low-temperature waste heat recovery.

Kokic, P., Crimp, S., & Howden, M. (2014). A probabilistic analysis of human influence on recent record global mean temperature changes. *Climate Risk Management, 3*, 1-12.

Kuo, C.-R., Hsu, S.-W., Chang, K.-H., & Wang, C.-C. (2011). Analysis of a 50kW organic Rankine cycle system. *Energy, 36*(10), 5877-5885.

Law, R., Harvey, A., & Reay, D. (2013). Opportunities for low-grade heat recovery in the UK food processing industry. *Applied Thermal Engineering, 53*(2), 188-196.

LEGMAN, H., & Citrin, D. (2004). Low grade heat recovery. *World cement, 35*(4), 111-116.

Lemmon, E. W., Huber, M. L., & McLinden, M. O. (2002). NIST reference fluid thermodynamic and transport properties–REFPROP: version.

Liu, B.-T., Chien, K.-H., & Wang, C.-C. (2004). Effect of working fluids on organic Rankine cycle for waste heat recovery. *Energy, 29*(8), 1207-1217.

Liu, W., Meinel, D., Wieland, C., & Spliethoff, H. (2014). Investigation of hydrofluoroolefins as potential working fluids in organic Rankine cycle for geothermal power generation. *Energy, 67*, 106-116.

Luo, D., Mahmoud, A., & Cogswell, F. (2015). Evaluation of Low-GWP fluids for power generation with Organic Rankine Cycle. *Energy, 85*, 481-488.

Matsuda, K. (2014). Low heat power generation system. *Applied Thermal Engineering, 70*(2), 1056-1061.

Molés, F., Navarro-Esbrí, J., Peris, B., Mota-Babiloni, A., Barragán-Cervera, Á., & Kontomaris, K. K. (2014). Low GWP alternatives to HFC-245fa in Organic Rankine Cycles for low temperature heat recovery: HCFO-1233zd-E and HFO-1336mzz-Z. *Applied Thermal Engineering, 71*(1), 204-212.

Nasir, P., Jones, S., Buchanan, T., & Posner, D. (2004). Turning recovered heat to power. *Pipe and Technologies*.

Oluleye, G., Jobson, M., Smith, R., & Perry, S. J. (2016). Evaluating the potential of process sites for waste heat recovery. *Applied Energy, 161*, 627-646.

Patel, P. S., & Doyle, E. F. (1976). *Compounding the truck diesel engine with an organic Rankine-cycle system* (0148-7191). Retrieved from

Peralez, J., Tona, P., Lepreux, O., Sciarretta, A., Voise, L., Dufour, P., & Nadri, M. (2013). *Improving the control performance of an organic rankine cycle system for waste heat recovery from a heavy-duty diesel engine using a model-based approach.* Paper presented at the 52nd IEEE Conference on Decision and Control.

Peris, B., Navarro-Esbrí, J., & Molés, F. (2013). Bottoming organic Rankine cycle configurations to increase Internal Combustion Engines power output from cooling water waste heat recovery. *Applied Thermal Engineering, 61*(2), 364-371.

Petr, P., & Raabe, G. (2015). Evaluation of R-1234ze (Z) as drop-in replacement for R-245fa in Organic Rankine Cycles–From thermophysical properties to cycle performance. *Energy, 93*, 266-274.

Pischinger, R., Klell, M., & Sams, T. (2009). *Thermodynamik der Verbrennungskraftmaschine*: Springer-Verlag.

Protocol, K. (1997). United Nations framework convention on climate change. *Kyoto Protocol, Kyoto, 19*.

Protocol, M. (1987). Montreal protocol on substances that deplete the ozone layer. *Final Act, United Nations Environmental Program, Nairobi*.

Punov, P., Lacour, S., Périlhon, C., Podevin, P., Descombes, G., & Evtimov, T. (2015). Numerical study of the waste heat recovery potential of the exhaust gases from a tractor engine. *Proceedings of the Institution of Mechanical Engineers, Part D: Journal of Automobile Engineering*, 0954407015577530.

Qiu, K., & Hayden, A. (2012). Integrated thermoelectric and organic Rankine cycles for micro-CHP systems. *Applied Energy, 97*, 667-672.

Quoilin, S., & Lemort, V. (2009). Technological and economical survey of organic Rankine cycle systems.

Quoilin, S., Van Den Broek, M., Declaye, S., Dewallef, P., & Lemort, V. (2013). Techno-economic survey of Organic Rankine Cycle (ORC) systems. *Renewable and Sustainable Energy Reviews, 22*, 168-186.

Saleh, B., Koglbauer, G., Wendland, M., & Fischer, J. (2007). Working fluids for low-temperature organic Rankine cycles. *Energy, 32*(7), 1210-1221.

Secretariat, O. (2000). The Montreal protocol on substances that deplete the ozone layer. *United Nations Environment Programme, Nairobi, Kenya*.

Shu, G., Li, X., Tian, H., Liang, X., Wei, H., & Wang, X. (2014). Alkanes as working fluids for high-temperature exhaust heat recovery of diesel engine using organic Rankine cycle. *Applied Energy, 119*, 204-217.

Shu, G., Yu, G., Tian, H., Wei, H., & Liang, X. (2014). A multi-approach evaluation system (MA-ES) of Organic Rankine Cycles (ORC) used in waste heat utilization. *Applied Energy, 132*, 325-338.

Siddiqi, M. A., & Atakan, B. (2012). Alkanes as fluids in Rankine cycles in comparison to water, benzene and toluene. *Energy, 45*(1), 256-263.

SIEMENS. (2014). Waste Heat Recovery with Organic Rankine Cycle Technology. Retrieved from http://www.siemens.com/press/en/feature/2014/energy/2014-04-orc.php. N.p., n.d. Web.

Solomon, S., Mills, M., Heidt, L., Pollock, W., & Tuck, A. (1992). On the evaluation of ozone depletion potentials. *Journal of Geophysical Research: Atmospheres, 97*(D1), 825-842.

Sprouse, C., & Depcik, C. (2013). Review of organic Rankine cycles for internal combustion engine exhaust waste heat recovery. *Applied Thermal Engineering, 51*(1), 711-722.

Standard, A. (2001). Standard 34-2001. *Designation and Safety Classification of Refrigerant. ASHRAE: Atlanta, GA*.

Tartière, T. (2015). Analysis of the Organic Rankine Cycle Market. Retrieved from http://orc-world-map.org/analysis.html

Tchanche, B. F., Lambrinos, G., Frangoudakis, A., & Papadakis, G. (2011). Low-grade heat conversion into power using organic Rankine cycles–A review of various applications. *Renewable and Sustainable Energy Reviews, 15*(8), 3963-3979.

Teng, H. (2010a). Waste heat recovery concept to reduce fuel consumption and heat rejection from a diesel engine. *SAE International Journal of Commercial Vehicles, 3*(2010-01-1928), 60-68.

Teng, H. (2010b). Waste heat recovery concept to reduce fuel consumption and heat rejection from a diesel engine. *SAE International Journal of Commercial Vehicles, 3*(1), 60-68.

Teng, H., Klaver, J., Park, T., Hunter, G. L., & van der Velde, B. (2011). *A rankine cycle system for recovering waste heat from HD diesel engines-WHR system development* (0148-7191). Retrieved from

Tian, H., Chang, L., Gao, Y., Shu, G., Zhao, M., & Yan, N. (2017). Thermo-economic analysis of zeotropic mixtures based on siloxanes for engine waste heat recovery using a dual-loop organic Rankine cycle (DORC). *Energy Conversion and Management, 136*, 11-26.

Tian, H., Shu, G., Wei, H., Liang, X., & Liu, L. (2012). Fluids and parameters optimization for the organic Rankine cycles (ORCs) used in exhaust heat recovery of Internal Combustion Engine (ICE). *Energy, 47*(1), 125-136.

Unfccc, U. (2009). *Kyoto Protocol Reference Manual on Accounting of Emissions and Assigned Amount*. Retrieved from

Union, E. (2006). Directive 2006/40/EC of the European Parliament and of the Council of 17 May 2006 relating to emissions from air-conditioning systems in motor vehicles and Amending Council Directive 70/156/EEC. *Off J Eur Union, 1*.

UNION, P. (2006). REGULATION (EC) No 1907/2006 OF THE EUROPEAN PARLIAMENT AND OF THE COUNCIL.

Uusitalo, A., Honkatukia, J., Turunen-Saaresti, T., & Larjola, J. (2014). A thermodynamic analysis of waste heat recovery from reciprocating engine power plants by means of Organic Rankine Cycles. *Applied Thermal Engineering, 70*(1), 33-41.

Vaja, I., & Gambarotta, A. (2010). Internal combustion engine (ICE) bottoming with organic Rankine cycles (ORCs). *Energy, 35*(2), 1084-1093.

Wang, E., Zhang, H., Fan, B., Ouyang, M., Zhao, Y., & Mu, Q. (2011). Study of working fluid selection of organic Rankine cycle (ORC) for engine waste heat recovery. *Energy, 36*(5), 3406-3418.

Wang, Z., Zhou, N., Guo, J., & Wang, X. (2012). Fluid selection and parametric optimization of organic Rankine cycle using low temperature waste heat. *Energy, 40*(1), 107-115.

Weerasinghe, W., Stobart, R., & Hounsham, S. (2010). Thermal efficiency improvement in high output diesel engines a comparison of a Rankine cycle with turbo-compounding. *Applied Thermal Engineering, 30*(14), 2253-2256.

Yang, M.-H., & Yeh, R.-H. (2015). Thermo-economic optimization of an organic Rankine cycle system for large marine diesel engine waste heat recovery. *Energy, 82*, 256-268.

Yang, M.-H., & Yeh, R.-H. (2016). Economic performances optimization of an organic Rankine cycle system with lower global warming potential working fluids in geothermal application. *Renewable Energy, 85*, 1201-1213.

Yu, H., Feng, X., & Wang, Y. (2015). A new pinch based method for simultaneous selection of working fluid and operating conditions in an ORC (Organic Rankine Cycle) recovering waste heat. *Energy, 90*, 36-46.

Zhang, X., He, M., & Zhang, Y. (2012). A review of research on the Kalina cycle. *Renewable and Sustainable Energy Reviews, 16*(7), 5309-5318.

APPENDIX A

THE REFERENCE CALCULATIONS

1.The Simple Organic Rankine Cycle Calculation

The Properties of R134a,

$P_{critical}$= 4.059 MPa = 4059 kPa

$T_{critical}$= 374.2 K

1st Type of Generators' Calculations (TEKSAN)

The Properties of the Exhaust Gas,

$\dot{m}_{exh}$= 0.533 kg/sn

T_{exh}= 509 ^{0}C

$C_{p,exh=}$ 1.10 kJ/kg K (See Appendix B)

1st case,

$\frac{Peva}{Pcr} = 0.95$ and all the assumptions are the same as the previous calculations.

$P_{eva} = P_{cr} \times 0.95 = 4059 \times 0.95 = 3856.05\ kPa$

$P_{eva} = P_2 = P_2$,

State 1 (Saturated liquid)

T_{cond} = 35 ^{0}C so,

$P_{sat@35℃}$ = 887.91 kPa

$hf_{sat@35℃}$ = 249.2 kj/kg

$\vartheta_{fsat@35℃}$ = 0.0009 m^3/kg

$s_{gsat@35℃}$ = 1.7138 kJ/kg K

$h_{gsat@35℃}$=417.5 kJ/kg

State 2 (Compressed liquid but the state is assumed as saturated liquid)

$P_2 = 3856.05\ kPa$

$h_{2s} = h_1 + \vartheta_1 \times (P_2 - P_1) = 249.2 + 0.0009 \times (3856.05 - 887.91) = 251.87\ kJ/kg$

$$\frac{h_{2s} - h_1}{h_{2a} - h_1} = \eta s = \frac{251.87 - 249.2}{h_{2a} - 249.2} = 75\% \rightarrow h_{2a} = 252.76\ kJ/kg$$

$T_{2a} = 37.5℃$

$T_{min} = T_2 + \Delta T = 37.5℃ + 30 = 67.5\ ℃$

State 2' (Saturated liquid)

$T_{2'} = T_{sat@Peva} = T_{at@3856.05\ kPa} = 98.5\ ^0\text{C}$

$h_{2'} = h_{2'f} = 365\ kJ/kg$

$T_{pp} = T_{2'} + \Delta T_{pp} = 401.5\ K$ ps. $\Delta T_{pp} = 30\ K$

State 3 (Superheated Vapour)

$P_3 P3 = 3856.05\ kPa$

$s_{gsat@35℃} = s_3 = 1.7138\ kJ/kgK$

$T_3 = 105\ ℃$

$h_3 = 444\ kJ/kg$

1st energy balance inside the evaporator,

$$\dot{m}_{wf} = \frac{\dot{m}_{exhuast} \times Cp_{exhuast} \times (T_{exh,in} - T_{exh,pp})}{h_3 - h_{2'}} = \frac{0.533 \times 1.10 \times (782 - 401.5)}{(444 - 365)}$$

$$= 2.82\ kg/s$$

$$T_{exh,out} = T_{exh,pp} - \frac{(h_{2'} - h_2) \times \dot{m}_{wf1}}{\dot{m}_{exhuast} \times Cp_{exhuast}} = 401.5 - \frac{(365 - 252.76) \times 2.82}{(0.533 \times 1.10)}$$

$$= -138.35\ K < Tmin$$

2nd part of energy balance,

$$\dot{m}_{wf2} = \frac{\dot{m}_{exhuast} \times Cp_{exhuast} \times (T_{exh,in} - T_{min})}{h_3 - h_{2a}} = \frac{0.533 \times 1.10 \times (782 - 340.5)}{(444 - 252.76)}$$

$$= 1.35\ kg/s$$

$$\dot{Q}in = \dot{m}_{wf2} \times (h_3 - h_{2a}) = 1.35 \times (444 - 252.76) = 258.174\ kW$$

ps. $\frac{h3-h4a}{h3-h4s} = 0.80$; $\frac{444-h4a}{444-417.5} = 0.80 \rightarrow h4a = 422.8\ kJ/kg$

$$\dot{W}turbine = \dot{m}_{wf2} \times (h_3 - h_{4a}) = 1.35 \times (444 - 422.8) = 28.62\ kW$$

$$\dot{W}pump = \dot{m}_{wf2} \times (h_{2a} - h_1) = 1.35 \times (252.76 - 249.2) = 4.8\ kW$$

$$\dot{W}net = \dot{W}turbine - \dot{W}pump = 23.82\ kW$$

$$\eta cycle = \frac{\dot{W}net}{\dot{Q}in} = 0.09$$

2nd case,

$\frac{Peva}{Pcr} = 0.75$ and all the assumptions are the same as the previous calculations.

$$P_{eva} = P_{cr} \times 0.75 = 4059 \times 0.75 = 3044.25\ kPa$$

$$P_{eva} = P_2 = P_{2'}$$

State 1 (Saturated liquid)

$T_{cond} = 35\ ^0$C so,

$P_{sat@35℃} = 887.91$ kPa

$hf_{sat@35℃} = 249.2$ kJ/kg

$\vartheta_{fsat@35℃} = 0.0009$ m^3/kg

$s_{gsat@35℃} = 1.7138$ kJ/kg K

$h_{gsat@35℃} = 417.5$ kJ/kg

State 2 (Compressed liquid but the state is assumed as saturated liquid)

$P_2 = 3044.25\ kPa$

$h_{2s} = h_1 + \vartheta_1 \times (P_2 - P_1) = 249.2 + 0.0009 \times (3044.25 - 887.91) = 251.14\ kJ/kg$

$$\frac{h_{2s} - h_1}{h_{2a} - h_1} = \eta s = \frac{251.14 - 249.2}{h_{2a} - 249.2} = 75\% \rightarrow h_{2a} = 251.78\ kJ/kg$$

$T_{2a} = 36.5℃$

$T_{min} = T_2 + \Delta T = 36.5℃ + 30 = 66.5℃$

State 2' (Saturated liquid)

$T_{2'} = T_{sat@Peva} = T_{sat@3044.25kPa} = 87\ ^0$C

$h_{2'} = h_{2'f} = 336.9\ kJ/kg$

$T_{pp} = T_{2'} + \Delta T_{pp} = 390\ K$ ps. $\Delta T_{pp} = 30\ K$

State 3 (Superheated Vapour)

$P_3 = 3044.25\ kPa$

$s_{gsat@35℃} = s_3 = 1.7138\ kJ/kgK$

$T_3 = 93$ ℃

$h_3 = 441.4\ kJ/kg$

1st energy balance inside the evaporator,

$$\dot{m}_{wf} = \frac{\dot{m}_{exhuast} \times Cp_{exhuast} \times (T_{exh,in} - T_{exh,pp})}{h_3 - h_{2'}} = \frac{0.533 \times 1.10 \times (782 - 390)}{(441.4 - 336.9)}$$

$$= 2.19\ kg/s$$

$$T_{exh,out} = T_{exh,pp} - \frac{(h_{2'} - h_2)\times\dot{m}_{wf1}}{\dot{m}_{exhuast}\times Cp_{exhuast}} = 390 - \frac{2.19\times(336.9 - 251.78)}{(0.533\times1.10)}$$
$$= 70.69\ K < Tmin\ so,$$

2nd part of energy balance,

$\dot{m}wf2 = \frac{\dot{m}_{exhuast}\times Cp_{exhuast}\times(T_{exh,in} - T_{min})}{h_3 - h_{2a}} = \frac{0.533\times1.10\times(782-339.5)}{(441.4-251.78)} = 1.368\ kg/s$ (The mass flow rate of the system.)

$\dot{Q}in = \dot{m}_{wf2}\times(h_3 - h_{2a}) = 1.368\times(441.4 - 251.78) = 259.43\ kW$

ps. $\frac{h3-h4a}{h3-h4s} = 0.80$; $\frac{441.1-h4a}{441.1-417.5} = 0.80 \rightarrow h4a = 422.28\ kJ/kg$

$\dot{W}turbine = \dot{m}_{wf2}\times(h_3 - h_{4a}) = 1.368\times(441.1 - 422.28) = 26.156\ kW$

$\dot{W}pump = \dot{m}_{wf2}\times(h_{2a} - h_1) = 1.368\times(251.78 - 249.2) = 3.52\ kW$

$\dot{W}net = \dot{W}turbine - \dot{W}pump = 22.62\ kW$

$\eta cycle = \frac{\dot{W}net}{\dot{Q}in} = 8.7\%$

3rd case,

$\frac{P_{eva}}{P_{cr}} = 0.50$ and all the assumptions are the same as the previous calculations.

$P_{eva} = P_{cr}\times 0.75 = 4059\times0.50 = 2029.5\ kPa$
$P_{eva} = P_2 = P_{2'}$

State 1 (Saturated liquid)

$T_{cond} = 35\ ^0$C so,

$P_{sat@35℃} = 887.91$ kPa

hfsat@35℃ = 249.2 kJ/kg

$\vartheta_{fsat@35℃} = 0.0009$ m^3/kg

$s_{gsat@35℃} = 1.7138$ kJ/kg K

$h_{gsat@35℃}$=417.5 kj/kg

State 2 (Compressed liquid but the state is assumed as saturated liquid)

$P2 = 2029.5\ kPa$

$h_{2s} = h_1 + \vartheta_1 \times (P_2 - P_1) = 249.2 + 0.0009 \times (2029.5 - 887.91) = 250.22\ kJ/kg$

$$\frac{h_{2s} - h_1}{h_{2a} - h_1} = \eta s = \frac{250.22 - 249.2}{h2a - 249.2} = 75\% \rightarrow h2a = 250.56\ kJ/kg$$

$T_{2a} = 36℃$

$T_{min} = T_2 + \Delta T = 36℃ + 30 = 66℃$

State 2' (Saturated liquid)

$T2' = Tsat@Peva = Tsat@2029.5Pa = 68\ ^0$C

$h2' = h2'f = 301.3\ kj/kg$

$Tpp = T2' + \Delta Tpp = 371\ K$ ps. $\Delta Tpp = 30\ K$

State 3 (Superheated Vapour)

$P_3 = 2029.5\ kPa$

$s_{gsat@35℃} = s_3 = 1.7138\ kj/kgK$

$T_3 = 72$ ℃

$h_3 = 435\ kJ/kg$

1st energy balance inside the evaporator,

$$\dot{m}_{wf1}=\frac{\dot{m}_{exhuast}\times Cp_{exhuast}\times(T_{exh,in}-T_{exh,pp})}{h_3-h_{2\prime}}=\frac{0.533\times1.10\times(782-371)}{(435-301.3)}1.80\ kg/s$$

$$T_{exh,out}=T_{exh,pp}-\frac{(h_{2\prime}-h_2)\times\dot{m}_{wf1}}{\dot{m}_{exhuast}\times Cp_{exhuast}}=371-\frac{1.80\times(301.3-250.56)}{(0.533\times1.10)}=215$$

$$<Tmin$$

2nd part of energy balance,

$\dot{m}_{wf2}=\frac{\dot{m}_{exhuast}\times Cp_{exhuast}\times(T_{exh,in}-T_{min})}{h_3-h_{2a}}=\frac{0.533\times1.10\times(782-339)}{(435-250.56)}=1.40\ kg/s$ (The mass flow rate of the system.)

$$\dot{Q}in=\ \dot{m}_{wf2}\times(h_3-h_{2a})\ =1.40\times(435-250.56)=259.73\ kW$$

ps. $\frac{h3-h4a}{h3-h4s}=0.80$; $\frac{435-h4a}{435-417.5}=0.80\ \rightarrow h4a=421\ kj/kg$

$$\dot{W}turbine=\dot{m}_{wf2}\times(h_3-h_{4a})\ =1.40\times(435-421)=19.6\ kW$$

$$\dot{W}pump=\ \dot{m}_{wf2}\times(h_{2a}-h_1)\ \ =1.40\times(250.56-249.2)=1.904\ kW$$

$$\dot{W}net=\dot{W}turbine-\dot{W}pump=17.696\ kW$$

$$\eta cycle=\frac{\dot{W}net}{\dot{Q}in}=6.81\%$$

2.The Regenerative Organic Rankine Cycle Calculations

1st case,

$$\frac{Peva}{Pcr}=0.95$$

$$P_{eva}=P_{cr}\times0.95=4059\times0.95=3856.05\ kPa$$

$$P_{eva}=P_2=P_{2\prime}=P_{2R}$$

1st Type of Generators' Calculations (TEKSAN)

The Properties of the Exhaust Gas,

$\dot{m}_{exh}$= 0.533 kg/s

T_{exh}= 509 ^{0}C

- The Cp of the exhaust gas is calculated as 1.10 kJ/kg K

State 1 (Saturated liquid)

T_{cond} = 35 ^{0}C so,

$P_{sat@35℃}$ = 887.91 kPa

hfsat@35℃ = 249.2 kJ/kg

$\vartheta_{fsat@35℃}$ = 0.0009 m^3/kg

$s_{gsat@35℃}$ = 1.7138 kJ/kg K

$h_{gsat@35℃}$=417.5 kJ/kg

State 2 (Compressed liquid but the state is assumed as saturated liquid)

$P_2 = 3856.05\ kPa$

$h_{2s} = h_1 + \vartheta_1 \times (P_2 - P_1) = 249.2 + 0.0009 \times (3856.05 - 887.91) = 251.87\ kJ/kg$

$$\frac{h_{2s} - h_1}{h_{2a} - h_1} = \eta s = \frac{251.87 - 249.2}{h_{2a} - 249.2} = 75\% \rightarrow h2a = 252.76\ kJ/kg$$

$$T_{2a} = 37.5℃$$

State 2R (The state after the Heat Exchanger)

$h_{2R} - h_2 = h_4 - h_{4R}$

$h_{2R} = h_2 + (h_4 - h_{4R})$

$h_{2R} = 252.76 + (444.2 - 438) = 258.96\ kj/kg$

$T_{2R} = 43℃$

$T_{min} = T_{2R} + \Delta T = 43℃ + 30 = 73\ ℃$ ps.$\Delta T = 30\ K$

State 4R (Superheated Vapour)

$P_{cond} = P_{4R} = 887.5\ kPa$

$T_{4R} = T_2 + \Delta T_{approach} = 55℃ \qquad \Delta Tapp = 15K$

$h_{4R} = 438\ kJ/kg$

$s_{4R} = 1.7785\ kJ/kgK$

State 4 (Superheated Vapour)

$h_{4R} = h_{4s}\ (Assumption)$

$$\frac{h_3 - h_4}{h_3 - (h_{4s} = h_{4R})} = 0.80 = \frac{469 - h4}{469 - 438} = 0.80 \quad h4 = 444.2\ kJ/kg$$

State 2' (Saturated liquid)

$T_{2'} = T_{Sat@Peva} = T_{sat@3856.05\ kPa} = 98.5\ ^0\text{C}$

$h_{2'} = h_{2'f} = 365kJ/kg$

$T_{pp} = T_{2'} + \Delta T_{pp} = 401.5\ K \qquad \text{ps. } \Delta Tpp = 30\ K$

State 3 (Superheated Vapour)

$P_3 = 3856.05\ kPa$

$s_3 = s_{4R} = 1.7785\ kJ/kgK$

$T_3 = 120℃$

$h_3 = 469\ kJ/kg$

1st energy balance inside the evaporator,

$$\dot{m}_{wf1} = \frac{\dot{m}_{exhuast} \times Cp_{exhuast} \times (T_{exh,in} - T_{exh,pp})}{h_3 - h_{2'}} = \frac{0.553 \times 1.1 \times (782 - 401.5)}{(469 - 365)}$$

$$= 2.145\ kg/s$$

$$T_{exh,out} = T_{exh,pp} - \frac{(h_{2,} - h_2)\times \dot{m}_{wf1}}{\dot{m}_{exhuast}\times Cp_{exhuast}} \qquad = 401.5 - \frac{(365 - 258.96)\times 2.145}{0.533\times 1.10}$$

$$= 13.53\ K < Tmin$$

2nd part of energy balance,

$$\dot{m}wf2 = \frac{\dot{m}_{exhuast}\times Cp_{exhuast}\times(T_{exh,in} - T_{min})}{h_3 - h_{2R}} = \frac{0.533\times 1.10\times(782-(73+273)}{(469-258.96)} = 1.21\ kg/s$$

$$\dot{Q}in = \dot{m}_{wf2} \times (h_3 - h_{2R}) = 1.21\times(469 - 258.96) = 255.62\ kW$$

ps. $\frac{h3-h4a}{h3-h4s} = 0.80$; $\frac{469-h4a}{469-438} = 0.80 \rightarrow h4 = 444.2\ kj/kg$

$$\dot{W}turbine = \dot{m}_{wf2} \times (h_3 - h_{4a}) = 1.21\times(469 - 444.2) = 30\ kW$$

$$\dot{W}pump = \dot{m}_{wf2} \times (h_{2a} - h_1) = 1.21\times(252.76 - 249.2) = 4.3\ kW$$

$$\dot{W}net = \dot{W}turbine - \dot{W}pump = 25.69\ kW$$

$$\eta cycle = \frac{\dot{W}net}{\dot{Q}in} = 10\%$$

2nd case,

$$\frac{Peva}{Pcr} = 0.75$$

$$P_{eva} = P_{cr}\times 0.75 = 4059\times 0.75 = 3044.25\ kPa$$

$$P_{eva} = P_2 = P_{2,} = P_{2R}$$

State 1 (Saturated liquid)

T_{cond} = 35 ^{0}C so,

$P_{sat@35℃}$ = 887.91 kPa

$hf_{\text{sat@35℃}} = 249.2$ kJ/kg

$\vartheta_{f\text{sat@35℃}} = 0.0009$ m^3/kg

$s_{g\text{sat@35℃}} = 1.7138$ kJ/kg K

$h_{g\text{sat@35℃}} = 417.5$ kJ/kg

State 2 (Compressed liquid but the state is assumed as saturated liquid)

$P_2 = 3044.25\ kPa$

$h_{2s} = h_1 + \vartheta_1 \times (P_2 - P_1) = 249.2 + 0.0009 \times (3044.25 - 887.91) = 251.14\ kJ/kg$

$$\frac{h_{2s} - h_1}{h_{2a} - h_1} = \eta s = \frac{251.14 - 249.2}{h_{2a} - 249.2} = 75\% \rightarrow h_{2a} = 251.78\ kJ/kg$$

$T_{2a} = 36.5$℃

State 2R (The state after the Heat Exchanger)

$h_{2R} - h_2 = h_4 - h_{4R}$

$h_{2R} = h_2 + (h_4 - h_{4R})$

$h_{2R} = 251.78 + (438.36 - 433) = 257.14\ kj/kg$

$T_{2R} = 40.5$℃

$T_{min} = T_{2R} + \Delta T = 40.5℃ + 30 = 73.5$ ℃ ps. $\Delta T = 30\ K$

State 4R (Superheated Vapour)

$P_{cond} = P_{4R} = 887.5\ kPa$

$T_{4R} = T_2 + \Delta T_{approach} = 36.5℃ + 15 = 51.5℃ \qquad \Delta T app = 15K$

$h_{4R} = 433\ kJ/kg$

$s_{4R} = 1.7625\ kJ/kgK$

State 4 (Superheated Vapour)

$h_{4R} = h_{4s}\ (Assumption)$

$$\frac{h_3 - h_{4a}}{h_3 - (h_{4s} = h_{4R})} = 0.80 = \frac{459.8 - h_{4a}}{459.8 - 433} = 0.80 \quad h_{4a} = 443.36\ kj/kg$$

State 2' (Saturated liquid)

$T_{2'} = T_{sat@Peva} = T_{sat@3044.25\ kPa} = 87\ ^0\text{C}$

$h_{2'} = h_{2'f} = 336.9kJ/kg$

$T_{pp} = T_{2'} + \Delta T_{pp} = 390\ K$ ps. $\Delta Tpp = 30\ K$

State 3 (Superheated Vapour)

$P_3 = 3044.25\ kPa$

$s_3 = s_{4R} = 1.7625\ kJ/kgK$

$T_3 = 103℃$

$h_3 = 459.8\ kJ/kg$

1st energy balance inside the evaporator,

$$\dot{m}_{wf1} = \frac{\dot{m}_{exhuast} \times Cp_{exhuast} \times (T_{exh,in} - T_{exh,pp})}{h_3 - h_{2'}} = \frac{0.553 \times 1.1 \times (782 - 390)}{(459.8 - 336.9)}$$

$$= 1.87\ kg/s$$

$$T_{exh,out} = T_{exh,pp} - \frac{(h_{2'} - h_{2R}) \times \dot{m}_{wf1}}{\dot{m}_{exhuast} \times Cp_{exhuast}} = 390 - \frac{(336.9 - 257.14) \times 1.87}{0.533 \times 1.10} = 135\ K$$

$< Tmin$

2nd part of energy balance,

$$\dot{m}wf2 = \frac{\dot{m}_{exhuast} \times Cp_{exhuast} \times (T_{exh,in} - T_{min})}{h_3 - h_{2R}} = 1.26\ kg/s$$

$$\dot{Q}in = \dot{m}_{wf2} \times (h_3 - h_{2R})\ \ 1.26 \times (459.8 - 257.14) = 257.09\ kW$$

$\dot{W}turbine = \dot{m}_{wf2} \times (h_3 - h_{4a}) = 1.26 \times (459.8 - 438.36) = 27.01\ kW$

$\dot{W}pump = \dot{m}_{wf2} \times (h_{2a} - h_1) = 1.26 \times (251.78 - 249.2) = 3.25\ kW$

$\dot{W}net = \dot{W}turbine - \dot{W}pump = 23.75\ kW$

$\eta cycle = \frac{\dot{W}net}{\dot{Q}in} = 9\%$

3rd case,

$\frac{Peva}{Pcr} = 0.50$

$P_{eva} = P_{cr} \times 0.50 = 4059 \times 0.50 = 2029.5\ kPa$

$P_{eva} = P_2 = P_{2\prime} = P_{2R}$

State 1 (Saturated liquid)

T_{cond} = 35 ^{0}C so,

$P_{sat@35°C}$ = 887.91 kPa

$h_{fsat@35°C}$ = 249.2 kJ/kg

$\vartheta_{fsat@35°C}$ = 0.0009 m^3/kg

$s_{gsat@35°C}$ = 1.7138 kJ/kg K

$h_{gsat@35°C}$=417.5 kJ/kg

State 2 (Compressed liquid but the state is assumed as saturated liquid)

$P_2 = 2029.5\ kPa$

$h_{2s} = h_1 + \vartheta_1 \times (P_2 - P_1) = 249.2 + 0.0009 \times (2029.5 - 887.91) = 250.22\ kj/kg$

$\frac{h_{2s} - h_1}{h_{2a} - h_1} = \eta s = \frac{250.22 - 249.2}{h_{2a} - 249.2} = 75\% \rightarrow h_{2a} = 250.56\ kj/kg$

$T_{2a} = 36℃$

State 2R (The state after the Heat Exchanger)

$h_{2R} - h_2 = h_4 - h_{4R}$

$h_{2R} = h_2 + (h_4 - h_{4R})$

$h_{2R} = 250.56 + (434.4 - 432) = 252.96\ kj/kg$

$T_{2R} = 37.5℃$

$T_{min} = T_{2R} + \Delta T = 37.5℃ + 30 = 67.5\ ℃$ ps.$\Delta T = 30\ K$

State 4R (Superheated Vapour)

$P_{cond} = P_{4R} = 887.5\ kPa$

$T_{4R} = T_2 + \Delta T_{approach} = 36℃ + 15 = 51℃$ $\Delta Tapp = 15K$

$h_{4R} = 432\ kJ/kg$

$s_{4R} = 1.7620\ kJ/kgK$

State 4 (Superheated Vapour)

$h_{4R} = h_{4s}\ (Assumption)$

$$\frac{h_3 - h_{4a}}{h_3 - (h_{4s} = h_{4R})} = 0.80 = \frac{444 - h_{4a}}{444 - 432} = 0.80 \quad h4a = 434.4\ kj/kg$$

State 2' (Saturated liquid)

$T_{2'} = T_{Sat@Peva} = T_{sat@2029.5\ kPa} = 68\ ^0C$

$h_{2'} = h_{2'f} = 301.3kJ/kg$

$T_{pp} = T_{2'} + \Delta T_{pp} = 371\ K$ ps. $\Delta Tpp = 30\ K$

State 3 (Superheated Vapour)

$P_3 = 2029.5\ kPa$

$s_3 = s_{4R} = 1.7620\ kJ/kgK$

$T_3 = 83℃$

$h_3 = 444\ kJ/kg$

1st energy balance inside the evaporator,

$$\dot{m}_{wf1}=\frac{\dot{m}_{exhuast}\times Cp_{exhuast}\times(T_{exh,in}-T_{exh,pp})}{h_3-h_{2\prime}} = \frac{0.553\times1.1\times(782-371)}{(444-301.3)} = 1.68kg/s$$

$$Texh,\ out = Texh,\ pp - T_{exh,pp} - \frac{(h_{2\prime}-h_{2R})\times\dot{m}_{wf1}}{\dot{m}_{exhuast}\times Cp_{exhuast}} = 371 - \frac{(301.3-256.96)\times1.68}{0.533\times1.10} =$$

$231\ K < Tmin$

2nd part of energy balance,

$$\dot{m}_{wf2}=\frac{\dot{m}_{exhuast}\times Cp_{exhuast}\times(T_{exh,in}-T_{min})}{h_3-h_{2R}} = \frac{0.533\times1.10\times(782-340.5)}{(444-252.96)} = 1.35\ kg/s$$

$$\dot{Q}in = \dot{m}_{wf2}\times(h_3 - h_{2R}) = 1.35\times(444 - 252.96) = 257.9\ kW$$

$$\dot{W}turbine = \dot{m}_{wf2}\times(h_3 - h_{4a}) = 1.35\times(444 - 434.4) = 12.96\ kW$$

$$\dot{W}pump = \dot{m}_{wf2}\times(h_{2a} - h_1) = 1.35\times(250.56 - 249.2) = 1.836\ kW$$

$$\dot{W}net = \dot{W}turbine - \dot{W}pump = 11.124\ kW$$

$$\eta cycle = \frac{\dot{W}net}{\dot{Q}in} = 4\%$$

3.Pre-Heating and Regenerative Organic Rankine Cycle Calculations

1st case,

$$\frac{Peva}{Pcr} = 0.95$$

$$P_{eva} = P_{cr}\times 0.95 = 4059\times0.95 = 3856.05\ kPa$$

$P_{eva} = P_2 = P_{2P} = P_{2p'} = P_{2R}$

1st Type of Generators' Calculations (TEKSAN)

The Properties of the Exhaust Gas,

$\dot{m}_{exh}$= 0.533 kg/s

T_{exh}= 509 ^{0}C

- The Cp of the exhaust gas is calculated as 1.10 kJ/kg K

State 1 (Saturated liquid)

T_{cond} = 35 ^{0}C so,

$P_{sat@35℃}$ = 887.91 kPa

$h_{fsat@35℃}$ = 249.2 kJ/kg

$\vartheta_{fsat@35℃}$ = 0.0009 m^3/kg

$s_{gsat@35℃}$ = 1.7138 kJ/kg K

$h_{gsat@35℃}$=417.5 kJ/kg

State 2 (Compressed liquid but the state is assumed as saturated liquid)

$P_2 = 3856.05\ kPa$

$h_{2s} = h_1 + \vartheta_1 \times (P_2 - P_1) = 249.2 + 0.0009 \times (3856.05 - 887.91) = 251.87\ kJ/kg$

$$\frac{h_{2s} - h_1}{h_{2a} - h_1} = \eta s = \frac{251.87 - 249.2}{h_{2a} - 249.2} = 75\% \rightarrow h_{2a} = 252.76\ kj/kg$$

$T_{2a} = 37.5℃$

State 2R (The state after the Heat Exchanger)

$h_{2R} - h_2 = h_4 - h_{4R}$

$h_{2R} = h_2 + (h_4 - h_{4R})$

$h_{2R} = 252.76 + (444.2 - 438) = 258.96\ kj/kg$

$T_{2R} = 43℃$

State 4R (Superheated Vapour)

$P_{cond} = P_{4R} = 887.5\ kPa$

$T_{4R} = T_2 + \Delta T_{approach} = 55℃ \qquad \Delta Tapp = 15K$

$h_{4R} = 438\ kJ/kg$

$s_{4R} = 1.7785\ kJ/kgK$

State 4 (Superheated Vapour)

$h_{4R} = h_{4s}\ (Assumption)$

$$\frac{h_3 - h_4}{h_3 - (h_{4s} = h_{4R})} = 0.80 = \frac{469 - h_4}{469 - 438} = 0.80 \quad h4 = 444.2\ kJ/kg$$

State 2P (The state after the Pre-Heater)

The Energy Balance inside the pre-heater,

$\dot{m}_{wf1} \times (h_{2P} - h_{2R}) = \dot{m}_{water} \times Cp_{water} \times (T_{water,in} - T_{water,out})$

Assumptions,

- $\dot{m}_{water} = 1\ kg/s$
- $C_{pwater} = 4.22 \frac{kj}{kg} K$
- $T_{water,in} = 90℃$
- $T_{water,out} = 80℃$
- $T_{2p} = 65$ ℃ hence, $h_{2p} h2p$ can be obtained from the thermodynamic table for the specified working fluid.
- $h_{2p} = 296.2\ kJ/kg$

In this case, the mass flow rate of the working should be known in order to solve this equation. Since the enthalpy of the state 2P is still known. As a result of the first energy balance inside the evaporator, the mass flow rate can be obtained.

$$\dot{m}_{wf1} = \frac{\dot{m}_{water} \times Cp_{water} \times (T_{water,in} - T_{water,out})}{(h_{2p} - h_{2R})} = \frac{1 \times 4.22(90℃ - 80℃)}{(296.2 - 258.96)} = 1.13\ kg/sn$$

$T_{min} = T_{2p} + \Delta T = 65 + 30 = 95℃$

State 2P' (The saturated liquid)

$T_{2p'} = T_{Sat@Peva} = T_{sat@3856.05\ kPa} = 98.5\ ^0C$

$h_{2'} = h_{2'f} = 365kJ/kg$

$T_{pp} = T_{2p'} + \Delta T_{pp} = 401.5\ K$ ps. $\Delta Tpp = 30\ K$

State 3 (Superheated Vapour)

$P_3 = 3856.05\ kPa$

$s_3 = s_{4R} = 1.7785\ kj/kgK$

$T_3 = 120℃$

$h_3 = 469\ kJ/kg$

1st energy balance inside the evaporator,

$$\dot{m}_{wf1} = \frac{\dot{m}_{exhuast} \times Cp_{exhuast} \times (T_{exh,in} - T_{exh,pp})}{h_3 - h_{2p'}} = \frac{0.553 \times 1.1 \times (782 - 401.5)}{(469 - 365)} = 2.145\ kg/s$$

$$T_{exh,out} = T_{exh,pp} - \frac{(h_{2P'} - h_{2P}) \times \dot{m}_{wf1}}{\dot{m}_{exhuast} \times Cp_{exhuast}} = 401.5 - \frac{(365 - 296.2) \times 2.145}{(0.533 \times 1.10)} = 149\ K < Tmin$$

$$\dot{m}_{wf2} = \frac{\dot{m}_{exhuast} \times Cp_{exhuast} \times (T_{exh,in} - T_{min})}{h_3 - h_{2P}} = \frac{0.533 \times 1.10 \times (782 - 368)}{(469 - 296.2)} = 1.40\ kg/sn$$

$$\dot{Q}in = \dot{m}_{wf2} \times (h_3 - h_{2R}) = 1.40 \times (469 - 278.63) = 266.5\ kW$$

$$\dot{W}turbine = \dot{m}_{wf2} \times (h_3 - h_{4a}) = 1.40 \times (469 - 444.2) = 34.72\ kW$$

$$\dot{W}pump = \dot{m}_{wf2} \times (h_{2a} - h_1) = 1.40 \times (252.76 - 249.2) = 4.9\ kW$$

$$\dot{W}net = \dot{W}turbine - \dot{W}pump = 29.82\ kW$$

$\eta cycle = \frac{\dot{W}net}{\dot{Q}in} = 11\%$

2nd Case,

$\frac{Peva}{Pcr} = 0.75$

$P_{eva} = P_{cr} \times 0.75 = 4059 \times 0.75 = 3044.25\ kPa$

$P_{eva} = P_2 = P_{2P} = P_{2p\prime} = P_{2R}$

State 1 (Saturated liquid)

T_{cond} = 35 ^{0}C so,

$P_{\text{sat@35°C}}$ = 887.91 kPa

$hf_{\text{sat@35°C}}$ = 249.2 kJ/kg

$\vartheta_{f\text{sat@35°C}}$ = 0.0009 m^3/kg

$s_{g\text{sat@35°C}}$ = 1.7138 kJ/kg K

$h_{g\text{sat@35°C}}$=417.5 kJ/kg

State 2 (Compressed liquid but the state is assumed as saturated liquid)

$P_2 = 3044.25\ kPa$

$h_{2s} = h_1 + \vartheta_1 \times (P_2 - P_1) = 249.2 + 0.0009 \times (3044.25 - 887.91) = 251.14\ kj/kg$

$\frac{h_{2s} - h_1}{h_{2a} - h_1} = \eta s = \frac{251.14 - 249.2}{h_{2a} - 249.2} = 75\% \rightarrow h_{2a} = 251.78\ kJ/kg$

$T_{2a} = 36.5$°C

State 2R (The state after the Heat Exchanger)

$h_{2R} - h_2 = h_4 - h_{4R}$

$h_{2R} = h_2 + (h_4 - h_{4R})$

$h_{2R} = 251.78 + (438.36 - 433) = 257.14\ kj/kg$

$T_{2R} = 40.5$°C

State 4R (Superheated Vapour)

$P_{cond} = P_{4R} = 887.5\ kPa$

$T_{4R} = T_2 + \Delta T_{approach} = 36.5℃ + 15 = 51.5℃ \qquad \Delta Tapp = 15K$

$h_{4R} = 433\ kJ/kg$

$s_{4R} = 1.7625\ kJ/kgK$

State 4 (Superheated Vapour)

$h_{4R} = h_{4s}\ (Assumption)$

$$\frac{h_3 - h_{4a}}{h_3 - (h_{4s} = h_{4R})} = 0.80 = \frac{459.8 - h_{4a}}{459.8 - 433} = 0.80 \quad h_{4a} = 443.36\ kJ/kg$$

State 2P (The state after the Pre-Heater)

The Energy Balance inside the pre-heater,

$\dot{m}_{wf} \times (h_{2P} - h_{2R}) = \dot{m}_{water} \times Cp_{water} \times (T_{water,in} - T_{water,out})$

Assumptions,

- $\dot{m}_{water} = 1\ kg/s$
- $C_{pwater} = 4.22 \frac{kj}{kg} K$
- $T_{water,in} = 90℃$
- $T_{water,out} = 80℃$
- $T_{2p} = 65℃$ hence, $h2p$ can be obtained from the thermodynamic table for the specified working fluid.
- $h_{2p} = 296.2\ kJ/kg$

  $\dot{m}wf = \frac{\dot{m}_{water} \times Cp_{water} \times (T_{water,in} - T_{water,out})}{(h_{2p} - h_{2R})} = \frac{1 \times 4.22(90℃ - 80℃)}{(296.2 - 257.14)} = 1.08\ kg/s$

$T_{min} = T_{2P} + \Delta T = 65℃ + 30K = 95℃$

State 2P' (The saturated liquid)

$T_{2'} = T_{Sat@Peva} = T_{sat@3044.25\ kPa} = 87\ ^0\text{C}$

$h_{2'} = h_{2'f} = 336.9kJ/kg$

$T_{pp} = T_{2P'} + \Delta T_{pp} = 390\ K$ ps. $\Delta Tpp = 30\ K$

State 3 (Superheated Vapour)

$P_3 = 3044.25\ kPa$

$s_3 = s4R = 1.7625\ kj/kgK$

$T_3 = 103℃$

$h_3 = 459.8\ kj/kg$

1st energy balance inside the evaporator,

$\dot{m}_{wf1} = \frac{\dot{m}_{exhuast} \times Cp_{exhuast} \times (T_{exh,in} - T_{exh,pp})}{h_3 - h_{2P'}} = \frac{0.553 \times 1.1 \times (782-390)}{(459.8-336.9)} = 1.87\ kg/s$

$Texh,\ out = T_{exh,pp} - \frac{(h_{2O'} - h_{2p}) \times \dot{m}_{wf1}}{\dot{m}_{exhuast} \times Cp_{exhuast}} = 390 - \frac{1.87 \times (365-279.7)}{(0.533 \times 1.10)} = 117.8\ K < Tmin$

$\dot{m}_{wf2} = \frac{\dot{m}_{exhuast} \times Cp_{exhuast} \times (T_{exh,in} - T_{min})}{h_3 - h_{2P}} = \frac{0.533 \times 1.10 \times (782-368)}{(459.8-296.2)} = 1.48\ kg/s$ (The mass flow rate of the system.)

$\dot{Q}in = \dot{m}_{wf2} \times (h_3 - h_{2P}) = 1.48 \times (459.8 - 279.7) = 266.5\ kW$

$\dot{W}turbine = \dot{m}_{wf2} \times (h_3 - h_{4a}) = 1.48 \times (459.8 - 438.36) = 31.7\ kW$

$\dot{W}pump = \dot{m}_{wf2} \times (h_{2a} - h_1) = 1.48 \times (251.78 - 249.2) = 3.8\ kW$

$\dot{W}net = \dot{W}turbine - \dot{W}pump = 26.02\ kW$

$\eta cycle = \frac{\dot{W}net}{\dot{Q}in} = 10\%$

3rd Case,

$\frac{Peva}{Pcr} = 0.50$

$P_{eva} = P_{cr} \times 0.50 = 4059 \times 0.50 = 2029.5\ kPa$

$P_{eva} = P_2 = P_{2P} = P_{2p'} = P_{2R}$

State 1 (Saturated liquid)

T_{cond} = 35 ^{0}C so,

$P_{sat@35℃}$ = 887.91 kPa

hfsat@35℃ = 249.2 kJ/kg

$\vartheta_{fsat@35℃}$ = 0.0009 m^3/kg

$s_{gsat@35℃}$ = 1.7138 kJ/kg K

$h_{gsat@35℃}$=417.5 kJ/kg

State 2 (Compressed liquid but the state is assumed as saturated liquid)

$P_2 = 2029.5\ kPa$

$h_{2s} = h_1 + \vartheta_1 \times (P_2 - P_1) = 249.2 + 0.0009 \times (2029.5 - 887.91) = 250.22\ kJ/kg$

$\frac{h_{2s} - h_1}{h_{2a} - h_1} = \eta s = \frac{250.22 - 249.2}{h2a - 249.2} = 75\% \rightarrow h_{2a} = 250.56\ kJ/kg$

$T_{2a} = 36℃$

State 2R (The state after the Heat Exchanger)

$h_{2R} - h_2 = h_4 - h_{4R}$

$h_{2R} = h_2 + (h_4 - h_{4R})$

$h_{2R} = 250.56 + (434.4 - 432) = 252.96\ kj/kg$

$T_{2R} = 37.5℃$

State 4R (Superheated Vapour)

$P_{cond} = P_{4R} = 887.5\ kPa$

$T_{4R} = T_2 + \Delta T_{approach} = 36℃ + 15 = 51℃ \qquad \Delta Tapp = 15K$

$h_{4R} = 432\ kJ/kg$

$s_{4R} = 1.7620\ kJ/kgK$

State 4 (Superheated Vapour)

$h_{4R} = h_{4s}\ (Assumption)$

$$\frac{h_3 - h_{4a}}{h_3 - (h_{4s} = h_{4R})} = 0.80 = \frac{444 - h4a}{444 - 432} = 0.80 \quad h_{4a} = 434.4\ kJ/kg$$

State 2P (The state after the Pre-Heater)

The Energy Balance inside the pre-heater,

$\dot{m}_{wf} \times (h_{2P} - h_{2R}) = \dot{m}_{water} \times Cp_{water} \times (T_{water,in} - T_{water,out})$

Assumptions,

- $\dot{m}_{water} = 1\ kg/s$
- $C_{pwater} = 4.22 \frac{kj}{kg} K$
- $T_{water,in} = 90℃$
- $T_{water,out} = 80℃$
- $T_{2p} = 65℃$
- $h_{2p} = 296.2\ kJ/kg$

$$\dot{m}_{wf} = \frac{\dot{m}water \times cpwater \times (Twaterin - Twaterout)}{(h2p - h2R)} = \frac{1 \times 4.22 \times (90℃ - 80℃)}{(296.2 - 252.96)} = 0.97\ kg/s$$

State 2P' (The saturated liquid)

$T_{2P'} = T_{Sat@Peva} = T_{sat@2029.5\ kPa} = 68\ ^0$C

$h_{2p'} = h_{2',f} = 301.3kJ/kg$

$T_{pp} = T_{2'} + \Delta T_{pp} = 371\ K$ ps. $\Delta Tpp = 30\ K$

State 3 (Superheated Vapour)

$P_3 = 2029.5\ kPa$

$s_3 = s_{4R} = 1.7620\ kJ/kgK$

$T_3 = 83$ ℃

$h_3 = 444\ kJ/kg$

1st energy balance inside the evaporator,

$\dot{m}_{wf1} = \frac{\dot{m}_{exhuast} \times Cp_{exhuast} \times (T_{exh,in} - T_{exh,pp})}{h_3 - h_{2P'}} = \frac{0.553 \times 1.1 \times (782-390)}{(444-301.3)} = 1.68\ kg/s$

$Texh,\ out = T_{exh,pp} - \frac{(h_{2O'} - h_{2p}) \times \dot{m}_{wf1}}{\dot{m}_{exhuast} \times Cp_{exhuast}} = 371 - \frac{1.68 \times (301.3-278)}{(0.533 \times 1.10)} = 304\ K < Tmin$

$\dot{m}_{wf2} = \frac{\dot{m}_{exhuast} \times Cp_{exhuast} \times (T_{exh,in} - T_{min})}{h_3 - h_{2P}} = \frac{0.533 \times 1.10 \times (782-357)}{(444-278)} = 1.5\ kg/s$ (The mass flow rate of the system.)

$\dot{Q}in = \dot{m}wf2 \times (h3 - h2p) = 249.17$ kW

$\dot{W}turbine = \dot{m}wf2 \times (h3 - h4a) = 14.4$ kW

$\dot{W}pump = \dot{m}wf2 \times (h2a - h1) = 2.04$ kW

$\dot{W}net = \dot{W}turbine - \dot{W}pump = 12.36$ kW

$\eta cycle = \frac{\dot{W}net}{\dot{Q}in} = 4\%$

P.S.: In order to obtain much more accurate outcomes at 50% pressure ratio, the subcritical saturation cycle design should be employed instead of subcritical superheated cycle.

APPENDIX B

CALCULATION OF SPECIFIC HEAT VALUE OF EXHAUST GAS

The general formula of diesel fuel is $C_nH_{1.9n}$. In order to asses the accurate specific heat value of the exhaust gas of applied three engines, under the hypothesis of pure combustion of $C_{10}H_{20}$, the composition of the exhaust gases on the basis of molar has been calculated as,

The combustion of pure $C_{10}H_{20}$,

$C_{10}H_{20} + 15(O_2+3.76N_2) \rightarrow 10CO_2 + 10H_2O + (15\times3.76\ N_2)$

The mass flow rate of the fuel of the first engine at full load is obtained as 0.0165 kg/s, the exhaust mass flow rate is 0.533 kg/s.

$\dot{m}_{fuel}+\dot{m_{air}}= \dot{m}_{exhuast}$

$\dot{m}_{air} = 0.5165\ kg/s$

$\frac{\dot{m}_{air}}{\dot{m}_{fuel}} = 31.30 = \lambda\ \phi = \frac{1}{\lambda} = 0.467 \sim 0.5 < 1\ (lean\ mixture)$

$C_{10}H_{20} + 15\times2(O_2+3.76N_2) \rightarrow 10CO_2 + 10H_2O + (2\times15\times3.76\ N_2) + 15O_2$

n° of molar products= 147.8

Wet analysis is applied to obtain molar fractions of the products.

$CO_2\ \% = \frac{10}{147.8} = 6.76\ \%$

$O_2\ \% = \frac{10}{147.8} = 6.76\ \%$

$N_2\ \% = \frac{112.8}{147.8} = 76.31\ \%$

$O_2\% = \frac{15}{147.8} = 10.11\%$

In accordance with the inlet and minimum temperature of the exhaust gases for three engines, C_{pexh} is calculated.

For, $T_{exh,in}$= 509℃ and T_{min}= 70℃

$C_{pexh} = \sum_i xic_{pi} = n_{CO2}\times C_{pCO2} + n_{O2}\times C_{pO2} + n_{N2}\times C_{pN2} + n_{O2}\times C_{pO2}$

$C_{pexh} = 1.085$ kJ/kg K ($T_{exh,in}$)

$C_{pexh} = 1.04$ kJ/kg K (T_{min})

Taking into account for the temperature difference of the exhaust gases of the three engines, $C_{pexh} \cong 1.10$ kJ/kg K.